Title

Caveolin-3 Overexpression Increases the Responsivity of Beta Adrenergic Receptors in Cardiac Myocytes

Author

Busija, Anna

Publication Date

2017

Peer reviewed|Thesis/dissertation

UNIVERSITY OF CALIFORNIA, SAN DIEGO

Caveolin-3 Overexpression Increases the Responsivity of Beta Adrenergic Receptors in Cardiac Myocytes

A dissertation submitted in partial satisfaction of the requirements for the degree Doctor of Philosophy

in

Biomedical Sciences

by

Anna R. Busija

Committee in charge:

Professor Paul Insel, Chair
Professor Hemal Patel, Co-Chair
Professor Jeff Omens
Professor Farah Sheikh
Professor JoAnn Trejo

2017

The Dissertation of Anna R. Busija is approved, and it is acceptable in quality and form for publication on microfilm and electronically:

Co-Chair

Chair

University of California, San Diego

2017

DEDICATION

I dedicate this dissertation to my family.

TABLE OF CONTENTS

LIST OF FIGURES AND TABLES

LIST OF ABBREVIATIONS

8S-Cav – $8S_{20,w}$ oligomer of Cavs
60S-Cavin – $60S_{20,w}$ oligomer of cavins
70S-Cav – $70S_{20,w}$ oligomer of Cavs
80S – $80S_{20,w}$ complex of $70S_{20,w}$-Cav and $60_{20,w}$-Cavin
ACV/VI – Adenylyl cyclase isoforms V and VI
aka – Also known as
Akt – Protein kinase B
Ankrd13 – Ankyrin Repeat Domain-Containing Protein 13
AP-2 – Clathrin adaptor protein isoform 2
β_1AR – β_1 adrenergic receptor
β_2AR – β_2 adrenergic receptor
β_3AR – β_3 adrenergic receptor
βARK1 – βAR kinase isoform 1, aka GRK2
β-ARR1/2 – β-arrestin isoforms 1 and 2
cAMP – 3',5'-cyclic adenosine monophosphate
Cav – Caveolin
Cav3 OE – CM-specific Cav3-overexpressing mouse
CF – Caveolar fraction
CGP – CGP20712a
CM – Cardiac myocyte
COPII – Coat protein complex II
CSD – Caveolin scaffolding domain
CSK – c-Src tyrosine kinase
CRAC – Cholesterol recognition/interaction consensus sequence
DMSO – Dimethyl sulfoxide
DR1, DR2, DR3 – Disordered regions of Cavins
DRMs – Detergent-resistant membranes (lipid raft membranes)
eNOS – Endothelial nitric oxide synthase (aka NOS3)
EC50 – Half-maximal effective concentration
ER – Endoplasmic reticulum
ERAD – ER-associated degradation
ERES – ER exit site
ERK – Extracellular signal-related kinase (aka mitogen-activated protein kinase)
ESCRT – Endosomal sorting complexes required for transport
FAPP-1, FAPP-2 – Four phosphate adapter protein 1 and 2
Forsk – Forskolin
G_α, $G_{\beta\gamma}$ – Subunits of heterotrimeric G proteins
$G_{\alpha s}$, $G_{\alpha i}$ – Stimulatory and inhibitory G_α subunits
GLUT4 – Glucose transporter type 4
GPCR – G-protein coupled receptor
GPI – Glycosylphosphatidyl inositol
GRK – G-protein coupled receptor kinase
GSK3α/β – Glycogen synthase kinase 3

HR1, HR2 – Helical regions 1 and 2 of Cavins
IBMX – 3-isobutyl-1-methylxanthine
ICI – ICI118,551
Iso – Isoproterenol
K_v – Voltage-gated potassium channel
LQTS – Long QT syndrome
LTCC – L-type Ca^{2+} channel
LV -- Left ventricle
LVDP – Left ventricular developed pressure
MAPK – Mitogen-activated protein kinase (aka extracellular signal-related kinase)
MDCK – Madin-Darby Canine Kidney
MVB – Multivesicular bodies
Na_v – Voltage-gated sodium channel
NE -- Norepinephrine
nNOS – Neuronal nitric oxide synthase (aka NOS1)
OCR – Oxygen consumption rate
PA – Phosphatidic acid
PC – Phosphatidylcholine
$pCav1^{Y14}$ – Cav1 phosphorylated at tyrosine 14
PDE – Cyclic nucleotide phosphodiesterase
PDZ – Structural domain involved in cytoskeletal anchoring of membrane receptors
PE – Phosphatidylethanolamine
PG – Phosphatidylglycerol
PI3K – Phosphatidylinositol-4,5-bisphosphate 3-kinase
PI4P – Phosphatidylinositol 4-phosphate
$PI(4,5)P_2$ – Phosphatidylinositol 4,5-bisphosphate
PI – Phosphatidylinositol
$PI(3,4,5)P_3$ – Phosphatidylinositol (3,4,5)-triphosphate
PKA – Protein kinase A aka cAMP-dependent protein kinase
PLB – Phospholamban
PNGase F – Peptide-N-glycosidase F
PM – Plasma membrane
PP – Protein phosphatase
PR – Time between the start of the P wave until the beginning of the QRS complex in the cardiac electrical cycle
PS – Phosphatidylserine
PTM – Post-translational modification
QTcB – Time between the start of the Q wave and end of the T wave in the cardiac electrical cycle corrected for heart rate
Ryr – Ryanodine receptor
SAP97 – Synapse-associated protein 97
SERCA – Sarco/endoplasmic reticulum Ca^{2+}-ATPase
SHP-2 – Src homology 2 domain-containing protein tyrosine phosphatase 2
SM – Sphingomyelin
SR – Sarcoplasmic reticulum

Src – Proto-oncogene tyrosine-protein kinase Src
$t_{1/2}$ – Half-life
TGneg – Sibling transgene-negative control to Cav3 OE
TropI – Troponin I
TTCC – T-type Ca^{2+} channel
t-tubule – Transverse tubule
UbCav – Ubiquitinated Cav
monoUbCav – Monoubiquitinated Cav
polyUbCav – Polyubiquitinated Cav
UBXD1 – Ubiquitin Regulatory X (UBX) Domain-containing Protein 1
VCP – Valosin-containing protein

ACKNOWLEDGEMENTS

I would like to acknowledge Dr. Hemal Patel and Dr. Paul Insel for their support, scientific guidance, and patience throughout graduate school and for being the co-chairs of my committee. I would like to acknowledge Drs. Farah Sheikh, JoAnn Trejo, and Jeff Omens for the suggestions and guidance they have given me as members of my committee. I would also like to acknowledge the members of the Insel and Patel labs for their friendly support, enthusiasm for research, and helpful advice.

Chapter 1 is, in part, a reprint of the material as it appears in the American Journal of Physiology - Cell Physiology, in press, Busija, AR; Patel, HH; and Insel, PA. The dissertation/thesis author was the primary author of this paper.

Chapter 2 is, in part, in preparation for submission for publication of the material. The authors are Busija, Anna R; Schilling, Jan M.; Roth, David M.; Insel, Paul A.; and Patel, Hemal H. The dissertation author was the primary investigator and author of this material.

Chapter 3 is, in part, in preparation for submission for publication of the material. The authors are Busija, Anna R; Schilling, Jan M.; Roth, David M.; Insel, Paul A.; Patel, Hemal H. The dissertation author was the primary investigator and author of this material.

VITA

2009 Bachelor of Science, Duke University

2017 Doctor of Philosophy, University of California, San Diego

PUBLICATIONS

Busija AR, Fridolfsson HN, Patel HH. (2010) A new sense of protection: role of the Ca2+-sensing receptor in ischemic preconditioning. *Am J Physiol Heart Circ Physiol*. 299(5):H1300-1

Zemljic-Harpf AE, Godoy JC, Platoshyn O, Asfaw EK, **Busija AR**, Domenighetti AA, Ross RS. (2014) Vinculin directly binds zonula occludens-1 and is essential for stabilizing connexin-43-containing gap junctions in cardiac myocytes. *J Cell Sci.* 1;127(Pt 5):1104-16

See Hoe LE, Schilling JM, Tarbit E, Kiessling CJ, **Busija AR**, Niesman IR, Du Toit E, Ashton KJ, Roth DM, Headrick JP, Patel HH, Peart JN. (2014) Sarcollemal cholesterol and caveolin-3 dependence of cardiac function, ischemic tolerance, and opioidergic cardioprotection. *Am J Physiol Heart Circ Physiol.* 307(6):H895-903.

Mandyam CD, Schilling JM, Cui W, Egawa J, Niesman IR, Kellerhals SE, Staples MC, **Busija AR**, Risbrough VB, Posadas E, Grogman GC, Chang JW, Roth DM, Patel PM, Patel HH, Head BP. (2017) Neuron-Targeted Caveolin-1 Improves Molecular Signaling, Plasticity, and Behavior Dependent on the Hippocampus in Adult and Aged Mice. *Biol Psychiatry.* 81(2):101-110

Ray S, Kassan A, **Busija AR**, Rangamani P, Patel HH. (2016) The plasma membrane as a capacitor for energy and metabolism. *Am J Physiol Cell Physiol*. 310(3):C181-92

See Hoe LE, Schilling JM, **Busija AR**, Haushalter KJ, Ozberk V, Keshwani MM, Roth DM, Toit ED, Headrick JP, Patel HH, Peart JN. (2016) Chronic β_1-adrenoceptor blockade impairs ischaemic tolerance and preconditioning in murine myocardium. *Eur J Pharmacol.* 789:1-7

Busija AR, Patel HH, Insel PA. (2017) Hugh Davson Distinguished Lectureship Article Caveolins and cavins in the trafficking, maturation, and degradation of caveolae: implications for cell physiology. *Am J Physiol Cell Physiol*. ajpcell.00355.2016

RESEARCH EXPERIENCE

2009-2017 Department of Pharmacology, University of California, San Diego
Co-advisor: Dr. Paul Insel

Department of Anesthesiology, University of California, San Diego
Co-advisor: Dr. Hemal Patel

ABSTRACT OF THE DISSERTATION

Caveolin-3 Overexpression Increases the Responsivity
of Beta Adrenergic Receptors in Cardiac Myocytes

by

Anna R. Busija

Doctor of Philosophy in Biomedical Sciences

University of California, San Diego 2017

Professor Paul Insel, Chair
Professor Hemal Patel, Co-Chair

Heart failure is a leading cause of human morbidity and mortality and has been linked to neurohormonal dysregulation of β-adrenergic receptor (βAR) expression and responsivity that occurs with advancing age. No overarching mechanism for this age-dependent loss in βAR response has been identified. However, βARs localize to caveolae, membrane lipid raft microdomains formed by caveolin (Cav) proteins and expression of caveolin-3 (Cav3), the main Cav in caveolae of cardiac myocytes (CMs) decreases in an age-dependent manner. Therefore, aging-related reduction of Cav3 and

caveolae may influence the loss of βAR response, and increased Cav3 expression may alter the βAR responsivity of CMs and preserve βAR function into old age.

The studies presented in this dissertation were designed to understand the influence of Cav3 on the βAR signaling pathway. In chapter 1, we reviewed current knowledge of the biogenesis and degradation of Cavs and caveolae, described their composition and roles in compartmentalization of lipid and protein factors of cellular physiology, and identified unanswered questions informed by the state-of-the-art and human disease.

In chapter 2, we tested the hypothesis that CM-specific Cav3 overexpression (Cav3 OE) would modify βAR responsivity in young and aged hearts. We measured the physiological sequelae of activation of βARs in young and aged hearts with the synthetic catecholamine isoproterenol (Iso). We found significant amplification of Iso dose-induced increases in physiological contractility and relaxation of young Cav3 OE hearts, which also exhibited increased responses into old age.

In chapter 3, we tested the hypothesis that Cav3 OE increases caveolar compartmentation of βARs and/or downstream effectors of the βAR response and that the enhanced Cav3 OE response to Iso is mediated by β_1ARs or β_2ARs. Cav3 OE hearts did not demonstrate enhancement in targeted adenylyl cyclase- or βAR isoform-specific responses. However, we discovered that βAR-dependent cAMP production with Iso is subject to increased regulation by phosphodiesterase activity in Cav3 OE CMs, implicating Cav3 in differential regulation of βAR signals without significant changes in protein distribution.

Our findings from the studies in this dissertation support the hypothesis that Cav3 OE amplifies βAR function in young hearts and preserves responsivity in aged animals. These results are the first to demonstrate that Cav3 OE is protective against loss of βAR responsivity in aging hearts.

CHAPTER 1: CAVEOLINS AND CAVINS IN THE TRAFFICKING, MATURATION, AND DEGRADATION OF CAVEOLAE: IMPLICATIONS FOR CELL PHYSIOLOGY AND β-ADRENERGIC SIGNALING

Abstract

Caveolins (Cavs) are ~20 kDa scaffolding proteins that assemble as oligomeric complexes in lipid raft domains to form caveolae, flask-shaped plasma membrane (PM) invaginations. Caveolae ("little caves") require lipid-lipid, protein-lipid, and protein-protein interactions that can modulate the localization, conformational stability, ligand affinity, effector specificity, and other functions of Cav partner proteins. Cavs are assembled into small oligomers in the endoplasmic reticulum (ER), transported to the Golgi for assembly with cholesterol and other oligomers, and then exported to the PM as an intact coat complex. At the PM, cavins, ~50 kDa adapter proteins, oligomerize into an outer coat complex that remodels the membrane into caveolae. The structure of caveolae protects their contents (i.e., lipids and proteins) from degradation. Cellular changes, including signal transduction effects, can destabilize caveolae and produce cavin dissociation, restructuring of Cav oligomers, ubiquitination, internalization, and degradation. In this review, we provide a perspective of the life cycle (biogenesis to degradation), composition, and physiologic roles of Cavs and caveolae and identify unanswered questions regarding the roles of Cavs and cavins in caveolae and in regulating cell physiology. Additionally, we give an overview of how β-adrenergic receptors may interact with the caveolar environment to alter signaling pathways in health and disease.

Introduction:

Caveolins (Cavs) are ~20kDa oligomeric proteins required for the formation of caveolae, which are lipid raft plasma membrane (PM) domains enriched in proteins and lipids, including cholesterol and sphingolipids (1). Caveolae are flask-shaped membrane invaginations, formed by *cis/medial*-Golgi-PM transport of oligomeric Cavs embedded in cholesterol-rich membranes. Upon arrival at the cell surface, these complexes interact with cavins, adapter proteins that form oligomers and assist in membrane curvature (reviewed in (2, 3)). Based, at least in part, on the ability of Cavs to scaffold protein partners, caveolae play key roles in a variety of cellular responses, including: signal transduction (**Table 1.1**); transport of nutrients into and out of cells (e.g., insulin receptor activation stimulates translocation of the GLUT4 glucose transporter to caveolae in adipocytes (4)); and cellular entry of certain pathogens, toxins, and endocytic cargo (e.g., simian virus 40 (5), cholera toxin (6), albumin (7)). Caveolae and the functions they regulate have been recently reviewed: e.g., caveolae as membrane sensors and organizers (2, 8), in cytoskeletal interactions (9), endo/exocytosis (10), and signal transduction (11). Moreover, mutations in Cavs and Cavins are associated with a variety of diseases **(Table 1.2).**

There are three Cav isoforms: Cav1, Cav2, and Cav3. Cav1 and Cav3 are necessary and sufficient for caveolae formation in most tissues and striated muscle, respectively. Cav2 associates with Cav1 in hetero-oligomers and does not independently form caveolae (12, 13). The four Cav domains **(Figure 1.1) are**: 1) an *N-terminal domain,* which includes a Cav1 phosphorylation site ($Cav1^{Y14}$),

ubiquitination sites in Cav1, and SUMOylation sites in Cav3; 2) an α-helical *caveolin scaffolding domain (CSD)* (implicated in protein-protein interactions, oligomerization, and inhibition of signaling proteins) with a cholesterol recognition/interaction consensus sequence (CRAC) and ubiquitination or SUMOylation sites; 3) a *membrane domain* that interacts with PM lipids through an atypical helix-turn-helix motif that exposes both the N- and C-termini of Cav to the cytoplasm; and 4) a *C-terminal domain* with three palmitoylated cysteines involved in oligomerization, protein binding, and Cav stability.

Cavin proteins aid oligomerized Cavs to form flask-shaped caveolae. Four cavin isoforms have been identified: Cavin1 (aka polymerase I and transcript release factor [PTRF]), Cavin2 (aka serum deprivation response protein [SDPR]), Cavin3 (aka serum deprivation response factor-related gene product that binds to C-kinase [SRBC]), and Cavin4 (aka muscle-restricted coiled-coil [MURC]). Cavins homo- and hetero-trimerize with two Cavin1 proteins and one Cavin1, Cavin2, or Cavin3 via an α-helical domain, bind to caveolae membranes by basic regions on the helical domains, and assist Cavs in the membrane curvature that forms caveolae **(Figure 1.2).**

Interactions of Cavs with binding partners during trafficking, at the PM, and as part of signal transduction events modulate the behavior of caveolae as structural and functional microdomains. This review follows the life cycle of Cavs from the ER to

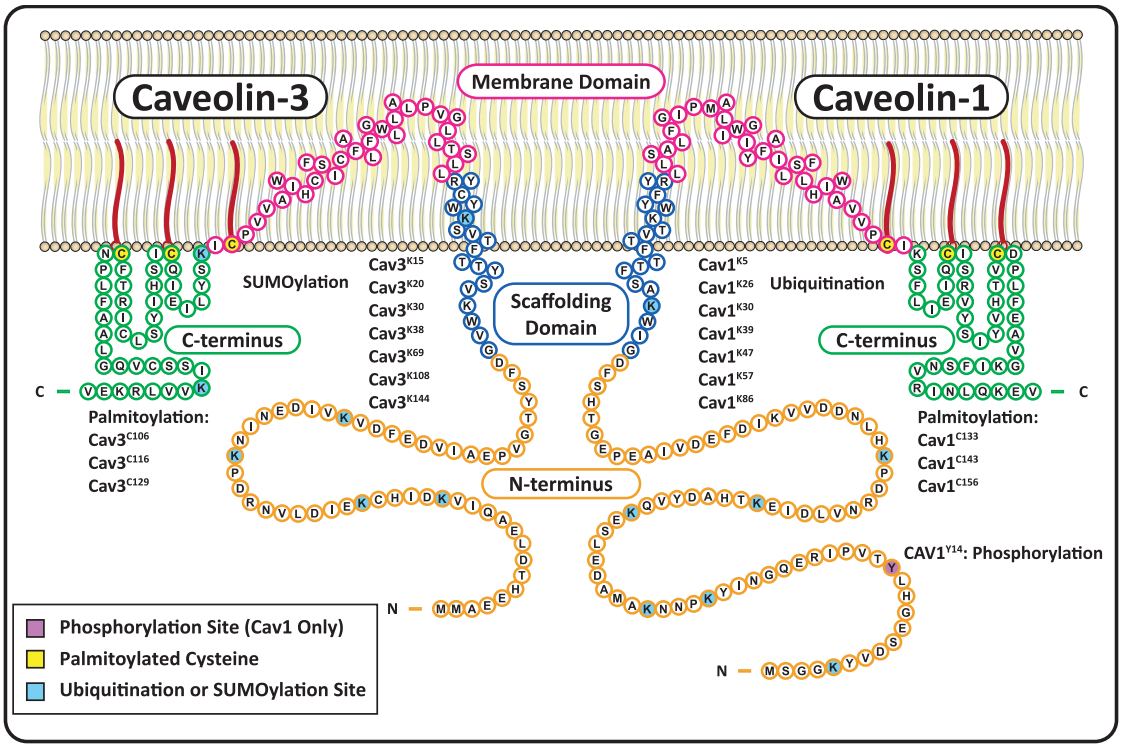

Figure 1.1: Structure and post-translational modifications of Caveolin-1 (Cav1) and Caveolin-3 (Cav3). Cav1 and Cav3 have four primary domains: **1)** N-terminal domains (orange) with multiple ubiquitination/SUMOylation sites on both Cavs, as well as a splice site and phosphorylation site on Cav1; **2)** scaffolding domains (blue) that form α-helices and are inserted into the membrane, with a cholesterol recognition/interaction amino acid consensus (CRAC) composed of the eight residues proximal to the membrane domain; **3)** helix-turn-helix membrane domains (fuchsia) that exit the membrane at a palmitoylation site; and **4)** C-terminal domains (green) with two more palmitoylated cysteines and two SUMOylation sites on Cav3.

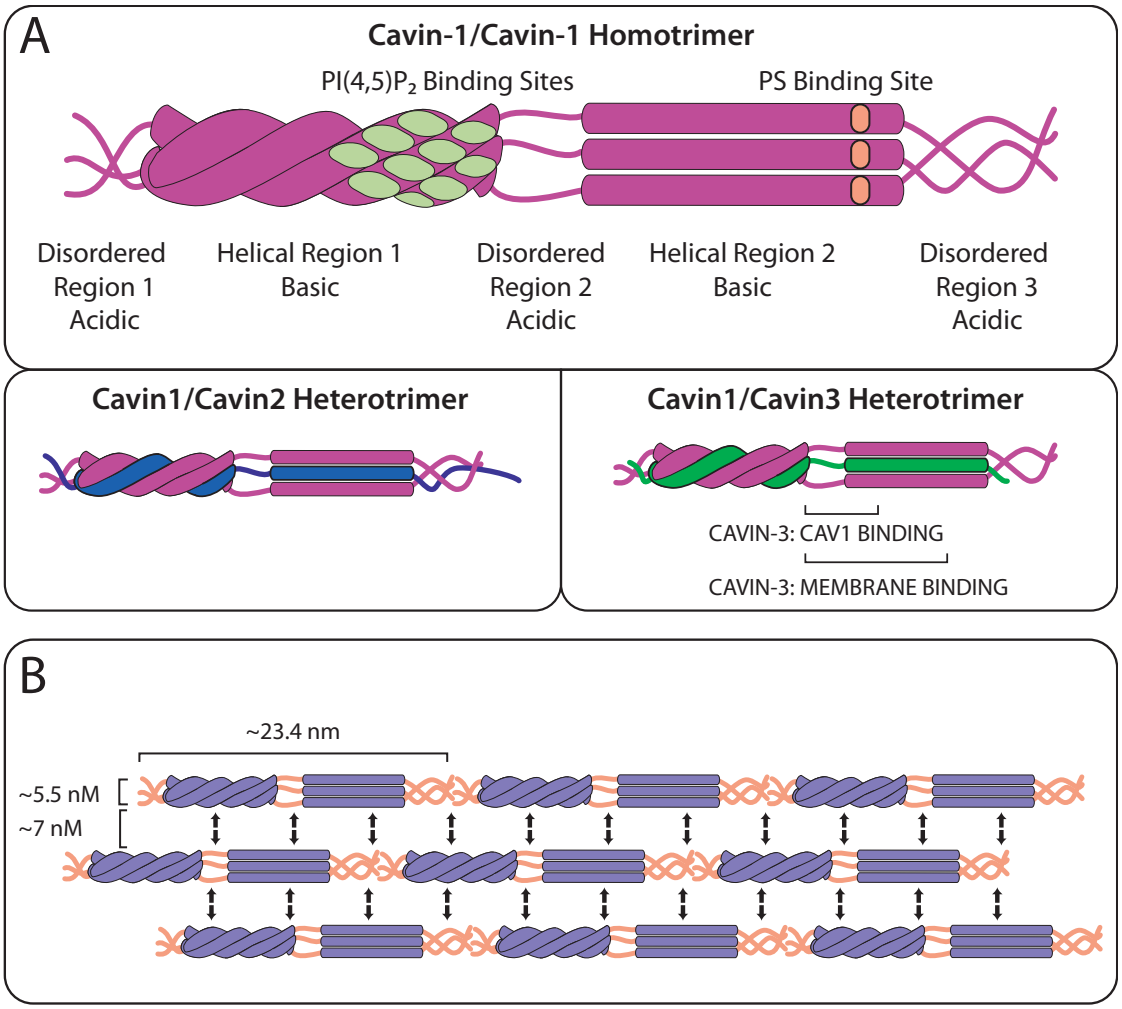

Figure 1.2: Structure of Cavins
(A) Cavins are cytosolic proteins with three disordered regions (DR1, DR2, DR3) alternating with two helical regions (HR1 and HR2). Two Cavin1's homo- and hetero-trimerize with a Cavin1, Cavin2, or Cavin3 monomer via an extended coiled-coil structure in HR1, which drives HR2 to generate an α-helical structure. Cavin1 has membrane binding sites, including a phosphatidylinositol (4,5)-bisphosphate ($PI(4,5)P_2$)-binding site composed of four basic regions in close proximity on HR1 and a phosphatidylserine (PS)-binding basic site on HR2. **(B)** Cavins detected on cellular membranes with electron microscopy form rod-like structures that are 5.5 nm wide and 23.4 nm long and associate laterally in 7 nM intervals. One idea, as described in the text and shown here, proposes that electrostatic interactions between alternating acidic DRs (orange) and basic HRs (purple) may facilitate these lateral associations while permitting flexibility in the cavin coat complex.

the lysosome and explores the roles of lipid and protein interactions within caveolae that contribute to aspects of cell physiology.

Trafficking of Cavs and Cavins for the formation of caveolae

Studies of caveolae formation have used primary cultures of epithelial cells (e.g., human lung microvascular endothelial cells) or fibroblasts (e.g., human skin fibroblasts, primary mouse embryonic fibroblasts), various epitheloid (e.g., Chinese hamster ovary, MDCK, Fischer rat thyroid), fibroblast-like (e.g., CV-1 and COS-7 from African green monkey kidney, NIH mouse 3T3), adipocyte (e.g., 3T3-L1), cancer (e.g., MCF-7 and MDA-MB-231 breast cancer, PC3 prostate cancer, A431 epidermoid carcinoma) cells, and/or other commonly used systems (e.g., HeLa, HEK293, *E. coli* cells). Cav3, Cavin1, and Cavin4 studies have also been performed in primary skeletal or cardiac muscle isolates or in the immortalized cardiac myoblastic cell lines H9C2 (rat) or HL-1 (mouse). Some of these cells provide null (or near-null) backgrounds for Cav expression; for example, MCF-7 cells have very low Cav1 expression, do not express cavins and do not form caveolae, and PC3 cells express Cav1 at high levels but do not express cavins (14-16). MDCK, A431, and MEF cells all express Cav1, Cavins 1-3, and form caveolae at the PM (15-18). The diversity of cellular backgrounds in research on caveolae can contribute to differences in results; for example, in studies of polarized epithelial cells, apical and basolateral membranes perform distinct roles in endo/exocytosis, signal transduction, mechanosensation, adherence, junction formation, and/or migration compared with studies of caveolae in

a sessile adipocyte, contractile primary skeletal muscle cell, or HEK293 cell (9). Cav1 and Cav3 may differ in their biogenesis of caveolae. However, most data on caveolae formation are based on studies of Cav1-expressing systems, in which the basic components and pathway of caveolae formation appear to be similar among different cell types and thus are the focus of this review.

Early steps in caveolae assembly: Membrane insertion, 8S-Cav oligomerization, and endoplasmic reticulum (ER) to Golgi transition

Caveolae are constructed in a complex, stepwise assembly process that involves ER membrane insertion, oligomerization, and export of Cav; Golgi Cav-cholesterol association, oligomerization, and export to the PM; palmitoylation near the PM; and addition of cavins at the PM to form invaginated structures (reviewed in (2, 19)) **(Figure 1.3).** The timeline from Cav translation to cavin addition at the PM in CV1 cells includes ER exit site (ERES) localization and initial oligomer (8S-Cav) formation within 5 min; Golgi localization within 15 min; secondary oligomer (70S-Cav) formation, cholesterol addition, and PM translocation by ~60 min; and accumulation of cavin at PM 70S-Cav oligomers that occurs over >25 min (20). Cavs are the primary protein components of caveolae, influencing membrane composition and protein content from translation to degradation. Thus, the translation and early oligomerization of Cavs begin the caveolae biogenesis pathway.

Formation of caveolae is initiated by the co-translational ER membrane insertion of monomeric Cav1 in a signal recognition particle-dependent manner (20, 21). As quickly as 5 min after synthesis in the ER, Cav1 forms $8S_{20,w}$ oligomers (8S-

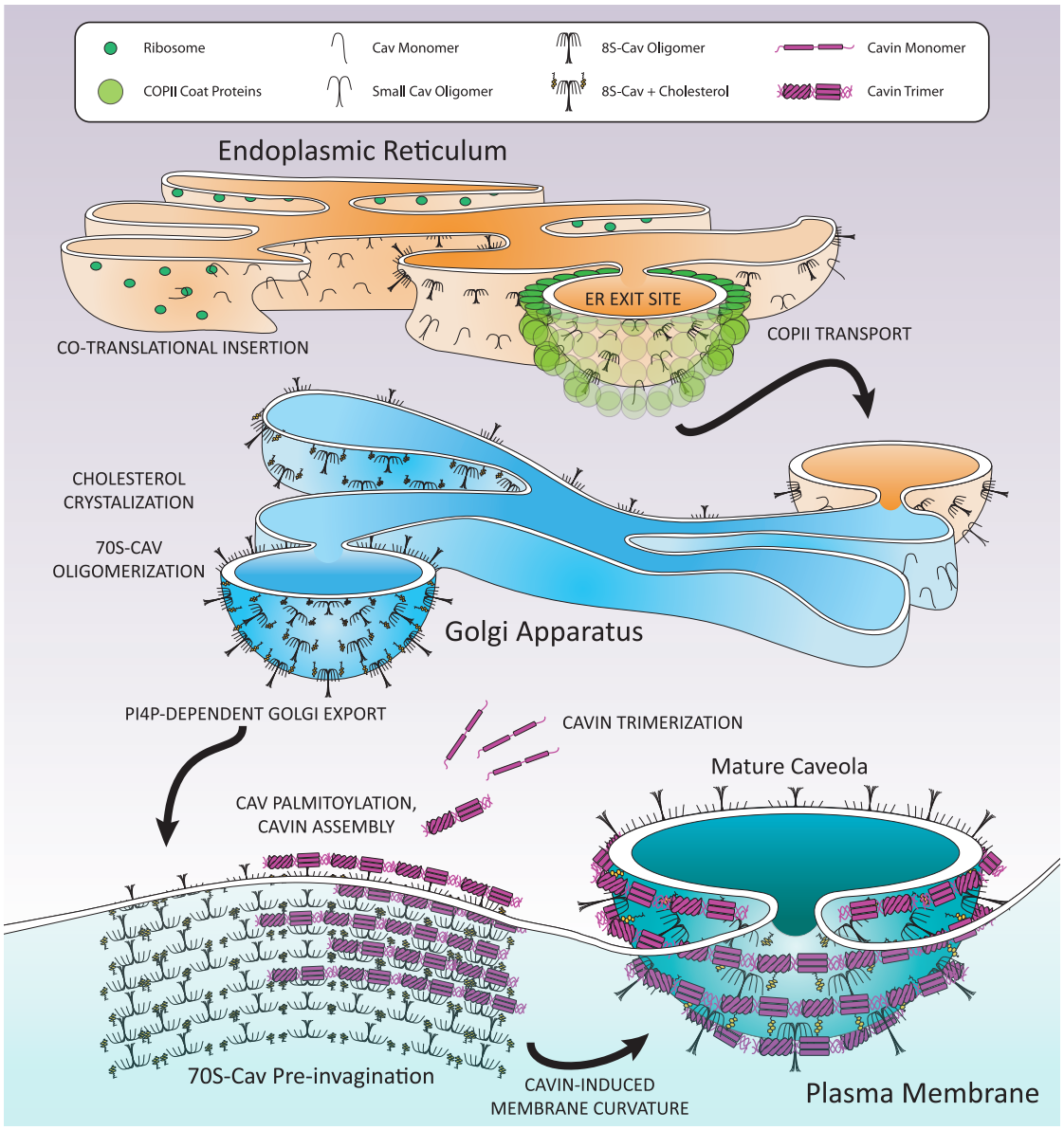

Figure 1.3: Maturation of Caveolae
Cav1 and Cav2 monomers are co-translationally inserted into the endoplasmic reticulum (ER) membrane and swiftly oligomerized into 8S-Cav oligomers containing 7-14 Cavs. These oligomers are transported to ER exit sites (ERES) within 5 min of synthesis for COPII-dependent transport to the Golgi apparatus 15 min post-synthesis. In the Golgi, cholesterol crystalizes in the membrane and assists in the formation of 70S-Cav complexes composed of 18-25 8S-Cav subunits by ~60 min after synthesis, whereupon 70S-Cav is transported to the PM by a four phosphate-adapter protein (FAPP-1, -2)-dependent secretory vesicles. Near or on the PM, palmitoyl acyltransferases palmitoylate 70S-Cav oligomers. Also on the PM, cavin proteins that trimerize in the cytosol gradually aggregate on the 70S-Cav membrane over the course of more than 25 min and assist in membrane curvature. Mature caveolae consist of three layers: a cholesterol and anionic lipid-rich membrane embedded with a palmitoylated 70S-Cav coat, which is surrounded by a striated oligomerized 60S-Cavin coat.

Cav, (150-200 kDa with a minor species around 443-669 kDa) that is estimated to contain 7-14 Cavs in a Cav1:Cav2 ratio of 2-4:1 (20-25). The formation of 8S-Cav oligomers depends upon aa residues $Cav1^{66-70}$, $Cav1^{81-100}$ (i.e., the CSD), and $Cav1^{134-178}$ (i.e., the C-terminus) (23, 26, 27). No molecular chaperone has been identified for the formation of 8S-Cav.

8S-Cav complexes translocate to the ERES, where recognition of a N-terminal diacidic sequence motif, Asp-X-Glu ($Cav1^{67DFE69}$), results in COPII vesicle-dependent export to the Golgi by ~15 min after synthesis (20, 28, 29). Disruption of this signal (e.g., $Cav1^{D67G}$) delays ER export and leads to accumulation in tubular-reticular ER structures and lipid droplets (20, 29). Experimental overexpression of Cav1 exhibits similar trafficking errors, implying that this export pathway may be a potentially saturable step in Cav maturation (30, 31). 8S oligomer formation is a prerequisite for caveolae formation (28) but Cav1 monomers and small oligomers reach the ER and may be subject to the same COP II-dependent export pathway as 8S complexes (20).

Intermediary steps in caveolae assembly: 70S-Cav oligomerization, cholesterol incorporation, and PM insertion

Golgi-localized 8S-Cav oligomerizes by ~60 min after synthesis into $70S_{20,w}$ complexes (70S-Cav) of ~3.3 MDa, predicted to comprise ~160 Cav1 and Cav2 molecules in 15-25 8S-Cav subunits (20, 32). Recent work suggests that the mature caveolae coat has a single 70S-Cav unit; thus, 70S-Cav formation is the penultimate step of Cav maturation (20, 25, 32-34). 70S-Cav oligomerization is restricted to the

Golgi: treatment with brefeldin A (which inhibits protein transport from the ER to the Golgi) prevents 70S-Cav oligomerization (20).

During the oligomerization step, 70S-Cav-associated membranes attain a high content of cholesterol, which is thought to involve a *cholesterol recognition/interaction amino acid consensus* of Cavs (CRAC: -Leu/Val-X_{1-5}-Tyr-X_{1-5}-Arg/Lys- where X_{1-5} represents one to five residues of any aa). The CRAC of Cav1 (^{94}VTK**Y**WF**Y**R^{101}) induces cholesterol crystallization in the membrane and results in deeper Cav1 peptide insertion (35). Cholesterol depletion reduces 70S-Cav complex formation, implying that oligomerization depends on membrane integration of cholesterol (20). Cavs that lack the CRAC allow 8S-Cav oligomerization but can prevent Cav association with lipid rafts in the Golgi and 70S-Cav formation, suggesting that 8S-Cav oligomers are not sufficient to establish the cholesterol-rich environment of caveolae (26, 36). The properties of the Golgi that allow 70S-Cav formation and cholesterol aggregation are not well-defined, nor are the chaperones or cofactors involved in assembly of 70S-Cav oligomers.

After oligomerization, 70S-Cav is exported to the PM from the *cis/medial*-Golgi network in carrier-dependent, dynamin-2-independent secretory vesicles within 60 min of synthesis (20). Transport is directed by four phosphate adapter protein 1 and 2 (FAPP-1, -2) that interact with phosphatidylinositol-4-phosphate (PI4P), the primary phosphoinositide (PI) species in the Golgi, to generate post-Golgi vesicles for transport (20, 37, 38). These small, uniform 70S-Cav-cholesterol vesicles can transport cargo, including glycosylphosphatidyl inositol (GPI)-linked proteins that

associate with lipid rafts (20, 39). Vesicle fusion with the PM allows GPI-linked proteins to diffuse laterally while the Cav coat remains at the point of integration (20).

70S-Cav complexes encounter palmitoyl acyltransferases near the PM, which palmitoylate Cavs on 3 cysteines in the late membrane/early C-terminal domains ($Cav1^{C133, C143, C156}$, $Cav3^{C106, C116, C124}$) **(Figure 1.1)** (40-43). Palmitoylation in many proteins is dynamic but Cav1 palmitoyl modifications are stable for at least 24 h in endothelial cells (42). Palmitoylation is not essential for membrane localization of Cavs. Although palmitoylation-deficient Cav1 mutants ($Cav1^{Cys-}$) form high molecular weight oligomers in detergent-resistant membranes (DRMs, i.e., lipid raft domains) at the PM, they exhibit reduced stability (44, 45). The lipid affinities of Cav domains and palmitoylation sites can influence the oligomerization and stability of Cavs at the PM. The composition of the lipids in caveolae stabilizes proteins and influences protein function, as we will discuss subsequently.

Terminal steps in caveolae assembly: cavin association, invagination, and stabilization

Once 70S-Cav oligomers and their cholesterol-rich membranes reach the PM, ~60-80 cavin proteins accumulate in caveolae over >25 min and create a striated coat (detected by electron microscopy (20, 46-48)). Cavins can assemble into cytoplasmic complexes in the absence of Cav1 but cavins are gradually added to 70S-Cav at the PM (20, 49). Cavins are not primarily bound to Cavs at the membrane: Cavin3 is the only isoform known to directly interact with Cav1 (in the CSD and middle domains of Cav1 and Cavin3, respectively) **(Figure 1.2)** (50). However, cavins have binding sites

for the anionic phospholipids phosphatidylserine (PS) and phosphatidylinositol (4,5)-bisphosphate (PI4,5P) that are locally concentrated in caveolae membranes (15, 25, 49, 51-53). All four cavin proteins have a C-terminal basic domain putatively involved in membrane association (54). Cavin1 also has an N-terminal leucine zipper domain (aa 53-75) that enables membrane association, while Cavin4 uses its N-terminal coiled-coil domain (aa 44-77) to localize to the PM (55, 56).

The basic oligomeric unit of cavin proteins is a trimer composed of two Cavin1 units with a monomer of Cavin1, Cavin2 or Cavin3 (Cavin4 has not been studied), interacting through helical region 1 (HR1); after HR1 trimerization, helical region 2 (HR2) undergoes conformational changes and forms an α-helical secondary structure, enabling further oligomerization (25, 49) (**Figure 1.2**). A 9 cavin complex forms from identical cavin trimers: Cavin1/Cavin2 and Cavin1/Cavin3 are mutually excluded from such trimeric-trimer-cavin complexes and segregate separately on the caveolae surface, implying that Cavin1/Cavin2 or Cavin1/Cavin3 oligomers may have distinct roles (49). Cavin-cavin interactions yield $60S_{20,w}$ complexes (60S-Cavin, predicted ~2.5 MDa) which, with addition of 70S-Cav, forms an 80S complex (3, 20).

Membrane invagination in a nascent caveola depends upon localized biophysical properties of the lipid bilayer and the intrinsic membrane-remodeling capacity of Cavs, cavins, and lipids (33, 48, 54) (**Figure 1.3)**. Cav1 or Cavin1 expressed alone can independently influence membrane curvature and in mammalian cells can form tubular membrane structures (54, 57). Cavs interact with phospholipid headgroups of the membrane through a helix-turn-helix membrane domain that enters and exits from the cytosol **(Figure 1.1)** (58). Additionally, the three palmitoylated

cysteines of Cavs stabilize Cav oligomers in the caveolae membrane (44, 45) and may participate in membrane curvature (58). Membrane lipids, such as PI4P in Golgi export vesicles, may also contribute to membrane curvature and caveolae invagination (59, 60).

A proposed mechanism of cavin-driven membrane remodeling is that alternation between basic HR1 and HR2 domains interspersed with acidic disordered regions 1, 2, and 3 (DR1-3) (**Figure 1.2**) allows DRs of one cavin trimer to recognize HRs of a trimer in the adjacent parallel striation and vice versa, thereby creating a flexible lattice of lateral cavin-cavin interactions around caveolae that exert curve-inducing forces on the membrane (3). Supporting this idea are observations of a zigzag appearance of cavin striations around the caveolae coat, with cavin subunits alternating in proximity to adjacent striations (47). Details of membrane invagination are not well defined, for example, the roles of other binding partners of Cavs and cavins and of cytoskeletal components.

70S-Cav and 60S-Cavin together form mature, stable caveolae that have three layers: a cholesterol- and negatively-charged phospholipid-enriched membrane, 8S-Cav subunits organized into a palmitoylated 70S-Cav coat, and a 60S-Cavin complex that spirals around the outside of the 70S-Cav coat. These mature caveolae (**Figures 1.3 and 1.4**) stabilize and protect Cavs from degradation by preventing lateral movement and exchange of Cavs and cavins (20, 61, 62). Cavs and caveolae proteins are also protected from ubiquitination and depalmitoylation. An example of this is G_{α} protein (GTP-binding proteins in $\alpha\beta\gamma$ heterotrimers): palmitoyl turnover of G_{α} proteins is increased by receptor activation and G_{α} dissociation from $G_{\beta\gamma}$ and caveolae,

implying that caveolae may exclude acyl thioesterases (63-66). Cavins are also protected from degradation within caveolae: a PI binding site on HR1 of Cavin1 is a major ubiquitination site that is obscured by membrane association (16).

Cav1 has a reported half-life ($t_{1/2}$) of > 24 h (42, 67, 68), although some studies report other values (69-71). Cavin1 knockdown destabilizes caveolae and reduces the $t_{1/2}$ of Cav1 to 7 h (15). Similarly, truncation constructs of Cav1 that cannot oligomerize have a decreased half-life and do not form stable caveolae (26). Cav3 appears to have a shorter $t_{1/2}$ than Cav1 (5.5-7 h) and mutant forms of Cav3 can have an even shorter $t_{1/2}$ (45-60 min) because of ubiquitination and proteosomal degradation (72-74). Cavin1 has a $t_{1/2}$ that ranges between 5-8 h; however, in the absence of Cav1, the $t_{1/2}$ decreases by almost half (16).

Thus, in the process of caveolae biogenesis, unstructured 18-21 kDa Cav monomers assemble in a tightly controlled fashion to form 8S-Cav, 70S-Cav-cholesterol, and finally, 80S-Cav-Cholesterol-Cavin complexes that are protected from degradation.

Processes of caveolae disassembly

Stability of caveolae at the PM requires that Cav and cavin oligomers remain tightly associated. Disruption of that structural stability by mechanical stress, endocytic activity, or signal transduction pathways dissociates cavins from caveolae and leads to endocytosis of Cavs **(Figure 1.4).** In contrast to the maturation and stability of 70S-Cav, which requires constitutive, stable palmitoylation, caveolae

disassembly and 70S-Cav dissociation involve dynamic PTMs of Cavs that include phosphorylation, S-nitrosylation, and ubiquitination.

Cavs are subject to multiple endocytic pathways, two of which are depicted in **Figure 1.4**: Caveolae, including the 70S-Cav complex, can be endocytosed as a result of Src-dependent phosphorylation (75-78) or the PM can undergo mechanical stresses that flatten caveolae and dissociate 60S-Cavin complexes, after which Cav is ubiquitinated (UbCav1) and endocytosed (79, 80). The pathways are likely more complex than described below and in **Figure 1.4**. Key to both pathways are Cavin dissociation, endocytosis, Cav ubiquitination, and endosomal processing of UbCav1, in which mono- and poly-UbCav1 is directed to intraluminal vesicles for lysosomal degradation (20, 80) and poly-UbCav1 undergoes proteosomal processing (79).

Cavin dissociation occurs in both pathways portrayed in **Figure 1.4**. If caveolae lose structural integrity in response to mechanical stress or vesiculation, 60S-Cavin dissociates into the cytosol and separates into trimeric-trimer-cavin units (3, 49, 81, 82). Because cavin associates with the lipids of caveolae, its departure does not directly affect 70S-Cav localization to the PM (15, 52, 53, 68). For example, although Cav3, Cavin1, and Cavin4 co-localize at the PM of myocytes, during hypo-osmotic stress Cav3, but not Cavin1 or Cavin4, is present in membrane blebs, suggesting that membrane stress leads to dissociation of the Cavins but not Cav3 (82). Cholesterol depletion with U18666A (which inhibits cholesterol trafficking in cells) also results in 60S-Cavin dissociation from the PM (68).

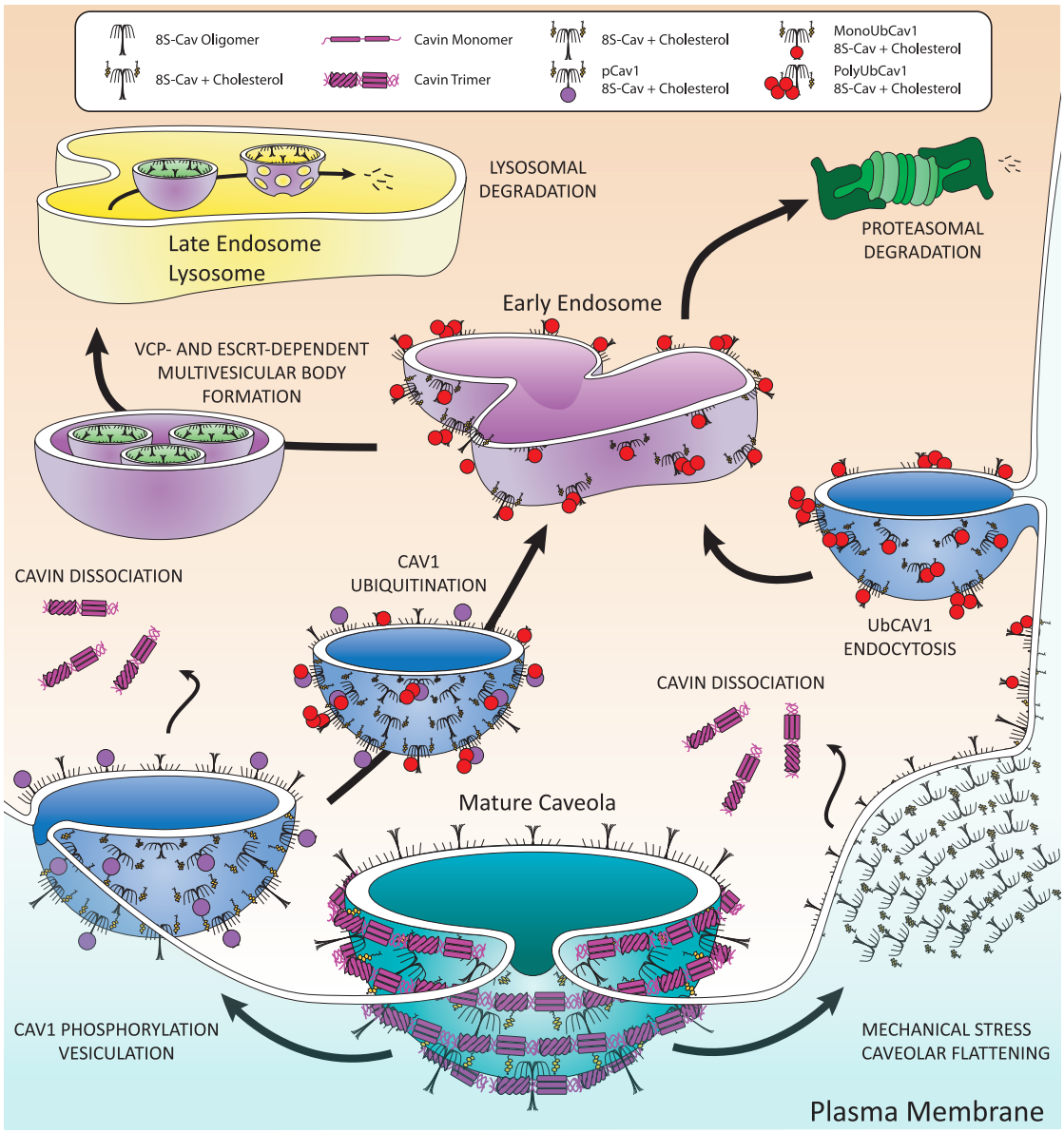

Figure 1.4: Disassembly and Degradation of Caveolae
Caveolae disassembly begins at the plasma membrane. Examples shown here are Src-dependent phosphorylation of Cav1 and membrane stretch. Cav1 phosphorylation initiates dynamin-dependent vesiculation that distorts caveolae, dislodging cavin trimers, and leads to ubiquitination of Cavs (UbCav) during vesicular transport to the early endosome. Mechanical stress displaces cavin from the membrane, followed by ubiquitination and subsequent endocytosis of Cav1 to the early endosome. Endosomal UbCav and cholesterol associate with valosin-containing protein (VCP) and are packaged in multivesicular bodies by endosomal sorting complexes required for transport (ESCRT) complex proteins for transport to and degradation in the late endosome/lysosome. Some polyUbCav is degraded by the proteasome.

Cytosolic Cavin1 is susceptible to ubiquitination on Lys residues within PI binding sites (i.e., groupings of surface-exposed basic residues) in the HR1 region that are occluded by membrane contact **(Figure 1.5)** (16). Mutation of the five Lys and Arg residues in this region reduces Cavin1 ubiquitination and turnover by the proteasome (16) without substantially influencing Cav1 co-localization or caveolae formation (48). Such data imply that the co-localization of the PI binding/ubiquitination site selectively protects Cavin1 from ubiquitination while bound to caveolae and leads to the ubiquitination of cytosolic Cavin1 (16).

Src-dependent phosphorylation of Cav1 is implicated as a control point of clathrin-independent membrane protein internalization and macromolecular cargo endocytosis (7, 83-85). Phosphorylation of Cav1 by Src kinases on an N-terminal tyrosine (p-Cav1^{Y14}) is an interaction that requires C-terminal palmitoylation of Cav1^{C156} and the myristoyl plus basic motif of Src (7, 86-92). p-Cav1^{Y14} also adds a binding site on Cav1 to the SH2 domain of Src, thereby scaffolding this kinase more closely to Cav1 after Src activation (93).

Cav1 phosphorylation and sustained Src signaling initiates endocytosis by phosphorylating dynamin-2 to close off and detach caveolae from the membrane, recruiting actin and the actin regulator cortactin, and cross-linking p-Cav1^{Y14} to filamin A (76-78, 94-97). p-Cav1^{Y14} regulates the duration of Src activity by binding kinases and phosphatases: p-Cav1^{Y14} recruits c-Src tyrosine kinase (Csk) to inhibit Src via Src^{Y527} phosphorylation, while recruitment of Src homology 2 domain-containing protein tyrosine phosphatase 2 (SHP-2) interferes with Csk-p-Cav1^{Y14} complex

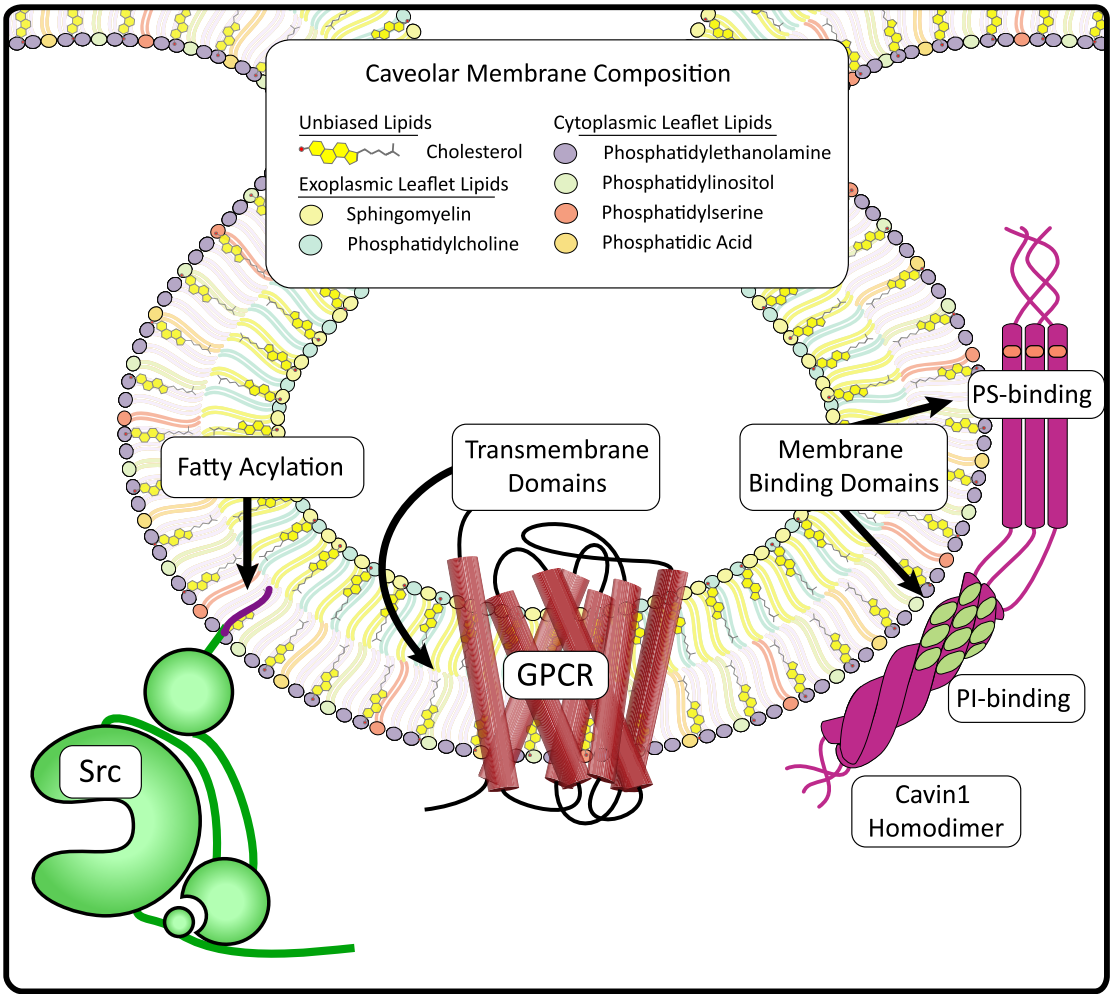

Figure 1.5: Caveolae membrane composition and caveolae targeting signals
Caveolae membranes are enriched in phospholipids, sphingolipids, and cholesterol. This diagram depicts the distribution of membrane lipid species within a caveolae bilayer. Cholesterol is concentrated within caveolae, representing a third of all lipids, and is present in both leaflets of the bilayer. Sphingomyelin is slightly more prevalent than PC in the exofacial leaflet of caveolae, while PE composes more than half of the cytoplasmic leaflet. Also in the cytoplasmic leaflet, the anionic phospholipids PI, PS, and PA compose the minor fraction of lipid content with PI roughly twice as prevalent as PS and PA at half the concentration of PS. Proteins can be targeted to caveolae through transmembrane domains (e.g., GPCRs, Cavs), fatty acylations (e.g., Src myristoylation) and membrane binding domains (e.g., Cavin1 PI and PS binding domains).

formation and preserves Src activity **(Figure 1.6)** (98, 99). The balance between Csk and SHP-2 action on p-Cav^{Y14} thus may control Src-mediated caveolae endocytosis.

Cav1^{Y14} phosphorylation also destabilizes 70S-Cav oligomers by altering the relationships between oligomerized Cav1: pCav1^{Y14} or phosphomimetic Cav1^{Y14D} increases the intermolecular distance between Cavs in caveolae vesicles, resulting in dissociation of higher-order Cav1 oligomers (100). Phosphorylation-induced loss of 70S-Cav integrity may be a mechanism by which the previously stable structure is made accessible to ubiquitination enzymes, acyl-protein thioesterases, and other degradative influences. Addition of a cell-permeable CSD peptide, which directly blocks Src-dependent Cav1^{Y14} phosphorylation, stabilizes large oligomers (100).

Mechanical effects on the PM that flatten caveolae initiate another type of caveolae disassembly. Flattening can result from cholesterol depletion (101, 102), hypo-osmotic stress (82), and substrate stretch (16, 81). The flattening of caveolae after mechanical stress may be a protective mechanism that provides a reservoir of PM to prevent membrane tension and injury by increasing PM surface area (82). Caveolae in skeletal muscle cluster in PM surface-connected rosettes; under hypo-osmotic stress, caveolae density decreases and reduces the ratio of rosettes to independent caveolae (82). Treatment of mouse lung endothelial cells with methyl-β-cyclodextrin, which depletes the PM of cholesterol, increases membrane tension during hypotonic stress (81).

The flattening of caveolae is ATP- and actin-independent. During recovery from nonlethal hypotonic stress, caveolae re-form by integrating the PM-localized pool of Cav1 with Cavin1 within 10 min to form an equal number of caveolae; this

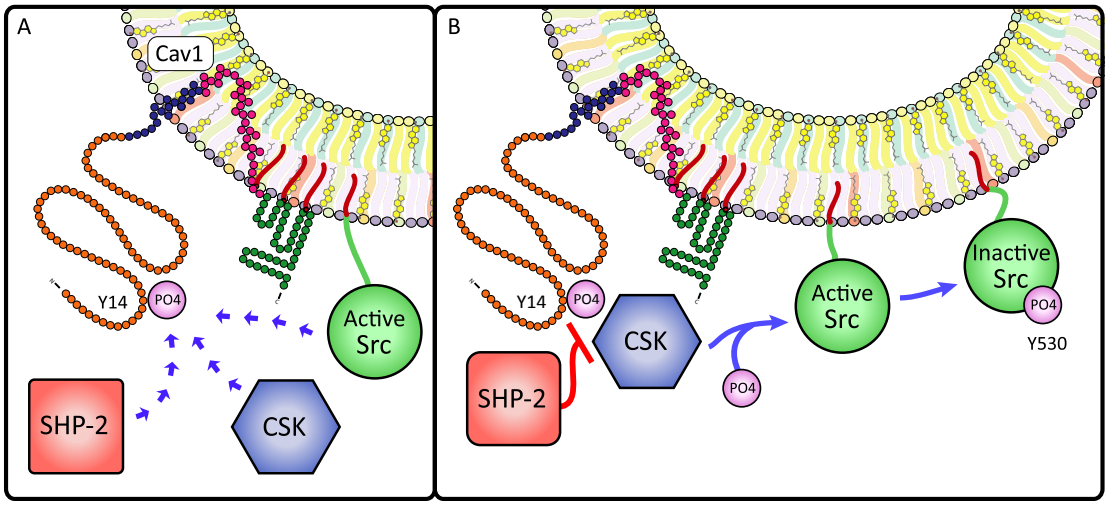

Figure 1.6: Cav1 phosphorylation influences Src signaling
(A) Cav1^{Y14} phosphorylation creates a Src Homology 2 (SH2) binding site that regulates Src activity through binding of Src and recruitment of two cytosolic Src-regulating enzymes: C-terminal Src Kinase (CSK) and SH2 domain-containing non-transmembrane protein tyrosine phosphatase (SHP-2). **(B)** When recruited to caveolae by pCav1^{Y14}, CSK deactivates Src by phosphorylating Src^{Y530}; however, pCav1^{Y14} binding to SHP-2 blocks CSK recruitment and prevents Src^{Y530} phosphorylation, increasing the duration of Src activity. Thus, Cav1 phosphorylation permits a rheostat-like control of Src signaling.

requires ATP but not actin remodeling (81). Chronic and repetitive shear stress, such as at the luminal PM of endothelial cells exposed to laminar flow, can increase PM caveolae number without increasing mRNA, suggesting that signaling induced by shear stress increases Golgi processing and export of Cav1 (103, 104). The number of caveolae increases only at the shear-exposed membrane, where they may play roles in translocating proteins to caveolae and activation of signaling cascades (103-105)**.** Caveolae flattening thus protects the PM from rupture by reducing PM tension during transient stress.

Absence of cavins from caveolae through mechanical detachment, cholesterol depletion, or knock-down disrupts 70S-Cav oligomers into their 8S-Cav subunits and induces Cav1 ubiquitination, caveolae-independent packaging, and endocytosis of UbCav1 to the early endosome (68). The cholesterol-rich membranes surrounding 8S-Cav units are transported to the endosome and lysosome, indicating that Cavs can maintain their membrane localization even with loss of the 70S-Cav structure (106).

Cav1 separated from mature caveolae can be monoubiquitinated on six N-terminal lysines ($Cav1^{K5, K26, K30, K39, K47, K57}$)(80), polyubiquitinated on $Cav1^{K86}$ (79), and may have other states of ubiquitination. The most prevalent ubiquitination is monoUbCav1. PolyUbCav1 is divided into two groups: 64% Lys-63-linked and 28% Lys-48-linked (68, 107, 108). p-$Cav1^{Y14}$ undergoes $Cav1^{K86}$ polyubiquitination and proteosomal degradation (79). Additionally, Cav1 and DRMs are implicated in the inhibition of lysosomal function, which may influence Cav1 degradation (17). Cav3 ubiquitination of specific lysines has not been shown; however, a small ubiquitin-like modifier (SUMO) can be added by the E3 ligase PIASγ to lysines on Cav3 that are

homologous to the ubiquitin sites on Cav1, suggesting that such sites may be loci for ubiquitination (109).

After ubiquitination and translocation of Cav to endosomes, it is degraded by proteosomal and lysosomal pathways (68, 79). Mono- and polyUbCav1 are packaged within multivesicular bodies (MVB) by endosomal sorting complexes required for transport (ESCRT) and an AAA+-type ATPase, valosin-containing protein (VCP; aka p97, Cdc48) (68, 80, 107, 108). VCP uses conformational changes from ATP hydrolysis to extract polypeptides from larger assemblies of oligomers or membranes, regulates endosome size and sorting, and with the cofactor UBXD1 enables MVB formation (107, 110-115). UBXD1 and Ankrd13, two mutually exclusive VCP cofactors, regulate VCP interaction with monoUbCav1 and mono/polyUbCav1, respectively and can drive Cav segregation to intraluminal vesicles (80, 107, 108, 111). VCP preferentially interacts with higher-order Cav oligomers (8S-Cav, ~150-200 kDa major species and 443-669 kDa minor species (20)) but it is unknown whether VCP also interacts with 70S-Cav (24, 107, 108). 8S-Cav and VCP interaction is disrupted by the depletion of membrane cholesterol, suggesting that VCP-dependent regulation of Cav oligomers occurs after cholesterol membrane integration in the Golgi and that cholesterol remains in the local membrane environment of Cavs during endocytosis and endosomal sorting (107).

PolyUb chains on residue $Cav1^{K86}$ direct it to proteasomes for degradation. The proteasomal inhibitor MG132 reduces Cav1 degradation but also prevents acidification of Cav1-containing endosomes; thus, Cav1 may be packaged in MVB before proteasomal and endosomal processing **(Figure 1.4)** (68). Because VCP is

typically involved in membrane protein extraction and proteasomal transport (111) and UbCav1 interacts with VCP, VCP complexes may also be involved in the proteasomal pathway of UbCav1 degradation; however, the process by which polyUbCav1 is trafficked to the proteasome is not known.

Importantly, tagged, overexpressed, and/or mutant Cav constructs are subject to defective 8S-Cav and 70S-Cav oligomerization, lipid raft exclusion, intracellular accumulation/aggregation, and increased turnover (30, 31, 68, 80, 107, 108). However, many studies use tagged Cavs to assess turnover, intracellular Cavs, or interaction of Cavs with partners. Cav1 oligomerization is also influenced by experimental tagging: overexpression of GFP-, mCherry- or C-myc-tagged Cav1 yields aberrant Cav1 oligomers that do not interact with endogenous Cav1 or Cav2 (31). Tags and overexpression can also affect localization to lipid rafts: tagged mutant $Cav1^{P132L}$ (a mutation in multiple diseases) is more sensitive to oligomer and lipid raft disruption than is $Cav1^{WT}$ (31). Differences in the reported $t_{1/2}$ of Cav1 can at least partially be attributed to the use of tagged proteins: in one study, endogenous Cav1 and Cav1-HA had $t_{1/2}$'s of >24 h and 13.6 h, respectively (68). Because of the role of VCP in ER-associated degradation (ERAD, in which misfolded or incomplete protein assemblies are dislocated from the ER and degraded by the ubiquitin-proteasome system (114, 116)), tagged/overexpressed Cav1 in the biogenesis pathway may be a target of VCP and yield non-physiologic results. Thus, careful attention must be paid in Cav trafficking and signaling studies to identify possible artifacts created by expression constructs with abnormal trafficking characteristics.

Composition and roles of the caveolae lipid microenvironment

The protein complex of caveolae comprises 80S-Cav multimers: ~160 membrane-bound, palmitoylated Cavs bound in close proximity to cholesterol-rich membranes and complexed with ~50 cavin oligomers. Interactions between Cavs, cavins, lipids, and other proteins create an unique protein, lipid, and lipoprotein microenvironment. Cavs shape this environment not only through cholesterol binding and palmitoylation but also by interaction with the inner leaflet of membrane lipids by a hairpin helix-turn-helix membrane domain. This domain includes Cav1$^{T91,\ K96,\ Y97,\ R101,\ Y118}$, which preferentially interact with phospholipid headgroups of the cytosolic PM leaflet, and Cav1^{G108} which interacts with the exofacial leaflet (34, 58, 117). Cavins are dependent upon the lipid composition of caveolae because they have affinities for negatively charged phospholipids (PS, PI(4,5)P_2) and cholesterol in caveolae membranes and their lipid binding may occlude ubiquitination sites, thereby protecting them from degradation (15, 25, 49, 52, 53). Other proteins localize to caveolae by association with Cavs, the caveolae membrane, and/or scaffolding proteins that associate with caveolae. Major factors that influence these interactions are caveolae lipid composition, PTMs, and activation state changes that exchange proteins between caveolae and cytosolic or PM domains.

The lipidome of caveolae appears to depend on the cell type studied, the method used to isolate caveolae, and the physiological "state" (e.g., mechanical stress or signal transduction events). Cavs are inserted and exit through the cytoplasmic leaflet of the PM, which is enriched in PS, phosphatidylethanolamine (PE),

phosphatidylinositol (PI), and phosphatidylcholine (PC), while the outer leaflet is enriched in sphingolipids (including glycolipids) and phosphatidylcholine (PC) (118, 119). Caveolae isolated without detergents have more than twice the molar concentration of lipid per mg of protein than do PM membranes (120, 121). These isolates are highly enriched in phospholipids, cholesterol, and sphingomyelin (SM) when compared with non-caveolae membranes: caveolae contain 3-5 times more PS, 2-5 times more cholesterol and SM, 2-4 times more phosphatidic acid (PA), and ~2-fold more PE (which composes around 40% of all membrane phospholipids) **(Figure 1.5)** (120, 121). However, studies disagree about PC and PI concentrations: a concanavalin-A affinity chromatography method of caveolae isolation in murine L-cell fibroblasts identified a 15-fold increase in PC and 3-fold increase in PI within caveolae, whereas an Optiprep density gradient centrifugation method in KB human epidermal cancer cells expressing exogenous Cav1 found a minimal increase in PC or PI species (120, 121). Caveolae membranes contain higher concentrations of unsaturated, saturated, and mono-unsaturated fatty acid species (121). Caveolae isolated with 1% Triton X-100 are enriched in cholesterol and SM without the glycerophospholipid enrichment seen in non-detergent-isolated lipid rafts (120). Thus, detergent treatment of PMs may preferentially extract exoplasmic leaflet lipids but not anionic inner leaflet glycerophospholipids (122). However, when Cav1 is not present in cells, non-detergent lipid rafts contain similar proportions of lipids as do those isolated from Cav1-expressing cells except that cholesterol is reduced (120). Thus, caveolae are distinct from other PM lipid rafts primarily due to caveolin and its interaction with cholesterol.

Cholesterol has a large role in the formation and structure of caveolae. Because the integration of cholesterol is necessary for 70S-Cav assembly from 8S-Cav subunits, cholesterol is essential for caveolae formation; however, it is also necessary for the stability, structure, and function of caveolae at the PM. Cholesterol increases the ordering and packing of lipid membranes and has numerous effects, for example, increasing resistance to disruption by mechanical stress (123, 124), membrane thickness (125), and depth of Cav CSD peptide insertion into membranes (35). Cholesterol depletion distorts caveolae, implying that PMs do not maintain an invaginated morphology without cholesterol (46, 126). Substitution of cholesterol with its precursor, desmosterol, reduces Cav affinity for sterol and results in enlarged caveolae with increased $Cav1^{Y14}$ phosphorylation (127).

Proteins associate with PM lipids through transmembrane domains, membrane-interacting sites, and/or fatty acid PTMs; however, conformational changes, binding site obstruction, and de-lipidation can alter lipid affinities, which may influence movement of proteins into and out of caveolae. Protein-protein, protein-lipid, and lipid-lipid associations can reciprocally stabilize and concentrate binding partners (128). For instance, membrane cholesterol and other lipids within caveolae influence conformational plasticity of the β_2AR, receptor ligand affinity, activation/inhibition, and G-protein affinity and activation; importantly, lipids that stabilize the β_2AR concentrate in its local membrane (129-132). Certain lipids can also be allosteric modifiers of β_2AR activity (132). Membrane lipid composition thus influences the stability and behavior of the receptor, which can influence the lipid composition in its local environment. In conjunction with evidence that agonist-stimulated β_2AR

dissociates laterally from lipid rafts to undergo β-arrestin-mediated clathrin endocytosis and degradation (132-134), localization within or outside caveolae may influence receptor behavior independent of protein scaffolds, activators, and downstream effectors. Therefore, by aggregating certain lipid species within caveolae, Cavs may stabilize proteins in conformations that can regulate ligand affinity, protein-protein interactions and signal transduction; in addition, conformational changes and/or PTMs that change lipid affinities may alter protein localization in caveolae (63, 64, 129-131, 135). In light of the data I will discuss in Chapters 2 and 3, these factors may play subtle but profound roles in the signaling characteristics of βARs within caveolae.

Stable membrane-bound homeostasis and stimulus-dependent dynamic behavior or modification occur with other caveolae-resident proteins. For example, nitric oxide (NO) production in endothelial cells is a key regulator of vascular smooth muscle relaxation. Within caveolae, eNOS is constitutively bound and inhibited by Cav1 (136, 137). Src activity enabled by Cav1 binding can lead to eNOS dissociation from Cav1 and eNOS activation: Src phosphorylates $Cav1^{Y14}$, which causes dissociation of eNOS; Src phosphorylates PI3K, which phosphorylates Akt, which phosphorylates uninhibited cytosolic eNOS at the activating Ser^{1177} site; and p-$eNOS^{S1177}$ produces more NO to stimulate smooth muscle relaxation **(Figure 1.7)** (138). Each component of this pathway has membrane and/or protein affinities that change upon activation or modification. Proteins can cycle out of caveolae and be activated; others may cycle into them upon stimulation.

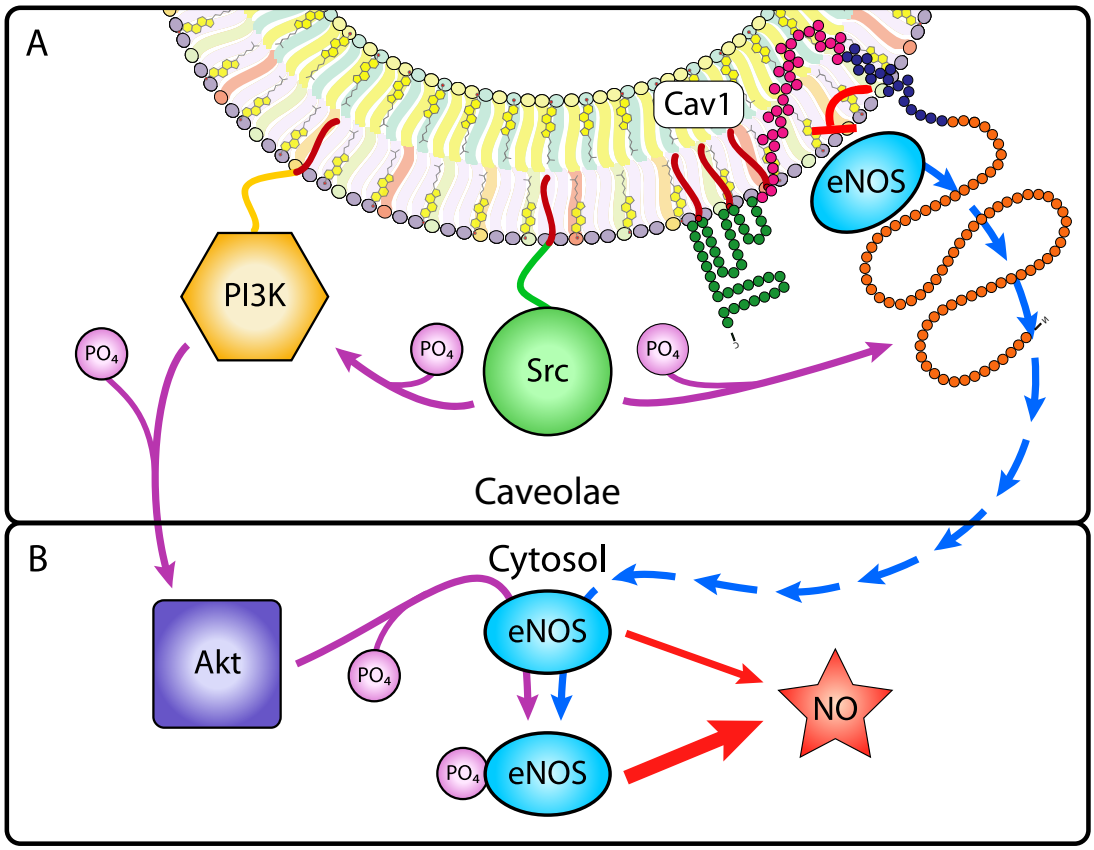

Figure 1.7: Caveolae-cytosol exchange of eNOS increases NO production
(A) Within caveolae, Src phosphorylates Cav1, leading to the release of eNOS from Cav1 inhibition (blue arrows). Src also phosphorylates and activates PI3K, which phosphorylates and activates Akt. **(B)** In the cytosol, free eNOS is phosphorylated by Akt, which increases NO production.

Fatty acylations (e.g., palmitoylation, myristoylation, GPI-link formation) influence caveolae localization and protein association in caveolae. Palmitoylation does not influence Cav1 stabilization in cholesterol-enriched membranes but interacts with other lipid components of the membrane and perturbs conformational dynamics (139). Cavs are palmitoylated near the PM after oligomerization, implying that palmitoylation has a limited role in lipid species selection or Golgi-localized oligomerization (40-42). However, the caveolae lipid environment can aggregate proteins (e.g., GPCRs, G_{α}'s, Ras, c-Src), with fatty modifications (135, 140, 141). In some cases, acylation is required for protein-protein associations: c-Src is localized to caveolae as a consequence of its myristoylation and binds to Cav1 through Cav^{C156} palmitoylation (39, 92, 140). Cav^{C156} can be S-nitrosylated secondary to eNOS activation, acting as potent negative regulator of Cav palmitoylation and thus palmitoylation-dependent binding activity.

Much is unknown regarding the facilitation by fatty acylation of membrane, Cav1 binding, and caveolae localization. The complexity of these interactions is illustrated by the behavior of G_{α} isoforms. G_{α} isoforms are CSD-associated and subject to dynamic palmitoylation but $G_{\alpha i/o/z}$ possess an additional myristoylation site that localizes them to caveolae (140-142). Palmitoylation of G_{α} and all three Cav1 cysteines is required for binding (141). Palmitoylation-deficient, but not myristoylation-deficient, $G_{\alpha i}$ is trafficked to caveolae but binding to Cav1 is abrogated, implying that caveolae localization requires myristoylation but Cav1 binding requires palmitoylation and thus suggesting a two-step mechanism for $G_{\alpha i}$ localization and association with Cav1 (141). By contrast, $G_{\alpha s}$ has no myristoylation

site and thus its PM localization and subsequent palmitoylation depend on its association with isoprenylated $G_{\beta\gamma}$ subunits (142). Localization of G_{α} is also dependent upon its activation state: GPCR-mediated activation of G_{α} subunits induces $G_{\beta\gamma}$ dissociation, separation from Cav1, and accelerates G_{α} depalmitoylation, thus delaying re-association of G_{α} and Cav1 (63, 64). Cav1 expression also modifies the palmitoylation state of certain proteins (143), and palmitoylation of $Cav1^{C143+C156}$ is required for the efficient transport of GPI-anchored proteins to the cell surface (39). Taken together, these data demonstrate that fatty acylations may induce differential localization and Cav binding behavior between protein isoforms, thus altering the stoichiometry or function of signal transduction proteins.

In summary, the microenvironment of caveolae represents a multifaceted, interrelated, and dynamic collaboration between Cavs, cholesterol, cavins, membrane lipids, and other membrane-interacting proteins. Forces within and outside caveolae can influence signal transduction paradigms in a variety of ways. Prior research has only begun to address this complexity.

Caveolae biogenesis, degradation, and lipid composition: discussion and unanswered questions

This review focuses on the biogenesis and degradation of caveolae microdomains and the roles of the lipid and protein components in those microdomains and in aspects of cell physiology. Much is known regarding caveolae biogenesis and degradation but many questions remain.

Caveolae biogenesis is sensitive to changes in protein structure, oligomerization, cholesterol, and PTMs. For example, numerous mutations in Cav1, Cav3, Cavin1, and Cavin4 have been associated with human diseases **(Table 2)**. Most of these mutations cause defects in Cav localization and loss of morphological caveolae and result in diseases in adipose tissue (Cav1, Cavin1) (144, 145), pulmonary endothelium and smooth muscle (Cav1) (146), skeletal muscle (Cav3) (147, 148), and cardiac muscle (Cav3, Cavin1, Cavin4) (144, 149, 150). Some Cav1 mutations occur in certain cancers (151-153). Cav biogenesis can be disrupted by epitope tags, Cav constructs, and Cav overexpression that recapitulate some disease-related defects (26, 27, 30, 31, 154-157). The disease-related mutations in these proteins reinforce the idea that the caveolae biogenesis system is physiologically relevant in numerous tissues. Normal Cav function may be tightly controlled by factors and/or chaperones that require unaltered Cav subunits to properly oligomerize, traffic to and function in the PM, and be degraded.

8S-Cav must be formed before COP II-dependent ER export to generate 70S-Cav in the Golgi. As Cav proteins localize to ERES within 5 min of synthesis and reach the Golgi by 15 min, 8S-Cav oligomerization is a relatively rapid process (20). The lack of substantial secondary or tertiary structural stability in Cav may make this initial oligomerization step slower if Cav is modified or mutated. Indeed, if given more time, conditions that facilitate protein folding (e.g., incubation at 30ºC or 10% glycerol supplementation), or inhibition of proteasomal degradation (e.g., with MG-132), some trafficking-deficient Cav3 is competent to reach the PM, accrue in lipid

rafts, and be protected from premature degradation (74). Even so, chaperones and information regarding the requirements for 8S-Cav oligomerization remain unknown.

Tagged, mutant, and/or overexpressed Cavs can form aggregates larger than 8S-Cav (30, 31, 73) and raise the question: how do 8S-Cav oligomers assemble into immobile and protected 70S-Cav structures with cholesterol in the Golgi? A mixture of incomplete Cav oligomers and monomers can be transported to the Golgi, but 8S-Cav does not form outside of the ER (20). Might unknown factors facilitate 70S-Cav assembly from 8S-Cav subunits (31, 35)? Perhaps long-lived caveolae structures require strict steric precision to prevent degradation, such that sequence changes lead to premature loss of oligomers, e.g., when Src-dependent Cav1^{Y14} phosphorylation wedges apart 8S-Cav clusters at the PM (100). Without 70S-Cav-cholesterol and 60S-Cavin complexed at the PM, "exposed" ubiquitination, palmitoylation, and/or phosphorylation sites may direct Cavs to degradation (74).

Another poorly understood aspect is the recognition pathway for 70S-Cav export from the Golgi. 8S-Cav is partially competent to reach the PM, but aggregates substantially larger than 8S-Cav are unable to reach the PM and may accumulate insufficient cholesterol to become buoyant lipid rafts (36). Are 70S-Cav-driven changes in Golgi lipid membrane composition a prerequisite for efficient export? Although FAPP-1 and -2 are components of the secretory pathway, their binding target PI4P is the most prevalent Golgi phospholipid and not unique to 70S-Cav (37, 38). Is there a cofactor that recognizes cholesterol, another enriched lipid, or Cav oligomers and drives the 70S-Cav Golgi export pathway?

Alternating acidic/basic domains in neighboring striations of the outer cavin coat have been proposed to exert forces for membrane curvature, but more information is needed regarding cavin recruitment, the role of cavins in caveolae curvature, determinants of cavin stability, and detachment of the cavin complex (20, 81, 82). Tomographic reconstruction of caveolae complexes has yielded promising data on the ultrastructure of the complete caveolae coat (25, 47) and the crystal structure of cavin (48) has helped advance understanding of cavins. By contrast, the lack of a crystal structure for Cavs has hampered the collection of more precise information of their structure and function.

The degradation pathways of caveolae and their resident proteins are less well-defined than those of biogenesis. In view of the trafficking and aggregation problems of tagged Cav constructs, their use may reveal information that identifies the sequelae of structural instability. Such "artifacts" can be useful, e.g., HA-Cav1 has a shorter $t_{1/2}$ than wild-type Cav1, thus facilitating cell culture experiments (108). However, most studies of Cav degradation cited in this review used tagged Cav1 to draw conclusions about the endocytic, endosomal, lysosomal, and/or proteasomal degradation pathway of Cavs (68, 80, 107, 108). The lack of data on the degradation of endogenous Cavs and cavins (3) is thus an important gap in terms of normal cell physiology.

In summary, sixty years after their discovery (158), caveolae remain enigmatic dark caves. Our understanding of Cavs, cavins, their maturation and degradation processes, and the dynamic complexity of their lipid and protein components remains a work in progress.

βAR function and caveolae in the heart

Heart failure is the leading cause of morbidity and mortality for the aging population in the United States (159, 160). Age-related cardiac dysfunction is heralded by a loss of β-adrenergic receptor (βAR) responsivity to adrenaline and noradrenaline, and so the leading therapies against heart disease, β-blockers, focus on improving the capability of the sympathetic nervous system to activate βARs when they are needed (161-165). However, druggable regulatory interventions to enhance cardiac health and βAR responsivity remain elusive and the mechanism for this age-dependent loss in βAR response is not known. However, expression of Cav-3 decreases in the aged heart and aging is associated with loss of Cav-3 from membrane caveolae (166, 167). Therefore, the loss of Cav-3 and caveolae with aging, and as a consequence, a loss of scaffolding and co-localization of βARs and downstream signaling components in caveolae may provide such a mechanism.

βARs are seven-transmembrane domain G-protein coupled receptors that activate the stimulatory ($G_{\alpha s}$) and inhibitory ($G_{\alpha i}$) G-proteins to influence adenylyl cyclase (AC) production of cAMP (168). Their actions have been extensively studied in terms of their influence on cardiovascular function and health. In early heart failure, decreased cardiac output promotes an activation of the sympathetic nervous system that increases circulating catecholamines, which activate cardiac βARs to increase heart rate, the speed and force of contractility, and the rate of relaxation (163). However, as heart failure progresses, the chronic neurohormonal activation of βARs drives negative feedback processes within cardiac myocytes (CMs) which lead to

~50% reduction of βAR density and βAR-dependent contractility (169, 170). Chronic activation of the βARs can also cause cardiac myocyte (CM) apoptosis (171, 172). The administration of β-blockers preserves the βAR signaling system from driving the heart into further failure and improves cardiac function but does not repair the damage inflicted by persistent catecholaminergic toxicity and apoptosis (159, 161, 162, 173, 174).

β_1ARs and β_2ARs are the two principal βARs expressed in cardiac myocytes (CMs). The predominant βAR isoform, β_1ARs, are major contributors toward global cAMP elevation that activates PKA to produce increased contractility, and, when overstimulated, myocardial apoptotic signals (171, 172). The β_2ARs stimulate transient, compartmentalized cAMP production that induces PKA-dependent positive inotropic responses through $G_{\alpha s}$, followed by negative responses attributed to β_2AR phosphorylation and coupling to $G_{\alpha i}$, protecting CMs from apoptosis via a $G_{\alpha i}$-phosphatidylinositol 3-kinase (PI3K)-Akt pathway (168, 170, 175). Interestingly, these different behaviors may depend on caveolar localization: the β_2ARs and some β_1ARs localize to sarcolemmal caveolae where their activation is characterized by tightly regulated and locally limited cAMP signaling (168, 171, 172).

The effects of differential regulation of the two βAR sub-types are complex. For example, β_1ARs are thought to be less susceptible to rapid downregulation by activation-induced feedback than are β_2ARs, but β_1ARs are implicated as the major isoform that is lost in advancing age and heart failure (171). β_2ARs, on the other hand, are subject to activation-promoted downregulation, but they are also linked to survival signaling (176). Additionally, when β_2ARs are displaced from caveolar domains, the

disinhibited cAMP signal strongly resembles that of the β_1ARs (177). Therefore, the distinct signaling paradigms of these two isoforms of βAR may depend upon their proximity to other components of the cAMP signaling pathway or regulatory influences rather than intrinsic differences in activation.

In adult CMs, caveolae compartmentalize and regulate βAR signaling pathway components that exhibit changes in function and expression as the heart ages, including β_2AR, $G_{\alpha s}$ and $G_{\alpha i}$, ACs, G protein coupled receptor kinases (GRKs), PKA catalytic subunits, and LTCCs (178). Interventions to increase βAR function in failing hearts have targeted the ACs with some success: increasing AC isoform VI in the heart increases contractile function in human patients with heart failure (179, 180). This work has not linked these changes to alterations in the membrane domain in which cAMP pathway proteins reside (178, 181-184), however, the differential regulation of βARs may provide an opportunity to develop interventions that increase the beneficial effects of comparmentalized βAR signaling without risking the negative sequelae of global increases in cAMP (172, 175, 185, 186). T-tubular localization of Cav-3 and β_2ARs places them in close apposition with the sarcoplasmic reticulum (SR), increasing the interaction of cAMP production and LTCC activation with ryanodine receptors in the SR, also enhancing cAMP degradation by localized phosphodiesterases (PDEs) and AC inhibition through $G_{\alpha i}$ signaling (187, 188). Redistribution of β_2ARs from Cav-3-rich domains results in a greater stimulatory effect on cAMP, generation of a diffuse cAMP pool, and loss of the protective aspects of β_2AR signaling (177, 186, 189). In summary, the compartments inhabited by β_2ARs and some β_1ARs tightly regulate the local concentraton of cAMP via multiple

components, including the following: ACs and cAMP-dependent signaling cascades they activate, the PDEs that hydrolyse cAMP, the protein phosphatases that reverse kinase-dependent activation of downstream signaling proteins, and the intrinsic residents and architects of these domains, caveolins, that scaffold and inhibit signal transduction molecules and create structures in the sarcolemmal membrane that bring all of these participants of signal transduction activity together (167, 185, 186). Therefore, the altered Cav-3 localization noted in aged animals and the potential changes in caveolar regulation of βAR pathway components may be important contributors to the decrease in βAR responses observed in the aged heart.

Cav3 is necessary and sufficient for the formation of caveolae in CMs (13, 190). Caveolins and caveolae have been extensively studied since their discovery by electron microscopy (158). In CMs, Cav3 forms caveolae at the sarcolemma and is prevalent within the t-tubules that are closely tied to domains of sarcoplasmic reticulum, an association that implicates Cav3 in the regulation of ion channels, nitric oxide synthases, and other regulators of cardiovascular function (191-193). Our laboratory and others have investigated the role of Cav3 in the heart. Our findings indicate that Cav3 expression is a control point of cardiovascular health and thus a target for therapeutic intervention (194-199). Therefore, our laboratory generated a CM-specific Cav3 overexpressing (Cav3 OE) mouse to investigate the impact of Cav3 on cardiovascular health and signaling of the heart.

As the heart ages, Cav3 expression is reduced and caveolae are less common at the sarcolemmal membrane. These changes have effects on βAR responses in the heart, since β_2ARs outside of caveolar/t-tubule domains increase cAMP levels and are

no longer controlled by caveolar regulatory processes, generating a β_1AR-like signal that loses protective aspects of β_2AR signaling (177, 186, 189). The possible relationship between aging-induced loss of Cavs and βAR dysregulation led us to ask whether increased Cav3 expression might prevent such effects in the heart by increased compartmentation of βAR signaling proteins **(Figure 1.8)**. Therefore, in the studies presented in this dissertation, I hypothesized that Cav3 overexpression (Cav3 OE) modifies βAR activity in CMs and sought to accomplish two major aims:

1. Determine whether Cav3 OE alters the βAR responsivity of the murine heart and if those changes alter the age-related loss of βAR responses in the heart.
2. Determine which mediators of the βAR signaling pathway are regulated by Cav3 OE and whether they depend upon increased localization or regulation by caveolar domains.

To accomplish these aims, I worked with the physiological responses to βAR stimulation that are lost in aging-related cardiac dysfunction. Thus, I investigated the role of Cav3 OE using pharmacological agents in the Langendorff isolated heart perfusion model, which enables observation and analysis of the contractile, relaxation, pressure development, and heart rate responses to stimulation. I also investigated the sequelae of βAR signaling in isolated adult myocytes, which provided findings regarding βAR-activated cAMP activity in Cav3 OE CMs and the mitochondrial respiration responses to βAR activation. My findings revealed a role for Cav3 OE in the regulation of the βAR response system in young and aged murine hearts (Chapter

2) and provided insight into the complex interactions between βARs, ACs, and Cav3 (Chapter 3).

Chapter 1, is, in part, a reprint of the material as it appears in American Journal of Physiology, Cell Physiology, in press, Busija, AR; Patel, HH; Insel, PA. The dissertation/thesis author was the primary author of this paper.

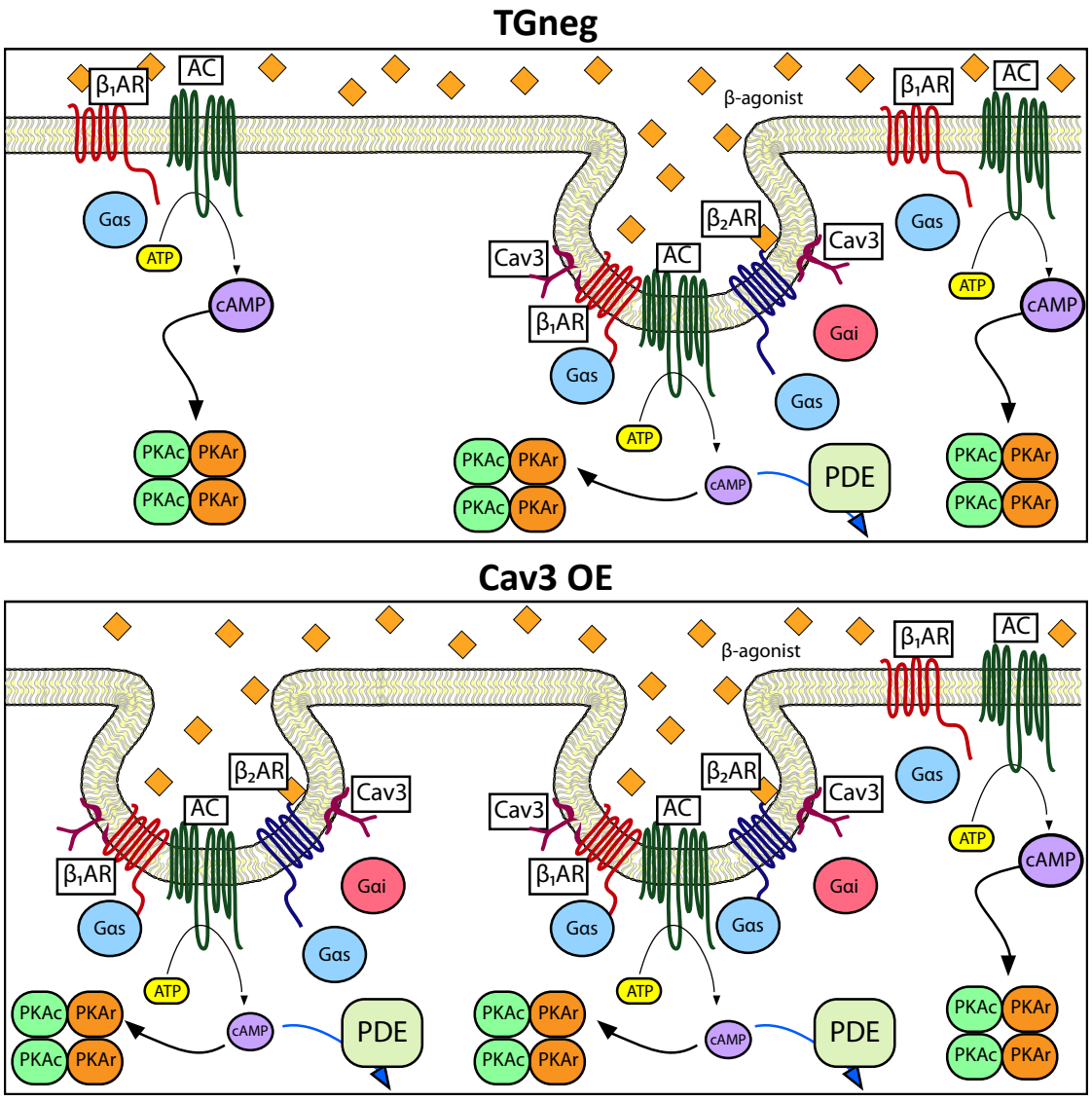

Figure 1.8: Schematic representation of (top) TGneg and (bottom) Cav3 OE sarcolemmal membranes. Due to the role of Cav3 in localization of βAR isoforms, Gα proteins, AC isoforms, PKA proteins, and PDE subtypes, I hypothesized that Cav3 OE hearts may demonstrate altered distribution of these key cAMP pathway proteins. Studies in this dissertation will address signaling through βARs, ACs, and PDEs to activate downstream physiological responses and cAMP signals.

Table 1.1: Examples of caveolae-associated signal transduction proteins. Adapted from (200).

Signal transduction protein	Mechanism(s) of association	References
Receptors		
G Protein-Coupled Receptors (GPCRs, e.g., adrenergic, adenosine, angiotensin-1, opioid, serotonin)	Transmembrane (TM), fatty acylation (FA), Cav association (Cav)	(109, 185, 201-203)
Steroid hormone acceptors (e.g., estrogen receptor α)	TM, FA, Cav	(204-206)
Transforming growth factor-β receptors (e.g., Bone Morphogenic Receptor II)	TM, Cav	(207)
Tyrosine kinase (e.g., insulin, EGFR, NGF, IGF, PDGF)	TM, FA, Cav	(208-210)
inositol 1,4,5-triphosphate receptor (IP3R)	TM, FA, Cav	(211, 212)
Ion channels, reporters, and exchangers		
Ca^{2+}-ATPase	TM, Cav	(211)
Ca^{2+} pumps (e.g. Na(+)-Ca(2+) exchanger type 1)	TM, Cav	(213)
L-type Ca^{2+}	TM, Cav	(213, 214)
Large-conductance Ca^{2+}-activated K^+	TM, Cav	(215)
Transient Receptor Potential Cation (TRPC)	TM, Cav	(216-219)
Na/K-ATPase	TM, Cav	(220, 221)
Voltage-gated K^+	TM, Cav	(193, 222, 223)
K_{ATP}	TM, Cav	(224)
Kinases		
Src-family	FA, Cav	(91, 92, 225-232)
Protein Kinase A	Cav	(224, 233-236)
Protein Kinase Cα, ζ	Cav	(237-239)
p42/p44 Mitogen Activated Protein Kinase	Cav	(240-242)
p38 Mitogen Activated Protein Kinase	Cav	(242)
Phosphatidylinositol-4,5-bisphosphate 3-kinase	$PI(4,5)P_2$ binding	(243, 244)
Protein kinase B	$PI(3,4,5)P_3$ binding	(243-251)
Other post-receptor components		
Heterotrimeric GTP binding (G) protein α subunits	FA, Cav	(64, 202, 203, 222, 226, 252-255)
Heterotrimeric GTP binding (G) protein βγ subunits	FA	(253)
Ras	FA, Cav	(135, 256, 257)
Adenylyl Cyclases (AC, e.g., AC3, 5, 6)	TM, Cav	(185, 202, 258-260)
Cyclic nucleotide phosphodiesterase (PDE3B)	Cav	(261)
Endothelial nitric oxide synthase (eNOS/NOS3)	Cav	(136, 235, 262-269)
Neuronal nitric oxide synthase (nNOS/NOS1)	Cav	(136, 263, 269-272)

Table 1.2: Examples of diseases associated with Cav or Cavin mutations

Disease	Clinical Features	Mutated protein	References
Bernardinelli-Seip Congenital Generalized Lipodystrophy types 3 (Cav1) and 4 (Cavin1)	Lack of adipose tissue, hypertriglyceridemia, insulin resistance, diabetes mellitus, hypertrophic cardiomyopathy, hepatic steatosis	Cav1, Cavin1	(144, 145)
Pulmonary arterial hypertension	Pulmonary vascular remodeling and proliferation, high pulmonary arterial blood pressure, right ventricular failure	Cav1	(146)
Limb-Girdle Muscular Dystrophy type 1C	Symmetric, progressive, proximal weakness of the limb girdle muscles, myoglobinuria, myotonia, elevated serum creatine kinase	Cav3	(148)
Rippling Muscle Disease	Mechanically-triggered contractions of skeletal muscle; subsequent electrically silent muscle contraction cascades	Cav3	(147)
Long QT Syndrome	Extended Q-T interval on electrocardiogram, arrhythmias, ventricular fibrillation	Cav3, Cavin1	(144)
Sudden Infant Death Syndrome	Sudden death of an infant unexplained by medical history or autopsy	Cav3	(150)
Hypertrophic or Dilated Cardiomyopathy	Thickened myocardium, non-ischemic cardiomyopathy, reduced cardiac function	Cav3, Cavin1, Cavin4	(144, 149) (150)
Cancer (implicated)	Breast, prostate, ovarian, and pancreatic	Cav1	(151-153)

REFERENCES

1. Pike LJ. Rafts defined: a report on the Keystone Symposium on Lipid Rafts and Cell Function. J Lipid Res. 2006;47(7):1597-8.

2. Parton RG, del Pozo MA. Caveolae as plasma membrane sensors, protectors and organizers. Nat Rev Mol Cell Biol. 2013;14(2):98-112.

3. Kovtun O, Tillu VA, Ariotti N, Parton RG, Collins BM. Cavin family proteins and the assembly of caveolae. Journal of cell science. 2015;128(7):1269-78.

4. Scherer PE, Lisanti MP, Baldini G, Sargiacomo M, Mastick CC, Lodish HF. Induction of caveolin during adipogenesis and association of GLUT4 with caveolin-rich vesicles. The Journal of cell biology. 1994;127(5):1233-43.

5. Norkin LC. Simian virus 40 infection via MHC class I molecules and caveolae. Immunol Rev. 1999;168:13-22.

6. Orlandi PA, Fishman PH. Filipin-dependent inhibition of cholera toxin: evidence for toxin internalization and activation through caveolae-like domains. J Cell Biol. 1998;141(4):905-15.

7. Minshall RD, Tiruppathi C, Vogel SM, Niles WD, Gilchrist A, Hamm HE, Malik AB. Endothelial cell-surface gp60 activates vesicle formation and trafficking via G(i)-coupled Src kinase signaling pathway. J Cell Biol. 2000;150(5):1057-70.

8. Ray S, Kassan A, Busija AR, Rangamani P, Patel HH. The plasma membrane as a capacitor for energy and metabolism. Am J Physiol Cell Physiol. 2016;310(3):C181-92.

9. Head BP, Patel HH, Insel PA. Interaction of membrane/lipid rafts with the cytoskeleton: impact on signaling and function: membrane/lipid rafts, mediators of cytoskeletal arrangement and cell signaling. Biochim Biophys Acta. 2014;1838(2):532-45.

10. Cheng JP, Nichols BJ. Caveolae: One Function or Many? Trends Cell Biol. 2016;26(3):177-89.

11. Schilling JM, Roth DM, Patel HH. Caveolins in cardioprotection - translatability and mechanisms. Br J Pharmacol. 2015;172(8):2114-25.

12. Li S, Galbiati F, Volonte D, Sargiacomo M, Engelman JA, Das K, Scherer PE, Lisanti MP. Mutational analysis of caveolin-induced vesicle formation. Expression of caveolin-1 recruits caveolin-2 to caveolae membranes. FEBS Lett. 1998;434(1-2):127-34.

13. Song KS, Scherer PE, Tang Z, Okamoto T, Li S, Chafel M, Chu C, Kohtz DS, Lisanti MP. Expression of caveolin-3 in skeletal, cardiac, and smooth muscle cells. Caveolin-3 is a component of the sarcolemma and co-fractionates with dystrophin and dystrophin-associated glycoproteins. J Biol Chem. 1996;271(25):15160-5.

14. Lavie Y, Fiucci G, Liscovitch M. Up-regulation of caveolae and caveolar constituents in multidrug-resistant cancer cells. J Biol Chem. 1998;273(49):32380-3.

15. Hill MM, Bastiani M, Luetterforst R, Kirkham M, Kirkham A, Nixon SJ, Walser P, Abankwa D, Oorschot VM, Martin S, Hancock JF, Parton RG. PTRF-Cavin, a conserved cytoplasmic protein required for caveola formation and function. Cell. 2008;132(1):113-24.

16. Tillu VA, Kovtun O, McMahon KA, Collins BM, Parton RG. A phosphoinositide-binding cluster in cavin1 acts as a molecular sensor for cavin1 degradation. Mol Biol Cell. 2015;26(20):3561-9.

17. Shi Y, Tan SH, Ng S, Zhou J, Yang ND, Koo GB, McMahon KA, Parton RG, Hill MM, Del Pozo MA, Kim YS, Shen HM. Critical role of CAV1/caveolin-1 in cell stress responses in human breast cancer cells via modulation of lysosomal function and autophagy. Autophagy. 2015;11(5):769-84.

18. Bastiani M, Liu L, Hill MM, Jedrychowski MP, Nixon SJ, Lo HP, Abankwa D, Luetterforst R, Fernandez-Rojo M, Breen MR, Gygi SP, Vinten J, Walser PJ, North KN, Hancock JF, Pilch PF, Parton RG. MURC/Cavin-4 and cavin family members form tissue-specific caveolar complexes. J Cell Biol. 2009;185(7):1259-73.

19. Root KT, Plucinsky SM, Glover KJ. Recent progress in the topology, structure, and oligomerization of caveolin: a building block of caveolae. Curr Top Membr. 2015;75:305-36.

20. Hayer A, Stoeber M, Bissig C, Helenius A. Biogenesis of caveolae: stepwise assembly of large caveolin and cavin complexes. Traffic. 2010;11(3):361-82.

21. Monier S, Parton RG, Vogel F, Behlke J, Henske A, Kurzchalia TV. VIP21-caveolin, a membrane protein constituent of the caveolar coat, oligomerizes in vivo and in vitro. Mol Biol Cell. 1995;6(7):911-27.

22. Scheiffele P, Verkade P, Fra AM, Virta H, Simons K, Ikonen E. Caveolin-1 and -2 in the exocytic pathway of MDCK cells. The Journal of cell biology. 1998;140(4):795-806.

23. Fernandez I, Ying Y, Albanesi J, Anderson RG. Mechanism of caveolin filament assembly. Proc Natl Acad Sci U S A. 2002;99(17):11193-8.

24. Sargiacomo M, Scherer PE, Tang Z, Kubler E, Song KS, Sanders MC, Lisanti MP. Oligomeric structure of caveolin: implications for caveolae membrane organization. Proc Natl Acad Sci U S A. 1995;92(20):9407-11.

25. Ludwig A, Howard G, Mendoza-Topaz C, Deerinck T, Mackey M, Sandin S, Ellisman MH, Nichols BJ. Molecular composition and ultrastructure of the caveolar coat complex. PLoS Biol. 2013;11(8):e1001640.

26. Machleidt T, Li WP, Liu P, Anderson RG. Multiple domains in caveolin-1 control its intracellular traffic. The Journal of cell biology. 2000;148(1):17-28.

27. Schlegel A, Lisanti MP. A molecular dissection of caveolin-1 membrane attachment and oligomerization. Two separate regions of the caveolin-1 C-terminal domain mediate membrane binding and oligomer/oligomer interactions in vivo. The Journal of biological chemistry. 2000;275(28):21605-17.

28. Mora R, Bonilha VL, Marmorstein A, Scherer PE, Brown D, Lisanti MP, Rodriguez-Boulan E. Caveolin-2 localizes to the golgi complex but

redistributes to plasma membrane, caveolae, and rafts when co-expressed with caveolin-1. The Journal of biological chemistry. 1999;274(36):25708-17.

29. Ostermeyer AG, Paci JM, Zeng Y, Lublin DM, Munro S, Brown DA. Accumulation of caveolin in the endoplasmic reticulum redirects the protein to lipid storage droplets. The Journal of cell biology. 2001;152(5):1071-8.

30. Hanson CA, Drake KR, Baird MA, Han B, Kraft LJ, Davidson MW, Kenworthy AK. Overexpression of caveolin-1 is sufficient to phenocopy the behavior of a disease-associated mutant. Traffic. 2013;14(6):663-77.

31. Han B, Tiwari A, Kenworthy AK. Tagging strategies strongly affect the fate of overexpressed caveolin-1. Traffic. 2015;16(4):417-38.

32. Pelkmans L, Zerial M. Kinase-regulated quantal assemblies and kiss-and-run recycling of caveolae. Nature. 2005;436(7047):128-33.

33. Walser PJ, Ariotti N, Howes M, Ferguson C, Webb R, Schwudke D, Leneva N, Cho KJ, Cooper L, Rae J, Floetenmeyer M, Oorschot VM, Skoglund U, Simons K, Hancock JF, Parton RG. Constitutive formation of caveolae in a bacterium. Cell. 2012;150(4):752-63.

34. Ariotti N, Rae J, Leneva N, Ferguson C, Loo D, Okano S, Hill MM, Walser P, Collins BM, Parton RG. Molecular Characterization of Caveolin-induced Membrane Curvature. The Journal of biological chemistry. 2015;290(41):24875-90.

35. Epand RM, Sayer BG, Epand RF. Caveolin scaffolding region and cholesterol-rich domains in membranes. J Mol Biol. 2005;345(2):339-50.

36. Ren X, Ostermeyer AG, Ramcharan LT, Zeng Y, Lublin DM, Brown DA. Conformational defects slow Golgi exit, block oligomerization, and reduce raft affinity of caveolin-1 mutant proteins. Mol Biol Cell. 2004;15(10):4556-67.

37. Godi A, Di Campli A, Konstantakopoulos A, Di Tullio G, Alessi DR, Kular GS, Daniele T, Marra P, Lucocq JM, De Matteis MA. FAPPs control Golgi-to-cell-surface membrane traffic by binding to ARF and PtdIns(4)P. Nat Cell Biol. 2004;6(5):393-404.

38. Vieira OV, Verkade P, Manninen A, Simons K. FAPP2 is involved in the transport of apical cargo in polarized MDCK cells. J Cell Biol. 2005;170(4):521-6.

39. Sotgia F, Razani B, Bonuccelli G, Schubert W, Battista M, Lee H, Capozza F, Schubert AL, Minetti C, Buckley JT, Lisanti MP. Intracellular retention of glycosylphosphatidyl inositol-linked proteins in caveolin-deficient cells. Mol Cell Biol. 2002;22(11):3905-26.

40. Dunphy JT, Greentree WK, Manahan CL, Linder ME. G-protein palmitoyltransferase activity is enriched in plasma membranes. J Biol Chem. 1996;271(12):7154-9.

41. Das AK, Dasgupta B, Bhattacharya R, Basu J. Purification and biochemical characterization of a protein-palmitoyl acyltransferase from human erythrocytes. J Biol Chem. 1997;272(17):11021-5.

42. Parat MO, Fox PL. Palmitoylation of caveolin-1 in endothelial cells is post-translational but irreversible. J Biol Chem. 2001;276(19):15776-82.

43. Baker TL, Booden MA, Buss JE. S-Nitrosocysteine increases palmitate turnover on Ha-Ras in NIH 3T3 cells. J Biol Chem. 2000;275(29):22037-47.

44. Monier S, Dietzen DJ, Hastings WR, Lublin DM, Kurzchalia TV. Oligomerization of VIP21-caveolin in vitro is stabilized by long chain fatty acylation or cholesterol. FEBS Lett. 1996;388(2-3):143-9.

45. Parat MO, Stachowicz RZ, Fox PL. Oxidative stress inhibits caveolin-1 palmitoylation and trafficking in endothelial cells. Biochem J. 2002;361(Pt 3):681-8.

46. Rothberg KG, Heuser JE, Donzell WC, Ying YS, Glenney JR, Anderson RG. Caveolin, a protein component of caveolae membrane coats. Cell. 1992;68(4):673-82.

47. Ludwig A, Nichols BJ, Sandin S. Architecture of the caveolar coat complex. J Cell Sci. 2016;129(16):3077-83.

48. Kovtun O, Tillu VA, Jung W, Leneva N, Ariotti N, Chaudhary N, Mandyam RA, Ferguson C, Morgan GP, Johnston WA, Harrop SJ, Alexandrov K, Parton RG, Collins BM. Structural insights into the organization of the cavin membrane coat complex. Dev Cell. 2014;31(4):405-19.

49. Gambin Y, Ariotti N, McMahon KA, Bastiani M, Sierecki E, Kovtun O, Polinkovsky ME, Magenau A, Jung W, Okano S, Zhou Y, Leneva N, Mureev S, Johnston W, Gaus K, Hancock JF, Collins BM, Alexandrov K, Parton RG. Single-molecule analysis reveals self assembly and nanoscale segregation of two distinct cavin subcomplexes on caveolae. Elife. 2013;3:e01434.

50. Mohan J, Moren B, Larsson E, Holst MR, Lundmark R. Cavin3 interacts with cavin1 and caveolin1 to increase surface dynamics of caveolae. J Cell Sci. 2015;128(5):979-91.

51. Wanaski SP, Ng BK, Glaser M. Caveolin scaffolding region and the membrane binding region of SRC form lateral membrane domains. Biochemistry. 2003;42(1):42-56.

52. Pike LJ, Casey L. Localization and turnover of phosphatidylinositol 4,5-bisphosphate in caveolin-enriched membrane domains. J Biol Chem. 1996;271(43):26453-6.

53. Fairn GD, Schieber NL, Ariotti N, Murphy S, Kuerschner L, Webb RI, Grinstein S, Parton RG. High-resolution mapping reveals topologically distinct cellular pools of phosphatidylserine. J Cell Biol. 2011;194(2):257-75.

54. Hansen CG, Bright NA, Howard G, Nichols BJ. SDPR induces membrane curvature and functions in the formation of caveolae. Nat Cell Biol. 2009;11(7):807-14.

55. Naito D, Ogata T, Hamaoka T, Nakanishi N, Miyagawa K, Maruyama N, Kasahara T, Taniguchi T, Nishi M, Matoba S, Ueyama T. The coiled-coil domain of MURC/cavin-4 is involved in membrane trafficking of caveolin-3 in cardiomyocytes. Am J Physiol Heart Circ Physiol. 2015;309(12):H2127-36.

56. Wei Z, Zou X, Wang H, Lei J, Wu Y, Liao K. The N-terminal leucine-zipper motif in PTRF/cavin-1 is essential and sufficient for its caveolae-association. Biochem Biophys Res Commun. 2015;456(3):750-6.

57. Verma P, Ostermeyer-Fay AG, Brown DA. Caveolin-1 induces formation of membrane tubules that sense actomyosin tension and are inhibited by polymerase I and transcript release factor/cavin-1. Mol Biol Cell. 2010;21(13):2226-40.

58. Rui H, Root KT, Lee J, Glover KJ, Im W. Probing the U-shaped conformation of caveolin-1 in a bilayer. Biophys J. 2014;106(6):1371-80.

59. Furse S, Brooks NJ, Seddon AM, Woscholski R, Templer RH, Tate EW, Gaffney PRJ, Ces O. Lipid membrane curvature induced by distearoyl phosphatidylinositol 4-phosphate. Soft Matter. 2012;8(11):3090-3.

60. Furse S, Brooks NJ, Woscholski R, Gaffney PRJ, Templer RH. Pressure-dependent inverse bicontinuous cubic phase formation in a phosphatidylinositol 4-phosphate/phosphatidylcholine system. Chemical Data Collections. 2016;3–4:15-20.

61. Thomsen P, Roepstorff K, Stahlhut M, van Deurs B. Caveolae are highly immobile plasma membrane microdomains, which are not involved in constitutive endocytic trafficking. Mol Biol Cell. 2002;13(1):238-50.

62. Tagawa A, Mezzacasa A, Hayer A, Longatti A, Pelkmans L, Helenius A. Assembly and trafficking of caveolar domains in the cell: caveolae as stable, cargo-triggered, vesicular transporters. J Cell Biol. 2005;170(5):769-79.

63. Wedegaertner PB, Bourne HR. Activation and depalmitoylation of Gs alpha. Cell. 1994;77(7):1063-70.

64. Li S, Okamoto T, Chun M, Sargiacomo M, Casanova JE, Hansen SH, Nishimoto I, Lisanti MP. Evidence for a regulated interaction between heterotrimeric G proteins and caveolin. The Journal of biological chemistry. 1995;270(26):15693-701.

65. Jones TL, Degtyarev MY, Backlund PS, Jr. The stoichiometry of G alpha(s) palmitoylation in its basal and activated states. Biochemistry. 1997;36(23):7185-91.

66. Mumby SM, Kleuss C, Gilman AG. Receptor regulation of G-protein palmitoylation. Proc Natl Acad Sci U S A. 1994;91(7):2800-4.

67. Lim JS, Nguyen KC, Han JM, Jang IS, Fabian C, Cho KA. Direct Regulation of TLR5 Expression by Caveolin-1. Mol Cells. 2015;38(12):1111-7.

68. Hayer A, Stoeber M, Ritz D, Engel S, Meyer HH, Helenius A. Caveolin-1 is ubiquitinated and targeted to intralumenal vesicles in endolysosomes for degradation. J Cell Biol. 2010;191(3):615-29.

69. Conrad PA, Smart EJ, Ying YS, Anderson RG, Bloom GS. Caveolin cycles between plasma membrane caveolae and the Golgi complex by microtubule-dependent and microtubule-independent steps. J Cell Biol. 1995;131(6 Pt 1):1421-33.

70. Forbes A, Wadehra M, Mareninov S, Morales S, Shimazaki K, Gordon LK, Braun J. The tetraspan protein EMP2 regulates expression of caveolin-1. J Biol Chem. 2007;282(36):26542-51.

71. Hung MJ, Cherng WJ, Hung MY, Wu HT, Pang JH. Interleukin-6 inhibits endothelial nitric oxide synthase activation and increases endothelial nitric oxide synthase binding to stabilized caveolin-1 in human vascular endothelial cells. J Hypertens. 2010;28(5):940-51.

72. Galbiati F, Volonte D, Minetti C, Chu JB, Lisanti MP. Phenotypic behavior of caveolin-3 mutations that cause autosomal dominant limb girdle muscular dystrophy (LGMD-1C). Retention of LGMD-1C caveolin-3 mutants within the golgi complex. J Biol Chem. 1999;274(36):25632-41.

73. Sotgia F, Woodman SE, Bonuccelli G, Capozza F, Minetti C, Scherer PE, Lisanti MP. Phenotypic behavior of caveolin-3 R26Q, a mutant associated with hyperCKemia, distal myopathy, and rippling muscle disease. Am J Physiol Cell Physiol. 2003;285(5):C1150-60.

74. Galbiati F, Volonte D, Minetti C, Bregman DB, Lisanti MP. Limb-girdle muscular dystrophy (LGMD-1C) mutants of caveolin-3 undergo ubiquitination and proteasomal degradation. Treatment with proteasomal inhibitors blocks the dominant negative effect of LGMD-1C mutanta and rescues wild-type caveolin-3. The Journal of biological chemistry. 2000;275(48):37702-11.

75. Cao H, Orth JD, Chen J, Weller SG, Heuser JE, McNiven MA. Cortactin is a component of clathrin-coated pits and participates in receptor-mediated endocytosis. Mol Cell Biol. 2003;23(6):2162-70.

76. Sverdlov M, Shinin V, Place AT, Castellon M, Minshall RD. Filamin A regulates caveolae internalization and trafficking in endothelial cells. Mol Biol Cell. 2009;20(21):4531-40.

77. Mundy DI, Machleidt T, Ying YS, Anderson RG, Bloom GS. Dual control of caveolar membrane traffic by microtubules and the actin cytoskeleton. J Cell Sci. 2002;115(Pt 22):4327-39.

78. Ahn S, Maudsley S, Luttrell LM, Lefkowitz RJ, Daaka Y. Src-mediated tyrosine phosphorylation of dynamin is required for beta2-adrenergic receptor internalization and mitogen-activated protein kinase signaling. J Biol Chem. 1999;274(3):1185-8.

79. Bakhshi FR, Mao M, Shajahan AN, Piegeler T, Chen Z, Chernaya O, Sharma T, Elliott WM, Szulcek R, Bogaard HJ, Comhair S, Erzurum S, van Nieuw Amerongen GP, Bonini MG, Minshall RD. Nitrosation-dependent caveolin 1 phosphorylation, ubiquitination, and degradation and its association with idiopathic pulmonary arterial hypertension. Pulm Circ. 2013;3(4):816-30.

80. Kirchner P, Bug M, Meyer H. Ubiquitination of the N-terminal region of caveolin-1 regulates endosomal sorting by the VCP/p97 AAA-ATPase. J Biol Chem. 2013;288(10):7363-72.

81. Sinha B, Koster D, Ruez R, Gonnord P, Bastiani M, Abankwa D, Stan RV, Butler-Browne G, Vedie B, Johannes L, Morone N, Parton RG, Raposo G, Sens P, Lamaze C, Nassoy P. Cells respond to mechanical stress by rapid disassembly of caveolae. Cell. 2011;144(3):402-13.

82. Lo HP, Nixon SJ, Hall TE, Cowling BS, Ferguson C, Morgan GP, Schieber NL, Fernandez-Rojo MA, Bastiani M, Floetenmeyer M, Martel N, Laporte J, Pilch PF, Parton RG. The caveolin-cavin system plays a conserved and critical role in mechanoprotection of skeletal muscle. The Journal of cell biology. 2015;210(5):833-49.

83. Parton RG, Joggerst B, Simons K. Regulated internalization of caveolae. J Cell Biol. 1994;127(5):1199-215.

84. John TA, Vogel SM, Tiruppathi C, Malik AB, Minshall RD. Quantitative analysis of albumin uptake and transport in the rat microvessel endothelial monolayer. Am J Physiol Lung Cell Mol Physiol. 2003;284(1):L187-96.

85. Predescu SA, Predescu DN, Timblin BK, Stan RV, Malik AB. Intersectin regulates fission and internalization of caveolae in endothelial cells. Mol Biol Cell. 2003;14(12):4997-5010.

86. Tiruppathi C, Song W, Bergenfeldt M, Sass P, Malik AB. Gp60 activation mediates albumin transcytosis in endothelial cells by tyrosine kinase-dependent pathway. J Biol Chem. 1997;272(41):25968-75.

87. Pelkmans L, Puntener D, Helenius A. Local actin polymerization and dynamin recruitment in SV40-induced internalization of caveolae. Science. 2002;296(5567):535-9.

88. Singh RD, Puri V, Valiyaveettil JT, Marks DL, Bittman R, Pagano RE. Selective caveolin-1-dependent endocytosis of glycosphingolipids. Mol Biol Cell. 2003;14(8):3254-65.

89. Wang H, Wang AX, Aylor K, Barrett EJ. Caveolin-1 phosphorylation regulates vascular endothelial insulin uptake and is impaired by insulin resistance in rats. Diabetologia. 2015;58(6):1344-53.

90. Sun Y, Hu G, Zhang X, Minshall RD. Phosphorylation of caveolin-1 regulates oxidant-induced pulmonary vascular permeability via paracellular and transcellular pathways. Circ Res. 2009;105(7):676-85, 15 p following 85.

91. Li S, Seitz R, Lisanti MP. Phosphorylation of caveolin by src tyrosine kinases. The alpha-isoform of caveolin is selectively phosphorylated by v-Src in vivo. The Journal of biological chemistry. 1996;271(7):3863-8.

92. Lee H, Woodman SE, Engelman JA, Volonte D, Galbiati F, Kaufman HL, Lublin DM, Lisanti MP. Palmitoylation of caveolin-1 at a single site (Cys-156) controls its coupling to the c-Src tyrosine kinase: targeting of dually acylated

molecules (GPI-linked, transmembrane, or cytoplasmic) to caveolae effectively uncouples c-Src and caveolin-1 (TYR-14). The Journal of biological chemistry. 2001;276(37):35150-8.

93. Gottlieb-Abraham E, Shvartsman DE, Donaldson JC, Ehrlich M, Gutman O, Martin GS, Henis YI. Src-mediated caveolin-1 phosphorylation affects the targeting of active Src to specific membrane sites. Mol Biol Cell. 2013;24(24):3881-95.

94. McNiven MA, Kim L, Krueger EW, Orth JD, Cao H, Wong TW. Regulated interactions between dynamin and the actin-binding protein cortactin modulate cell shape. J Cell Biol. 2000;151(1):187-98.

95. Krueger EW, Orth JD, Cao H, McNiven MA. A dynamin-cortactin-Arp2/3 complex mediates actin reorganization in growth factor-stimulated cells. Mol Biol Cell. 2003;14(3):1085-96.

96. Cao H, Courchesne WE, Mastick CC. A phosphotyrosine-dependent protein interaction screen reveals a role for phosphorylation of caveolin-1 on tyrosine 14: recruitment of C-terminal Src kinase. J Biol Chem. 2002;277(11):8771-4.

97. Rozelle AL, Machesky LM, Yamamoto M, Driessens MH, Insall RH, Roth MG, Luby-Phelps K, Marriott G, Hall A, Yin HL. Phosphatidylinositol 4,5-bisphosphate induces actin-based movement of raft-enriched vesicles through WASP-Arp2/3. Curr Biol. 2000;10(6):311-20.

98. Jo A, Park H, Lee SH, Ahn SH, Kim HJ, Park EM, Choi YH. SHP-2 binds to caveolin-1 and regulates Src activity via competitive inhibition of CSK in response to H2O2 in astrocytes. PLoS One. 2014;9(3):e91582.

99. Ren Y, Meng S, Mei L, Zhao ZJ, Jove R, Wu J. Roles of Gab1 and SHP2 in paxillin tyrosine dephosphorylation and Src activation in response to epidermal growth factor. J Biol Chem. 2004;279(9):8497-505.

100. Zimnicka AM, Husain YS, Shajahan AN, Sverdlov M, Chaga O, Chen Z, Toth PT, Klomp J, Karginov AV, Tiruppathi C, Malik AB, Minshall RD. Src-dependent phosphorylation of caveolin-1 Tyr-14 promotes swelling and release of caveolae. Mol Biol Cell. 2016;27(13):2090-106.

101. Vega-Moreno J, Tirado-Cortes A, Alvarez R, Irles C, Mas-Oliva J, Ortega A. Cholesterol depletion uncouples beta-dystroglycans from discrete sarcolemmal domains, reducing the mechanical activity of skeletal muscle. Cell Physiol Biochem. 2012;29(5-6):905-18.

102. Kozera L, White E, Calaghan S. Caveolae act as membrane reserves which limit mechanosensitive I(Cl,swell) channel activation during swelling in the rat ventricular myocyte. PLoS One. 2009;4(12):e8312.

103. Boyd NL, Park H, Yi H, Boo YC, Sorescu GP, Sykes M, Jo H. Chronic shear induces caveolae formation and alters ERK and Akt responses in endothelial cells. Am J Physiol Heart Circ Physiol. 2003;285(3):H1113-22.

104. Park H, Go YM, St John PL, Maland MC, Lisanti MP, Abrahamson DR, Jo H. Plasma membrane cholesterol is a key molecule in shear stress-dependent activation of extracellular signal-regulated kinase. J Biol Chem. 1998;273(48):32304-11.

105. Yang B, Rizzo V. Shear Stress Activates eNOS at the Endothelial Apical Surface Through beta1 Containing Integrins and Caveolae. Cell Mol Bioeng. 2013;6(3):346-54.

106. Mundy DI, Li WP, Luby-Phelps K, Anderson RG. Caveolin targeting to late endosome/lysosomal membranes is induced by perturbations of lysosomal pH and cholesterol content. Mol Biol Cell. 2012;23(5):864-80.

107. Ritz D, Vuk M, Kirchner P, Bug M, Schutz S, Hayer A, Bremer S, Lusk C, Baloh RH, Lee H, Glatter T, Gstaiger M, Aebersold R, Weihl CC, Meyer H. Endolysosomal sorting of ubiquitylated caveolin-1 is regulated by VCP and UBXD1 and impaired by VCP disease mutations. Nat Cell Biol. 2011;13(9):1116-23.

108. Burana D, Yoshihara H, Tanno H, Yamamoto A, Saeki Y, Tanaka K, Komada M. The Ankrd13 Family of Ubiquitin-interacting Motif-bearing Proteins Regulates Valosin-containing Protein/p97 Protein-mediated Lysosomal Trafficking of Caveolin 1. J Biol Chem. 2016;291(12):6218-31.

109. Fuhs SR, Insel PA. Caveolin-3 undergoes SUMOylation by the SUMO E3 ligase PIASy: sumoylation affects G-protein-coupled receptor desensitization. The Journal of biological chemistry. 2011;286(17):14830-41.

110. Ramanathan HN, Ye Y. The p97 ATPase associates with EEA1 to regulate the size of early endosomes. Cell Res. 2012;22(2):346-59.

111. Buchberger A, Schindelin H, Hanzelmann P. Control of p97 function by cofactor binding. FEBS Lett. 2015;589(19 Pt A):2578-89.

112. Rouiller I, Butel VM, Latterich M, Milligan RA, Wilson-Kubalek EM. A major conformational change in p97 AAA ATPase upon ATP binding. Mol Cell. 2000;6(6):1485-90.

113. Davies JM, Tsuruta H, May AP, Weis WI. Conformational changes of p97 during nucleotide hydrolysis determined by small-angle X-Ray scattering. Structure. 2005;13(2):183-95.

114. Ye Y, Meyer HH, Rapoport TA. Function of the p97-Ufd1-Npl4 complex in retrotranslocation from the ER to the cytosol: dual recognition of nonubiquitinated polypeptide segments and polyubiquitin chains. J Cell Biol. 2003;162(1):71-84.

115. Dai RM, Li CC. Valosin-containing protein is a multi-ubiquitin chain-targeting factor required in ubiquitin-proteasome degradation. Nat Cell Biol. 2001;3(8):740-4.

116. Ye Y, Shibata Y, Kikkert M, van Voorden S, Wiertz E, Rapoport TA. Recruitment of the p97 ATPase and ubiquitin ligases to the site of retrotranslocation at the endoplasmic reticulum membrane. Proc Natl Acad Sci U S A. 2005;102(40):14132-8.

117. Lee J, Glover KJ. The transmembrane domain of caveolin-1 exhibits a helix-break-helix structure. Biochim Biophys Acta. 2012.

118. van Meer G, Voelker DR, Feigenson GW. Membrane lipids: where they are and how they behave. Nat Rev Mol Cell Biol. 2008;9(2):112-24.

119. Maxfield FR, Mondal M. Sterol and lipid trafficking in mammalian cells. Biochem Soc Trans. 2006;34(Pt 3):335-9.

120. Pike LJ, Han X, Chung KN, Gross RW. Lipid rafts are enriched in arachidonic acid and plasmenylethanolamine and their composition is independent of caveolin-1 expression: a quantitative electrospray ionization/mass spectrometric analysis. Biochemistry. 2002;41(6):2075-88.

121. Atshaves BP, Gallegos AM, McIntosh AL, Kier AB, Schroeder F. Sterol carrier protein-2 selectively alters lipid composition and cholesterol dynamics of caveolae/lipid raft vs nonraft domains in L-cell fibroblast plasma membranes. Biochemistry. 2003;42(49):14583-98.

122. Pike LJ. Lipid rafts: bringing order to chaos. J Lipid Res. 2003;44(4):655-67.

123. Fernandez-Hernando C, Yu J, Davalos A, Prendergast J, Sessa WC. Endothelial-specific overexpression of caveolin-1 accelerates atherosclerosis in apolipoprotein E-deficient mice. The American journal of pathology. 2010;177(2):998-1003.

124. Shigematsu T, Koshiyama K, Wada S. Molecular dynamics simulations of pore formation in stretched phospholipid/cholesterol bilayers. Chem Phys Lipids. 2014;183:43-9.

125. Rog T, Murzyn K, Karttunen M, Pasenkiewicz-Gierula M. Nonpolar interactions between trans-membrane helical EGF peptide and phosphatidylcholines, sphingomyelins and cholesterol. Molecular dynamics simulation studies. J Pept Sci. 2008;14(4):374-82.

126. Pike LJ. The challenge of lipid rafts. J Lipid Res. 2009;50 Suppl:S323-8.

127. Jansen M, Pietiainen VM, Polonen H, Rasilainen L, Koivusalo M, Ruotsalainen U, Jokitalo E, Ikonen E. Cholesterol substitution increases the structural heterogeneity of caveolae. The Journal of biological chemistry. 2008;283(21):14610-8.

128. Kim JH, Peng D, Schlebach JP, Hadziselimovic A, Sanders CR. Modest effects of lipid modifications on the structure of caveolin-3. Biochemistry. 2014;53(27):4320-2.

129. Prasanna X, Sengupta D, Chattopadhyay A. Cholesterol-dependent Conformational Plasticity in GPCR Dimers. Sci Rep. 2016;6:31858.

130. Mancia F, Assur Z, Herman AG, Siegel R, Hendrickson WA. Ligand sensitivity in dimeric associations of the serotonin 5HT2c receptor. EMBO Rep. 2008;9(4):363-9.

131. Laganowsky A, Reading E, Allison TM, Ulmschneider MB, Degiacomi MT, Baldwin AJ, Robinson CV. Membrane proteins bind lipids selectively to modulate their structure and function. Nature. 2014;510(7503):172-5.

132. Dawaliby R, Trubbia C, Delporte C, Masureel M, Van Antwerpen P, Kobilka BK, Govaerts C. Allosteric regulation of G protein-coupled receptor activity by phospholipids. Nat Chem Biol. 2016;12(1):35-9.

133. Zocher M, Zhang C, Rasmussen SG, Kobilka BK, Muller DJ. Cholesterol increases kinetic, energetic, and mechanical stability of the human beta2-adrenergic receptor. Proc Natl Acad Sci U S A. 2012;109(50):E3463-72.

134. Goodman OB, Jr., Krupnick JG, Santini F, Gurevich VV, Penn RB, Gagnon AW, Keen JH, Benovic JL. Beta-arrestin acts as a clathrin adaptor in endocytosis of the beta2-adrenergic receptor. Nature. 1996;383(6599):447-50.

135. Song KS, Li S, Okamoto T, Quilliam LA, Sargiacomo M, Lisanti MP. Co-purification and direct interaction of Ras with caveolin, an integral membrane protein of caveolae microdomains. Detergent-free purification of caveolae microdomains. J Biol Chem. 1996;271(16):9690-7.

136. Garcia-Cardena G, Martasek P, Masters BS, Skidd PM, Couet J, Li S, Lisanti MP, Sessa WC. Dissecting the interaction between nitric oxide synthase (NOS) and caveolin. Functional significance of the nos caveolin binding domain in vivo. The Journal of biological chemistry. 1997;272(41):25437-40.

137. Michel JB, Feron O, Sacks D, Michel T. Reciprocal regulation of endothelial nitric-oxide synthase by Ca2+-calmodulin and caveolin. J Biol Chem. 1997;272(25):15583-6.

138. Banquet S, Delannoy E, Agouni A, Dessy C, Lacomme S, Hubert F, Richard V, Muller B, Leblais V. Role of G(i/o)-Src kinase-PI3K/Akt pathway and caveolin-1 in beta(2)-adrenoceptor coupling to endothelial NO synthase in mouse pulmonary artery. Cell Signal. 2011;23(7):1136-43.

139. Frank PG, Marcel YL, Connelly MA, Lublin DM, Franklin V, Williams DL, Lisanti MP. Stabilization of caveolin-1 by cellular cholesterol and scavenger receptor class B type I. Biochemistry. 2002;41(39):11931-40.

140. van't Hof W, Resh MD. Targeting proteins to plasma membrane and membrane microdomains by N-terminal myristoylation and palmitoylation. Methods Enzymol. 2000;327:317-30.

141. Galbiati F, Volonte D, Meani D, Milligan G, Lublin DM, Lisanti MP, Parenti M. The dually acylated NH2-terminal domain of gi1alpha is sufficient to target a green fluorescent protein reporter to caveolin-enriched plasma membrane domains. Palmitoylation of caveolin-1 is required for the recognition of dually acylated g-protein alpha subunits in vivo. J Biol Chem. 1999;274(9):5843-50.

142. Morales J, Fishburn CS, Wilson PT, Bourne HR. Plasma membrane localization of G alpha z requires two signals. Mol Biol Cell. 1998;9(1):1-14.

143. Baran J, Mundy DI, Vasanji A, Parat MO. Altered localization of H-Ras in caveolin-1-null cells is palmitoylation-independent. J Cell Commun Signal. 2007;1(3-4):195-204.

144. Rajab A, Straub V, McCann LJ, Seelow D, Varon R, Barresi R, Schulze A, Lucke B, Lutzkendorf S, Karbasiyan M, Bachmann S, Spuler S, Schuelke M. Fatal cardiac arrhythmia and long-QT syndrome in a new form of congenital generalized lipodystrophy with muscle rippling (CGL4) due to PTRF-CAVIN mutations. PLoS Genet. 2010;6(3):e1000874.

145. Cao H, Alston L, Ruschman J, Hegele RA. Heterozygous CAV1 frameshift mutations (MIM 601047) in patients with atypical partial lipodystrophy and hypertriglyceridemia. Lipids Health Dis. 2008;7:3.

146. Austin ED, Ma L, LeDuc C, Berman Rosenzweig E, Borczuk A, Phillips JA, 3rd, Palomero T, Sumazin P, Kim HR, Talati MH, West J, Loyd JE, Chung WK. Whole exome sequencing to identify a novel gene (caveolin-1) associated with human pulmonary arterial hypertension. Circulation Cardiovascular genetics. 2012;5(3):336-43.

147. Kubisch C, Schoser BG, von During M, Betz RC, Goebel HH, Zahn S, Ehrbrecht A, Aasly J, Schroers A, Popovic N, Lochmuller H, Schroder JM, Bruning T, Malin JP, Fricke B, Meinck HM, Torbergsen T, Engels H, Voss B, Vorgerd M. Homozygous mutations in caveolin-3 cause a severe form of rippling muscle disease. Annals of neurology. 2003;53(4):512-20.

148. Minetti C, Sotgia F, Bruno C, Scartezzini P, Broda P, Bado M, Masetti E, Mazzocco M, Egeo A, Donati MA, Volonte D, Galbiati F, Cordone G, Bricarelli FD, Lisanti MP, Zara F. Mutations in the caveolin-3 gene cause autosomal dominant limb-girdle muscular dystrophy. Nat Genet. 1998;18(4):365-8.

149. Rodriguez G, Ueyama T, Ogata T, Czernuszewicz G, Tan Y, Dorn GW, 2nd, Bogaev R, Amano K, Oh H, Matsubara H, Willerson JT, Marian AJ. Molecular genetic and functional characterization implicate muscle-restricted coiled-coil gene (MURC) as a causal gene for familial dilated cardiomyopathy. Circ Cardiovasc Genet. 2011;4(4):349-58.

150. Lariccia V, Nasti AA, Alessandrini F, Pesaresi M, Gratteri S, Tagliabracci A, Amoroso S. Identification and functional analysis of a new putative caveolin-3 variant found in a patient with sudden unexplained death. J Biomed Sci. 2014;21(1):58.

151. Li T, Sotgia F, Vuolo MA, Li M, Yang WC, Pestell RG, Sparano JA, Lisanti MP. Caveolin-1 mutations in human breast cancer: functional association with estrogen receptor alpha-positive status. Am J Pathol. 2006;168(6):1998-2013.

152. Patani N, Lambros MB, Natrajan R, Dedes KJ, Geyer FC, Ward E, Martin LA, Dowsett M, Reis-Filho JS. Non-existence of caveolin-1 gene mutations in human breast cancer. Breast Cancer Res Treat. 2012;131(1):307-10.

153. Han SE, Park KH, Lee G, Huh YJ, Min BM. Mutation and aberrant expression of Caveolin-1 in human oral squamous cell carcinomas and oral cancer cell lines. Int J Oncol. 2004;24(2):435-40.

154. Schlegel A, Arvan P, Lisanti MP. Caveolin-1 binding to endoplasmic reticulum membranes and entry into the regulated secretory pathway are regulated by serine phosphorylation. Protein sorting at the level of the endoplasmic reticulum. The Journal of biological chemistry. 2001;276(6):4398-408.

155. Woodman SE, Schlegel A, Cohen AW, Lisanti MP. Mutational analysis identifies a short atypical membrane attachment sequence (KYWFYR) within caveolin-1. Biochemistry. 2002;41(11):3790-5.

156. Song KS, Tang Z, Li S, Lisanti MP. Mutational analysis of the properties of caveolin-1. A novel role for the C-terminal domain in mediating homo-typic caveolin-caveolin interactions. The Journal of biological chemistry. 1997;272(7):4398-403.

157. Aoki S, Thomas A, Decaffmeyer M, Brasseur R, Epand RM. The role of proline in the membrane re-entrant helix of caveolin-1. J Biol Chem. 2010;285(43):33371-80.

158. Palade GE. Fine structure of blood capillaries. Journal of Applied Physics. 1953;24:1424.

159. Lakatta EG, Sollott SJ. The "heartbreak" of older age. Mol Interv. 2002;2(7):431-46.

160. Heron M. Deaths: Leading Causes for 2014. Natl Vital Stat Rep. 2016;65(5):1-96.

161. Boersma E, Pieper KS, Steyerberg EW, Wilcox RG, Chang WC, Lee KL, Akkerhuis KM, Harrington RA, Deckers JW, Armstrong PW, Lincoff AM, Califf RM, Topol EJ, Simoons ML. Predictors of outcome in patients with acute coronary syndromes without persistent ST-segment elevation. Results from an international trial of 9461 patients. The PURSUIT Investigators. Circulation. 2000;101(22):2557-67.

162. Fleg JL, Strait J. Age-associated changes in cardiovascular structure and function: a fertile milieu for future disease. Heart Fail Rev. 2012;17(4-5):545-54.

163. Bristow MR, Ginsburg R, Minobe W, Cubicciotti RS, Sageman WS, Lurie K, Billingham ME, Harrison DC, Stinson EB. Decreased catecholamine sensitivity and beta-adrenergic-receptor density in failing human hearts. N Engl J Med. 1982;307(4):205-11.

164. Bristow MR. Mechanism of action of beta-blocking agents in heart failure. Am J Cardiol. 1997;80(11A):26L-40L.

165. Eschenhagen T. Beta-adrenergic signaling in heart failure-adapt or die. Nat Med. 2008;14(5):485-7.

166. Kawabe JI, Grant BS, Yamamoto M, Schwencke C, Okumura S, Ishikawa Y. Changes in caveolin subtype protein expression in aging rat organs. Mol Cell Endocrinol. 2001;176(1-2):91-5.

167. Ratajczak P, Damy T, Heymes C, Oliviero P, Marotte F, Robidel E, Sercombe R, Boczkowski J, Rappaport L, Samuel JL. Caveolin-1 and -3 dissociations from caveolae to cytosol in the heart during aging and after myocardial infarction in rat. Cardiovasc Res. 2003;57(2):358-69.

168. Xiang Y, Rybin VO, Steinberg SF, Kobilka B. Caveolar localization dictates physiologic signaling of beta 2-adrenoceptors in neonatal cardiac myocytes. J Biol Chem. 2002;277(37):34280-6.

169. White M, Yanowitz F, Gilbert EM, Larrabee P, O'Connell JB, Anderson JL, Renlund D, Mealey P, Abraham WT, Bristow MR. Role of beta-adrenergic receptor downregulation in the peak exercise response in patients with heart failure due to idiopathic dilated cardiomyopathy. Am J Cardiol. 1995;76(17):1271-6.

170. Freedman NJ, Lefkowitz RJ. Desensitization of G protein-coupled receptors. Recent Prog Horm Res. 1996;51:319-51; discussion 52-3.

171. Xiao RP, Zhu W, Zheng M, Chakir K, Bond R, Lakatta EG, Cheng H. Subtype-specific beta-adrenoceptor signaling pathways in the heart and their potential clinical implications. Trends Pharmacol Sci. 2004;25(7):358-65.

172. Communal C, Singh K, Sawyer DB, Colucci WS. Opposing effects of beta(1)- and beta(2)-adrenergic receptors on cardiac myocyte apoptosis : role of a pertussis toxin-sensitive G protein. Circulation. 1999;100(22):2210-2.

173. Waagstein F, Caidahl K, Wallentin I, Bergh CH, Hjalmarson A. Long-term beta-blockade in dilated cardiomyopathy. Effects of short- and long-term metoprolol treatment followed by withdrawal and readministration of metoprolol. Circulation. 1989;80(3):551-63.

174. Heilbrunn SM, Shah P, Bristow MR, Valantine HA, Ginsburg R, Fowler MB. Increased beta-receptor density and improved hemodynamic response to catecholamine stimulation during long-term metoprolol therapy in heart failure from dilated cardiomyopathy. Circulation. 1989;79(3):483-90.

175. Hausdorff WP, Bouvier M, O'Dowd BF, Irons GP, Caron MG, Lefkowitz RJ. Phosphorylation sites on two domains of the beta 2-adrenergic receptor are involved in distinct pathways of receptor desensitization. J Biol Chem. 1989;264(21):12657-65.

176. Xiang Y, Kobilka B. The PDZ-binding motif of the beta2-adrenoceptor is essential for physiologic signaling and trafficking in cardiac myocytes. Proc Natl Acad Sci U S A. 2003;100(19):10776-81.

177. Nikolaev VO, Moshkov A, Lyon AR, Miragoli M, Novak P, Paur H, Lohse MJ, Korchev YE, Harding SE, Gorelik J. Beta2-adrenergic receptor redistribution in heart failure changes cAMP compartmentation. Science. 2010;327(5973):1653-7.

178. Balijepalli RC, Foell JD, Hall DD, Hell JW, Kamp TJ. Localization of cardiac L-type Ca(2+) channels to a caveolar macromolecular signaling complex is required for beta(2)-adrenergic regulation. Proc Natl Acad Sci U S A. 2006;103(19):7500-5.

179. Roth DM, Lai NC, Gao MH, Drumm JD, Jimenez J, Feramisco JR, Hammond HK. Indirect intracoronary delivery of adenovirus encoding adenylyl cyclase

increases left ventricular contractile function in mice. Am J Physiol Heart Circ Physiol. 2004;287(1):H172-7.

180. Hammond HK, Penny WF, Traverse JH, Henry TD, Watkins MW, Yancy CW, Sweis RN, Adler ED, Patel AN, Murray DR, Ross RS, Bhargava V, Maisel A, Barnard DD, Lai NC, Dalton ND, Lee ML, Narayan SM, Blanchard DG, Gao MH. Intracoronary Gene Transfer of Adenylyl Cyclase 6 in Patients With Heart Failure: A Randomized Clinical Trial. JAMA Cardiol. 2016;1(2):163-71.

181. Kandilci HB, Tuncay E, Zeydanli EN, Sozmen NN, Turan B. Age-related regulation of excitation-contraction coupling in rat heart. J Physiol Biochem. 2011;67(3):317-30.

182. Xiao RP, Tomhave ED, Wang DJ, Ji X, Boluyt MO, Cheng H, Lakatta EG, Koch WJ. Age-associated reductions in cardiac beta1- and beta2-adrenergic responses without changes in inhibitory G proteins or receptor kinases. J Clin Invest. 1998;101(6):1273-82.

183. Kilts JD, Akazawa T, Richardson MD, Kwatra MM. Age increases cardiac Galpha(i2) expression, resulting in enhanced coupling to G protein-coupled receptors. J Biol Chem. 2002;277(34):31257-62.

184. Kilts JD, Akazawa T, El-Moalem HE, Mathew JP, Newman MF, Kwatra MM. Age increases expression and receptor-mediated activation of G alpha i in human atria. J Cardiovasc Pharmacol. 2003;42(5):662-70.

185. Ostrom RS, Gregorian C, Drenan RM, Xiang Y, Regan JW, Insel PA. Receptor number and caveolar co-localization determine receptor coupling efficiency to adenylyl cyclase. J Biol Chem. 2001;276(45):42063-9.

186. Chen-Izu Y, Xiao RP, Izu LT, Cheng H, Kuschel M, Spurgeon H, Lakatta EG. G(i)-dependent localization of beta(2)-adrenergic receptor signaling to L-type Ca(2+) channels. Biophys J. 2000;79(5):2547-56.

187. Kerfant BG, Rose RA, Sun H, Backx PH. Phosphoinositide 3-kinase gamma regulates cardiac contractility by locally controlling cyclic adenosine monophosphate levels. Trends Cardiovasc Med. 2006;16(7):250-6.

188. Calaghan S, Kozera L, White E. Compartmentalisation of cAMP-dependent signalling by caveolae in the adult cardiac myocyte. J Mol Cell Cardiol. 2008;45(1):88-92.

189. Horikawa YT, Patel HH, Tsutsumi YM, Jennings MM, Kidd MW, Hagiwara Y, Ishikawa Y, Insel PA, Roth DM. Caveolin-3 expression and caveolae are required for isoflurane-induced cardiac protection from hypoxia and ischemia/reperfusion injury. J Mol Cell Cardiol. 2008;44(1):123-30.

190. Busija AR, Patel HH, Insel PA. Hugh Davson Distinguished Lectureship Article Caveolins and cavins in the trafficking, maturation, and degradation of caveolae: implications for cell physiology. Am J Physiol Cell Physiol. 2017:ajpcell 00355 2016.

191. Bean BP, Nowycky MC, Tsien RW. Beta-adrenergic modulation of calcium channels in frog ventricular heart cells. Nature. 1984;307(5949):371-5.

192. Xie YW, Wolin MS. Role of nitric oxide and its interaction with superoxide in the suppression of cardiac muscle mitochondrial respiration. Involvement in response to hypoxia/reoxygenation. Circulation. 1996;94(10):2580-6.

193. Martens JR, Sakamoto N, Sullivan SA, Grobaski TD, Tamkun MM. Isoform-specific localization of voltage-gated K+ channels to distinct lipid raft populations. Targeting of Kv1.5 to caveolae. J Biol Chem. 2001;276(11):8409-14.

194. Jo SH, Leblais V, Wang PH, Crow MT, Xiao RP. Phosphatidylinositol 3-kinase functionally compartmentalizes the concurrent G(s) signaling during beta2-adrenergic stimulation. Circ Res. 2002;91(1):46-53.

195. See Hoe LE, Schilling JM, Tarbit E, Kiessling CJ, Busija AR, Niesman IR, Du Toit E, Ashton KJ, Roth DM, Headrick JP, Patel HH, Peart JN. Sarcolemmal cholesterol and caveolin-3 dependence of cardiac function, ischemic tolerance, and opioidergic cardioprotection. Am J Physiol Heart Circ Physiol. 2014;307(6):H895-903.

196. Tsutsumi YM, Kawaraguchi Y, Niesman IR, Patel HH, Roth DM. Opioid-induced preconditioning is dependent on caveolin-3 expression. Anesth Analg. 2010;111(5):1117-21.

197. Tsutsumi YM, Kawaraguchi Y, Horikawa YT, Niesman IR, Kidd MW, Chin-Lee B, Head BP, Patel PM, Roth DM, Patel HH. Role of caveolin-3 and glucose transporter-4 in isoflurane-induced delayed cardiac protection. Anesthesiology. 2010;112(5):1136-45.

198. Horikawa YT, Panneerselvam M, Kawaraguchi Y, Tsutsumi YM, Ali SS, Balijepalli RC, Murray F, Head BP, Niesman IR, Rieg T, Vallon V, Insel PA, Patel HH, Roth DM. Cardiac-specific overexpression of caveolin-3 attenuates cardiac hypertrophy and increases natriuretic peptide expression and signaling. J Am Coll Cardiol. 2011;57(22):2273-83.

199. Wang J, Schilling JM, Niesman IR, Headrick JP, Finley JC, Kwan E, Patel PM, Head BP, Roth DM, Yue Y, Patel HH. Cardioprotective trafficking of caveolin to mitochondria is Gi-protein dependent. Anesthesiology. 2014;121(3):538-48.

200. Patel HH, Murray F, Insel PA. Caveolae as organizers of pharmacologically relevant signal transduction molecules. Annu Rev Pharmacol Toxicol. 2008;48:359-91.

201. Wyse BD, Prior IA, Qian H, Morrow IC, Nixon S, Muncke C, Kurzchalia TV, Thomas WG, Parton RG, Hancock JF. Caveolin interacts with the angiotensin II type 1 receptor during exocytic transport but not at the plasma membrane. The Journal of biological chemistry. 2003;278(26):23738-46.

202. Head BP, Patel HH, Roth DM, Lai NC, Niesman IR, Farquhar MG, Insel PA. G-protein-coupled receptor signaling components localize in both sarcolemmal and intracellular caveolin-3-associated microdomains in adult cardiac myocytes. J Biol Chem. 2005;280(35):31036-44.

203. Fujita T, Toya Y, Iwatsubo K, Onda T, Kimura K, Umemura S, Ishikawa Y. Accumulation of molecules involved in alpha1-adrenergic signal within caveolae: caveolin expression and the development of cardiac hypertrophy. Cardiovasc Res. 2001;51(4):709-16.

204. Chambliss KL, Yuhanna IS, Anderson RG, Mendelsohn ME, Shaul PW. ERbeta has nongenomic action in caveolae. Mol Endocrinol. 2002;16(5):938-46.

205. Acconcia F, Bocedi A, Ascenzi P, Marino M. Does palmitoylation target estrogen receptors to plasma membrane caveolae? IUBMB Life. 2003;55(1):33-5.

206. Li L, Haynes MP, Bender JR. Plasma membrane localization and function of the estrogen receptor alpha variant (ER46) in human endothelial cells. Proc Natl Acad Sci U S A. 2003;100(8):4807-12.

207. Ramos M, Lame MW, Segall HJ, Wilson DW. The BMP type II receptor is located in lipid rafts, including caveolae, of pulmonary endothelium in vivo and in vitro. Vascul Pharmacol. 2006;44(1):50-9.

208. Couet J, Sargiacomo M, Lisanti MP. Interaction of a receptor tyrosine kinase, EGF-R, with caveolins. Caveolin binding negatively regulates tyrosine and serine/threonine kinase activities. The Journal of biological chemistry. 1997;272(48):30429-38.

209. Huang CS, Zhou J, Feng AK, Lynch CC, Klumperman J, DeArmond SJ, Mobley WC. Nerve growth factor signaling in caveolae-like domains at the plasma membrane. J Biol Chem. 1999;274(51):36707-14.

210. Pike LJ. Growth factor receptors, lipid rafts and caveolae: an evolving story. Biochim Biophys Acta. 2005;1746(3):260-73.

211. Schnitzer JE, Oh P, Jacobson BS, Dvorak AM. Caveolae from luminal plasmalemma of rat lung endothelium: microdomains enriched in caveolin, Ca(2+)-ATPase, and inositol trisphosphate receptor. Proc Natl Acad Sci U S A. 1995;92(5):1759-63.

212. Fujimoto T, Miyawaki A, Mikoshiba K. Inositol 1,4,5-trisphosphate receptor-like protein in plasmalemmal caveolae is linked to actin filaments. J Cell Sci. 1995;108 (Pt 1):7-15.

213. Darby PJ, Kwan CY, Daniel EE. Caveolae from canine airway smooth muscle contain the necessary components for a role in Ca(2+) handling. Am J Physiol Lung Cell Mol Physiol. 2000;279(6):L1226-35.

214. Lohn M, Furstenau M, Sagach V, Elger M, Schulze W, Luft FC, Haller H, Gollasch M. Ignition of calcium sparks in arterial and cardiac muscle through caveolae. Circ Res. 2000;87(11):1034-9.

215. Wang XL, Ye D, Peterson TE, Cao S, Shah VH, Katusic ZS, Sieck GC, Lee HC. Caveolae targeting and regulation of large conductance Ca(2+)-activated K+ channels in vascular endothelial cells. J Biol Chem. 2005;280(12):11656-64.

216. Shaw L, Sweeney MA, O'Neill SC, Jones CJ, Austin C, Taggart MJ. Caveolae and sarcoplasmic reticular coupling in smooth muscle cells of pressurised arteries: the relevance for Ca2+ oscillations and tone. Cardiovasc Res. 2006;69(4):825-35.

217. Lockwich TP, Liu X, Singh BB, Jadlowiec J, Weiland S, Ambudkar IS. Assembly of Trp1 in a signaling complex associated with caveolin-scaffolding lipid raft domains. J Biol Chem. 2000;275(16):11934-42.

218. Kwiatek AM, Minshall RD, Cool DR, Skidgel RA, Malik AB, Tiruppathi C. Caveolin-1 regulates store-operated Ca2+ influx by binding of its scaffolding domain to transient receptor potential channel-1 in endothelial cells. Mol Pharmacol. 2006;70(4):1174-83.

219. Murata T, Lin MI, Stan RV, Bauer PM, Yu J, Sessa WC. Genetic evidence supporting caveolae microdomain regulation of calcium entry in endothelial cells. J Biol Chem. 2007;282(22):16631-43.

220. Liu L, Askari A. Beta-subunit of cardiac Na+-K+-ATPase dictates the concentration of the functional enzyme in caveolae. Am J Physiol Cell Physiol. 2006;291(4):C569-78.

221. Haas M, Askari A, Xie Z. Involvement of Src and epidermal growth factor receptor in the signal-transducing function of Na+/K+-ATPase. J Biol Chem. 2000;275(36):27832-7.

222. Cogolludo A, Moreno L, Lodi F, Frazziano G, Cobeno L, Tamargo J, Perez-Vizcaino F. Serotonin inhibits voltage-gated K+ currents in pulmonary artery smooth muscle cells: role of 5-HT2A receptors, caveolin-1, and KV1.5 channel internalization. Circ Res. 2006;98(7):931-8.

223. Abi-Char J, Maguy A, Coulombe A, Balse E, Ratajczak P, Samuel JL, Nattel S, Hatem SN. Membrane cholesterol modulates Kv1.5 potassium channel distribution and function in rat cardiomyocytes. J Physiol. 2007;582(Pt 3):1205-17.

224. Sampson LJ, Hayabuchi Y, Standen NB, Dart C. Caveolae localize protein kinase A signaling to arterial ATP-sensitive potassium channels. Circ Res. 2004;95(10):1012-8.

225. Song KS, Sargiacomo M, Galbiati F, Parenti M, Lisanti MP. Targeting of a G alpha subunit (Gi1 alpha) and c-Src tyrosine kinase to caveolae membranes: clarifying the role of N-myristoylation. Cell Mol Biol (Noisy-le-grand). 1997;43(3):293-303.

226. Li S, Couet J, Lisanti MP. Src tyrosine kinases, Galpha subunits, and H-Ras share a common membrane-anchored scaffolding protein, caveolin. Caveolin binding negatively regulates the auto-activation of Src tyrosine kinases. The Journal of biological chemistry. 1996;271(46):29182-90.

227. Lee H, Volonte D, Galbiati F, Iyengar P, Lublin DM, Bregman DB, Wilson MT, Campos-Gonzalez R, Bouzahzah B, Pestell RG, Scherer PE, Lisanti MP. Constitutive and growth factor-regulated phosphorylation of caveolin-1 occurs at the same site (Tyr-14) in vivo: identification of a c-Src/Cav-1/Grb7 signaling cassette. Mol Endocrinol. 2000;14(11):1750-75.

228. Smythe GM, Eby JC, Disatnik MH, Rando TA. A caveolin-3 mutant that causes limb girdle muscular dystrophy type 1C disrupts Src localization and activity and induces apoptosis in skeletal myotubes. J Cell Sci. 2003;116(Pt 23):4739-49.

229. Swaney JS, Patel HH, Yokoyama U, Head BP, Roth DM, Insel PA. Focal adhesions in (myo)fibroblasts scaffold adenylyl cyclase with phosphorylated caveolin. J Biol Chem. 2006;281(25):17173-9.

230. Del Pozo MA, Schwartz MA. Rac, membrane heterogeneity, caveolin and regulation of growth by integrins. Trends Cell Biol. 2007;17(5):246-50.

231. Patel HH, Tsutsumi YM, Head BP, Niesman IR, Jennings M, Horikawa Y, Huang D, Moreno AL, Patel PM, Insel PA, Roth DM. Mechanisms of cardiac

protection from ischemia/reperfusion injury: a role for caveolae and caveolin-1. Faseb J. 2007;21(7):1565-74.

232. Volonte D, Galbiati F, Pestell RG, Lisanti MP. Cellular stress induces the tyrosine phosphorylation of caveolin-1 (Tyr(14)) via activation of p38 mitogen-activated protein kinase and c-Src kinase. Evidence for caveolae, the actin cytoskeleton, and focal adhesions as mechanical sensors of osmotic stress. J Biol Chem. 2001;276(11):8094-103.

233. Razani B, Lisanti MP. Two distinct caveolin-1 domains mediate the functional interaction of caveolin-1 with protein kinase A. American journal of physiology Cell physiology. 2001;281(4):C1241-50.

234. Razani B, Rubin CS, Lisanti MP. Regulation of cAMP-mediated signal transduction via interaction of caveolins with the catalytic subunit of protein kinase A. The Journal of biological chemistry. 1999;274(37):26353-60.

235. Heijnen HF, Waaijenborg S, Crapo JD, Bowler RP, Akkerman JW, Slot JW. Colocalization of eNOS and the catalytic subunit of PKA in endothelial cell junctions: a clue for regulated NO production. J Histochem Cytochem. 2004;52(10):1277-85.

236. Levin AM, Coroneus JG, Cocco MJ, Weiss GA. Exploring the interaction between the protein kinase A catalytic subunit and caveolin-1 scaffolding domain with shotgun scanning, oligomer complementation, NMR, and docking. Protein Sci. 2006;15(3):478-86.

237. Rybin VO, Xu X, Steinberg SF. Activated protein kinase C isoforms target to cardiomyocyte caveolae : stimulation of local protein phosphorylation. Circ Res. 1999;84(9):980-8.

238. Fox TE, Houck KL, O'Neill SM, Nagarajan M, Stover TC, Pomianowski PT, Unal O, Yun JK, Naides SJ, Kester M. Ceramide recruits and activates protein kinase C zeta (PKC zeta) within structured membrane microdomains. J Biol Chem. 2007;282(17):12450-7.

239. Prevostel C, Alice V, Joubert D, Parker PJ. Protein kinase C(alpha) actively downregulates through caveolae-dependent traffic to an endosomal compartment. J Cell Sci. 2000;113 (Pt 14):2575-84.

240. Engelman JA, Chu C, Lin A, Jo H, Ikezu T, Okamoto T, Kohtz DS, Lisanti MP. Caveolin-mediated regulation of signaling along the p42/44 MAP kinase cascade in vivo. A role for the caveolin-scaffolding domain. FEBS Lett. 1998;428(3):205-11.

241. Galbiati F, Volonte D, Engelman JA, Watanabe G, Burk R, Pestell RG, Lisanti MP. Targeted downregulation of caveolin-1 is sufficient to drive cell transformation and hyperactivate the p42/44 MAP kinase cascade. Embo J. 1998;17(22):6633-48.

242. Ballard-Croft C, Locklar AC, Kristo G, Lasley RD. Regional myocardial ischemia-induced activation of MAPKs is associated with subcellular redistribution of caveolin and cholesterol. Am J Physiol Heart Circ Physiol. 2006;291(2):H658-67.

243. Shack S, Wang XT, Kokkonen GC, Gorospe M, Longo DL, Holbrook NJ. Caveolin-induced activation of the phosphatidylinositol 3-kinase/Akt pathway increases arsenite cytotoxicity. Mol Cell Biol. 2003;23(7):2407-14.

244. Smythe GM, Rando TA. Altered caveolin-3 expression disrupts PI(3) kinase signaling leading to death of cultured muscle cells. Exp Cell Res. 2006;312(15):2816-25.

245. Ha H, Pak Y. Modulation of the caveolin-3 and Akt status in caveolae by insulin resistance in H9c2 cardiomyoblasts. Exp Mol Med. 2005;37(3):169-78.

246. Zhang B, Peng F, Wu D, Ingram AJ, Gao B, Krepinsky JC. Caveolin-1 phosphorylation is required for stretch-induced EGFR and Akt activation in mesangial cells. Cell Signal. 2007;19(8):1690-700.

247. Sedding DG, Hermsen J, Seay U, Eickelberg O, Kummer W, Schwencke C, Strasser RH, Tillmanns H, Braun-Dullaeus RC. Caveolin-1 facilitates mechanosensitive protein kinase B (Akt) signaling in vitro and in vivo. Circ Res. 2005;96(6):635-42.

248. Zhuang L, Lin J, Lu ML, Solomon KR, Freeman MR. Cholesterol-rich lipid rafts mediate akt-regulated survival in prostate cancer cells. Cancer Res. 2002;62(8):2227-31.

249. Li L, Ren CH, Tahir SA, Ren C, Thompson TC. Caveolin-1 maintains activated Akt in prostate cancer cells through scaffolding domain binding site interactions with and inhibition of serine/threonine protein phosphatases PP1 and PP2A. Mol Cell Biol. 2003;23(24):9389-404.

250. Kim HA, Kim KH, Lee RA. Expression of caveolin-1 is correlated with Akt-1 in colorectal cancer tissues. Exp Mol Pathol. 2006;80(2):165-70.

251. Ono K, Iwanaga Y, Hirayama M, Kawamura T, Sowa N, Hasegawa K. Contribution of caveolin-1 alpha and Akt to TNF-alpha-induced cell death. Am J Physiol Lung Cell Mol Physiol. 2004;287(1):L201-9.

252. Murthy KS, Makhlouf GM. Heterologous desensitization mediated by G protein-specific binding to caveolin. J Biol Chem. 2000;275(39):30211-9.

253. Iiri T, Backlund PS, Jr., Jones TL, Wedegaertner PB, Bourne HR. Reciprocal regulation of Gs alpha by palmitate and the beta gamma subunit. Proc Natl Acad Sci U S A. 1996;93(25):14592-7.

254. Bhatnagar A, Sheffler DJ, Kroeze WK, Compton-Toth B, Roth BL. Caveolin-1 interacts with 5-HT2A serotonin receptors and profoundly modulates the signaling of selected Galphaq-coupled protein receptors. J Biol Chem. 2004;279(33):34614-23.

255. Oh P, Schnitzer JE. Segregation of heterotrimeric G proteins in cell surface microdomains. G(q) binds caveolin to concentrate in caveolae, whereas G(i) and G(s) target lipid rafts by default. Mol Biol Cell. 2001;12(3):685-98.

256. Prior IA, Harding A, Yan J, Sluimer J, Parton RG, Hancock JF. GTP-dependent segregation of H-ras from lipid rafts is required for biological activity. Nat Cell Biol. 2001;3(4):368-75.

257. Roy S, Plowman S, Rotblat B, Prior IA, Muncke C, Grainger S, Parton RG, Henis YI, Kloog Y, Hancock JF. Individual palmitoyl residues serve distinct roles in H-ras trafficking, microlocalization, and signaling. Mol Cell Biol. 2005;25(15):6722-33.

258. Ostrom RS, Bundey RA, Insel PA. Nitric oxide inhibition of adenylyl cyclase type 6 activity is dependent upon lipid rafts and caveolin signaling complexes. J Biol Chem. 2004;279(19):19846-53.

259. Fagan KA, Smith KE, Cooper DM. Regulation of the Ca2+-inhibitable adenylyl cyclase type VI by capacitative Ca2+ entry requires localization in cholesterol-rich domains. J Biol Chem. 2000;275(34):26530-7.

260. Head BP, Patel HH, Roth DM, Murray F, Swaney JS, Niesman IR, Farquhar MG, Insel PA. Microtubules and actin microfilaments regulate lipid raft/caveolae localization of adenylyl cyclase signaling components. J Biol Chem. 2006;281(36):26391-9.

261. Nilsson R, Ahmad F, Sward K, Andersson U, Weston M, Manganiello V, Degerman E. Plasma membrane cyclic nucleotide phosphodiesterase 3B (PDE3B) is associated with caveolae in primary adipocytes. Cell Signal. 2006;18(10):1713-21.

262. Garcia-Cardena G, Fan R, Stern DF, Liu J, Sessa WC. Endothelial nitric oxide synthase is regulated by tyrosine phosphorylation and interacts with caveolin-1. J Biol Chem. 1996;271(44):27237-40.

263. Venema VJ, Ju H, Zou R, Venema RC. Interaction of neuronal nitric-oxide synthase with caveolin-3 in skeletal muscle. Identification of a novel caveolin scaffolding/inhibitory domain. The Journal of biological chemistry. 1997;272(45):28187-90.

264. Razani B, Engelman JA, Wang XB, Schubert W, Zhang XL, Marks CB, Macaluso F, Russell RG, Li M, Pestell RG, Di Vizio D, Hou H, Jr., Kneitz B, Lagaud G, Christ GJ, Edelmann W, Lisanti MP. Caveolin-1 null mice are viable but show evidence of hyperproliferative and vascular abnormalities. The Journal of biological chemistry. 2001;276(41):38121-38.

265. Feron O, Kelly RA. The caveolar paradox: suppressing, inducing, and terminating eNOS signaling. Circ Res. 2001;88(2):129-31.

266. Sbaa E, Frerart F, Feron O. The double regulation of endothelial nitric oxide synthase by caveolae and caveolin: a paradox solved through the study of angiogenesis. Trends Cardiovasc Med. 2005;15(5):157-62.

267. Levin AM, Murase K, Jackson PJ, Flinspach ML, Poulos TL, Weiss GA. Double barrel shotgun scanning of the caveolin-1 scaffolding domain. ACS Chem Biol. 2007;2(7):493-500.

268. Chen Z, Bakhshi FR, Shajahan AN, Sharma T, Mao M, Trane A, Bernatchez P, van Nieuw Amerongen GP, Bonini MG, Skidgel RA, Malik AB, Minshall RD. Nitric oxide-dependent Src activation and resultant caveolin-1 phosphorylation promote eNOS/caveolin-1 binding and eNOS inhibition. Mol Biol Cell. 2012;23(7):1388-98.

269. Carnicer R, Crabtree MJ, Sivakumaran V, Casadei B, Kass DA. Nitric oxide synthases in heart failure. Antioxid Redox Signal. 2013;18(9):1078-99.

270. Damy T, Ratajczak P, Robidel E, Bendall JK, Oliviero P, Boczkowski J, Ebrahimian T, Marotte F, Samuel JL, Heymes C. Up-regulation of cardiac nitric oxide synthase 1-derived nitric oxide after myocardial infarction in senescent rats. Faseb J. 2003;17(13):1934-6.

271. Sato Y, Sagami I, Shimizu T. Identification of caveolin-1-interacting sites in neuronal nitric-oxide synthase. Molecular mechanism for inhibition of NO formation. The Journal of biological chemistry. 2004;279(10):8827-36.

272. Beigi F, Oskouei BN, Zheng M, Cooke CA, Lamirault G, Hare JM. Cardiac nitric oxide synthase-1 localization within the cardiomyocyte is accompanied by the adaptor protein, CAPON. Nitric Oxide. 2009;21(3-4):226-33.

CHAPTER 2: CARDIAC MYOCYTE-SPECIFIC CAVEOLIN-3 OVEREXPRESSION INCREASES β-ADRENERGIC RESPONSIVITY OF HEARTS FROM YOUNG AND AGED MICE

Abstract

Previous studies have demonstrated that Cav3 can compartmentalize βAR signaling and that Cav3 may help regulate cardiovascular health. However, the relationship between Cav3, βAR signaling, and the age-dependent changes in βAR responsivity have not been defined. In this study, I tested the hypothesis that CM-specific Cav3 overexpression (OE) in mice amplifies βAR response in young animals and preserves βAR responsivity into old age. Adult male Cav3 OE mice demonstrated increased Isoproterenol (Iso)-induced contractility and relaxation, cAMP generation, and mitochondrial respiration without major changes in phospholamban or troponin I phosphorylation or Iso-induced βAR response desensitization. Aged (20-24-month-old) Cav3 OE mice exhibited preserved *ex vivo* cardiac responsivity to Iso while TGneg sibling controls had severely blunted Iso responses. These data implicate Cav3 OE as a potent mediator of cardiovascular health, in particular throughout the lifespan, through preservation of the βAR system of the heart.

Experimental procedures

Animals

Laboratory Animals and protocols were approved by the VA San Diego Healthcare System IACUC and surgical procedures were carried out in accordance with the NIH Guide for the Care and Use of Laboratory Animals. Animals were maintained with *ad lib* access to food and water in a 12 h light-dark cycle in a temperature-controlled room. Heterozygous Cav3 OE mice were produced in a C57BL/6 background as previously described (1). Transgene negative siblings of Cav3 OE mice served as controls. Young mice were studied at age 2-4 months, and aged mice were between 20-24 months.

Langendorff isolated perfused heart model and Iso administrations

Mice were anesthetized with an intraperitoneal injection of sodium pentobarbital (50 mg kg^{-1}), followed by thoracotomy, heart excision, and immersion in ice-cold perfusion buffer to halt contraction and preserve myocyte viability during aortic dissection. The aorta was cannulated within 2 min of thoracotomy on a 21g stub needle attached to the Langendorff isolated heart apparatus for perfusion with oxygenated buffer at a constant pressure of 80 mmHg and constant temperature of 37°C. A modified Krebs-Henseleit perfusion buffer was used in all experiments: NaCl, 119 mM; d-glucose, 11 mM; $NaHCO_3$, 22 mM; KCl, 4.7 mM; $MgCl_2$, 1.2 mM; KH_2PO_4, 1.2 mM; $CaCl_2$, 2.5 mM; EDTA, 0.5 mM; and pyruvate, 2 mM. The buffer

was oxygenated with 95% O_2 and 5% CO_2 at 37°C to yield pH 7.4 and was filtered through an in-line 0.45 μm filter (Sterivex-HV, Millipore).

A polyethylene drain was inserted through the apex of the heart to vent fluid and a fluid-filled balloon was introduced into the left ventricle (LV) through an incision in the left atria. The balloon was connected via fluid-filled tubing to a pressure transducer and inflated to yield a LV end-diastolic pressure of 5 mmHg. Hearts were then immersed in a water-jacketed organ bath maintained at 37°C and acclimated to perfusion for 20 min. Coronary flow was measured using an in-line Doppler flow probe (Transonic Systems Inc). Flow and LV pressure signals were processed on a four-channel PowerLab data acquisition system (ADInstruments) and recorded by LabChart software. LV pressure recordings were analyzed to yield systolic, end-diastolic, and developed pressures (LVDP), heart rate, and the peak differentials of pressure change with time (+dP/dt, contractility and –dP/dt, relaxation).

Dose-response curves of Iso (Isuprel: Hospira Inc.) were administered after 20 min of cardiac acclimatization by bolus injection of 250 μl of the lowest concentration of Iso (1 nM) into the perfusion system proximal to the cardiac cannula (total volume after injection port = 500 μl). After a 10-min wash-out period, the serial doses of Iso were delivered and the wash-out was repeated. Peak LVDP, ±dP/dt, and heart rate were measured after each dose.

Infusions of Iso were performed by constant delivery of 10 μM Iso at 0.01x flow rate (effective dose: 100 nM) by a syringe driver (Harvard Apparatus) into a perfusion buffer proximal to the heart (total volume after injection port = 500 μl).

Hearts were frozen on the cannula with liquid nitrogen after 5 min of infusion for assessment of phospholamban (PLB) and troponin I phosphorylation. Measurements were taken every 5 min after the start of infusion for assessment of Iso-induced desensitization of βAR responses.

Adult mouse cardiac myocyte isolation

Materials for CM isolation were acquired from Sigma unless otherwise indicated. Adult mouse CM isolation was performed in pairs of Cav3 OE and TGneg sibling controls. Adult male C57BL/6 mice were anesthetized with pentobarbital, thoracotomy was performed, and hearts were excised and placed in ice-cold media for aortic dissection. Hearts were cannulated on a 21g stub needle and perfused at a rate of 3 ml/min with MEM Joklik's modified supplemented with: 10 mM HEPES pH 7.4 (Life Tech), 30 mM taurine, 2 mM ±carnitine HCl, 20 mM creatine, and 2 mM sodium pyruvate containing no Ca^{2+} (referred to as Joklik in following procedures) with 10 mM 2,3-Butanedione monoxime (BDM) for 4 min, followed by Joklik containing 10 mM BDM with: 20 μM $CaCl_2$ and 1.8 mg/ml collagenase II (Worthington: mitochondrial respiration) or 12.5 μM $CaCl_2$ with 0.25 mg/ml liberase TH (Roche: cAMP production) for 15 or 7 min, respectively. After perfusion, hearts were dissected, triturated with transfer pipettes, and washed to purify CMs. In brief, after perfusion CMs were allowed to precipitate (at gravity) for 6 min, followed by removal of supernatant and addition of 4:1 proportions of Joklik containing 10 mM BDM, 20 μM $CaCl_2$, and 1% BSA. This wash step was repeated twice, followed by introduction of $CaCl_2$ in four iterations of 250 μM with 4 min resting periods to achieve a slow

increase to a final Ca^{2+} concentration of 1.2 mM. Two more gravity precipitation wash steps were performed with Joklik without BDM supplemented with 1.2 mM $CaCl_2$, and cells were resuspended for plating in Joklik without BDM with 1.2 mM $CaCl_2$.

Seahorse Extracellular Flux Analyzer measurements

Isolated CMs were counted using an addition of 10 µl of cells to a hemocytometer and plated at 4,000 cells/well in a 96-well plate pre-coated with 10 µg/mL laminin (Life Tech.) for Seahorse XF Flux Analyzer procedures (mitochondrial respiration). After one hour, media was changed to XF Basal Media (Seahorse Bioscience, now Agilent Technologies) supplemented with 1 mM sodium pyruvate, 3 mM L-glutamine, and 5 mM HEPES (XF Assay media). A Seahorse Bioscience injection cassette was prepared with XF Assay media with added glucose (55 mM) and sodium pyruvate (30 mM) for 1:10 dilution upon automatic injection in port A and 1 µM Iso (Isuprel: Hospira Inc.) for 1:10 dilution in port B. The XF Analyzer was programmed to measure three 2-min periods at baseline, after glucose+pyruvate injection, and after Iso injection. Measurements included: 1.5 min mixing, 20 secs wait, and 2 min measurement. Data for oxygen consumption rate was exported to Microsoft Excel for analysis.

Measurement of cAMP production in adult mouse CMs

Adult CMs were plated on laminin-coated 24-well cell culture-treated plates for 1 h, after which media was exchanged for Joklik without BDM supplemented with 1.2 mM $CaCl_2$. Cells were prepared for cAMP accumulation by incubation with media

or 200 μM 3-isobutyl-1-methylxanthine (IBMX: Sigma) for 10 min. Agonists were introduced after cells were incubated with IBMX for 10 min: Iso (Isuprel: Hospira Inc.) was administered at 0.001, 0.01, 0.1, and 1 μM; Assay medium was aspirated and cells were washed once with ice-cold PBS, then ice-cold 7.5% w/v trichloroacetic acid (TCA) (Ricca Chemical Co.) was immediately added to each well.

TCA extracts were assayed for cAMP content using a competitive radioimmunoassay. TCA samples and a standard curve of cAMP (V6421: Promega) in a $\log_2$ distribution in concentration from 78.125 to 40,000 fM were diluted into 50 mM Sodium Acetate (NaAc) pH 4.75 and acetylated by addition of triethylamine (Alfa Aesar) and acetic anhydride (Fisher Sci.) at a 2:1 ratio, followed immediately by vortexing. Diluted acetylated samples and standards were incubated in a DuraPore membrane plate (EMD Millipore) overnight with anti-cAMP antibody (07-1497: EMD Millipore Corp) and adenosine 3',5'-cyclic phosphoric acid, 2`-O-succinyl [125I]-iodotyrosine methyl ester (I^{125}-cAMP: PerkinElmer); both primary antibody and I^{125}-cAMP were diluted in 50 mM NaAc pH 4.75 with 0.1% human γ-globulin (G4386: Sigma). Anti-rabbit BioMag secondary antibody (Qiagen) was added and incubated with samples for one h, followed by vacuum aspiration of unbound I^{125}-cAMP and three washes with superlative volumes of 12% polyethylene glycol (Sigma) in 10 mM NaAc pH 6.2. Wells were dried by vacuum and then punched out for quantification. Bound I^{125}-cAMP was quantified by a 2470 Wizard^2 gamma counter (PerkinElmer) and I^{125} counts per minute were compared against the standard curve. cAMP levels outside the linear portion of the standard curve were excluded; such samples were diluted and re-analyzed.

Immunoblots

Hearts were stimulated with vehicle or 100 nM Iso on the Langendorff apparatus for 5 min and frozen on the cannula, then pulverized on dry ice and lysed with 150 mM Na_2CO_3 pH 11, 1 mM EDTA, and 1x Halt protease and phosphatase inhibitor cocktail (Thermo Scientific) with 15 strokes in a glass-glass Dounce homogenizer, followed by sonication three times for 10 sec at 40% amplitude on ice (Sonics VibraCell). Protein levels were determined using the Bradford assay (Bio-Rad) and normalized, then mixed 1:2 with 4x LDS Laemmli loading buffer containing a final concentration of 100 mM dithiothreitol and subjected to sodium dodecyl sulfate polyacrylamide gel electrophoresis (SDS-PAGE) with 10% acrylamide using an SDS-MOPS buffer (ThermoFisher) followed by Western electrophoretic transfer to polyvinylidene fluoride membranes (PVDF pore size 0.2 μm). Blots were blocked with 3% BSA in Tris-buffered saline with 0.1% Tween 20 (TBST) for 1 h at room temperature and incubated with primary antibodies in 3% w/v bovine serum albumin (BSA) in TBST for 12-16 h at 4ºC. Antibodies to TropI (1:1000 #4002S, Cell Signaling Tech., 28 kDa detected band), p-TropI (1:1000 #4004S, Cell Signaling Tech., 28 kDa detected band), PLB (1:1000 ab2865, Abcam, 25 kDa pentameric detected band, 5 kDa monomeric detected band), p-PLB (1:1000 ab15000, Abcam, 5 kDa monomeric detected band), and β-actin (1:500 sc-1616, Santa Cruz Biotechnology, 45 kDa detected band) were used. Blots were washed thrice for 10 min in TBST at room temperature, then incubated at room temperature with 3% BSA-TBST containing horseradish peroxide-conjugated (HRP) secondary antibodies raised in mice against rabbit (Santa Cruz Biotechnology sc-2357: TropI, p-TropI, p-PLB), in

donkey against goat (Santa Cruz Biotechnology sc-2020), and in goat against mouse (Santa Cruz Biotechnology sc-2004: PLB) at 1:1000 dilutions. After three more washes with TBST, HRP activity was detected using SuperSignal West Dura chemiluminescence reagent (Thermo Scientific) and recorded using a UVP exposure box and CCD camera (UVP, LLC). Intensity values were measured with Image Studio Lite and signal normalized to β-actin for each blot, then phospho-protein over same-blot β-actin to yield a ratio over total protein over same-blot β-actin.

Statistical analysis

All data analysis and statistics were performed with GraphPad Prism 7 software (GraphPad Software Inc., La Jolla, CA). All data are expressed as mean ± S.E.M. Significant differences were accepted for α when $p < 0.05$ for all statistical tests.

2-way ANOVA of repeated measures

Peak responses after bolus for each Iso dose from Langendorff studies were analyzed by 2-way repeated measures analysis of variance (ANOVA: genotype x dose Iso) with subject matching, followed by the indicated multiple comparisons post-hoc tests on individual doses. The same analysis was performed on data from Iso perfusions, with time replacing Iso dose as the repeated measures variable (genotype x time).

EC50s and 2-way ANOVA

Due to a slight depression in LVDP, contractility, and relaxation at the smallest dose of Iso and in light of the similarities in baseline measurements in both genotypes, dose-response curve fitting was performed with the unstimulated values excluded to

provide accurate EC50 values. Dose-response data from all experiments were normalized to 0%-100% of response and fitted to a four-parameter dose-response curve with variable slope, from which LogEC50 values were calculated. LogEC50 values from the Iso-only young or aged groups were compared by unpaired t test. LogEC50 values were then compared between Iso±Aged groups by ordinary 2-way ANOVA (genotype x age) with the indicated post-hoc multiple comparisons tests. LogEC50 values were transformed to EC50 for graphical presentation and are presented as mean +S.E.M.

2-way ANOVA of cAMP accumulation and PKA substrate phosphorylation

Dose-responses for Iso-promoted cAMP were evaluated by ordinary two-way ANOVA (genotype x dose) and post-hoc multiple comparisons. Total and ratio of phosphorylated to total PLB or Trop I was analyzed by ordinary two-way ANOVA (genotype x Iso) for evaluation of PKA-mediated phosphorylation.

2-way repeated measures ANOVA of mitochondrial metabolism

Oxygen consumption rates (OCR) were compared after substrate addition and after addition of Iso using 2-way ANOVAs.

Results

Cav3 OE hearts exhibit enhanced dose-dependent increases in contractile and relaxation responses to Iso compared with TGneg hearts

Hearts from Cav3 OE and TGneg mice ($N = 7$ per group) were exposed to 1 nM – 1 μM Iso on the Langendorff apparatus and physiological responses were

measured. Cav3 OE mice showed enhanced Iso-induced responses in contractility and relaxation. Measurement of Iso-induced changes in contractility **(Figure 2.1A)** revealed a significant effect of Iso dose ($F(6, 72) = 72.35$, $p < 0.001$), with both strains responding to Iso. Subject matching was effective in controlling for variability between subjects ($F(12, 72) = 13.72$, $p < 0.001$), and responses between the genotypes were significantly different ($F(1, 12) = 7.36$, $p = 0.019$). There was a significant interaction between dose and genotype ($F(6, 72) = 6.26$, $p < 0.001$), indicating that genotypes responded differently to Iso and that post hoc tests should be performed. Sidak's multiple comparisons post-hoc test revealed that Cav3 OE hearts have increases in Iso-induced contractility of 4200 $mmHg*s^{-1}$ at 100 nM ($p = 0.015$), 5348 $mmHg*s^{-1}$ at 300 nM ($p = 0.001$), and 4955 $mmHg*s^{-1}$ at 1 μM ($p = 0.002$).

Measurement of Iso-induced changes in relaxation **(Figure 2.1B)** revealed a significant effect of dose ($F(6, 72) = 74.06$, $p < 0.001$), subject matching ($F(12, 72) = 10.38$, $p < 0.001$), and genotype ($F(1, 12) = 9.53$, $p = 0.009$). There was a significant interaction between dose and genotype ($F(6, 72) = 4.24$, $p = 0.001$). Sidak's multiple comparisons post-hoc test revealed that hearts from Cav3 OE had significantly amplified Iso-induced relaxation by 1632 $mmHg*s^{-1}$ at 100 nM ($p = 0.017$), 2292 $mmHg*s^{-1}$ at 300 nM ($p < 0.001$), and 1786 $mmHg*s^{-1}$ at 1 μM ($p = 0.007$).

Measurement of Iso-induced changes in left ventricular developed pressure (LVDP) **(Figure 2.1C)** indicated a significant effect of dose ($F(6, 72) = 37.56$, $p < 0.001$), subject matching ($F(12, 72) = 10.16$, $p < 0.001$), but neither for genotype ($F(1, 12) = 2.26$, $p = 0.159$) nor a significant interaction between dose and genotype (F

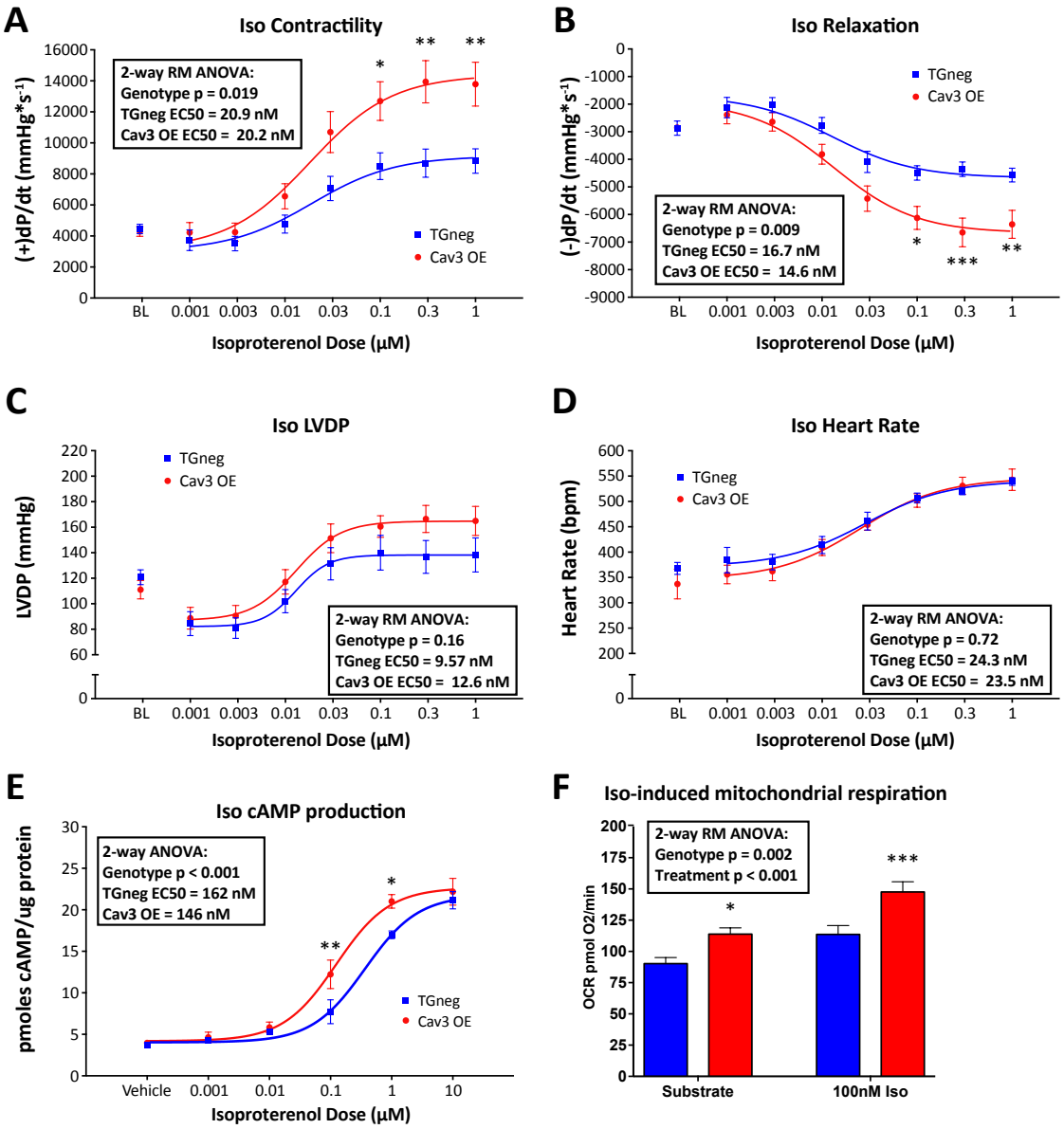

Figure 2.1: Cav3 OE increases contractility and relaxation in response to Iso. Iso dose-response curves in *ex vivo* hearts exhibit increased Cav3 OE responses in **(A)** contractility and **(B)** relaxation, but not **(C)** LVDP or **(D)** heart rate ($N = 7$/group). **(E)** Isolated CMs produce more cAMP in response to Iso stimulation in the presence of 200 µM IBMX at 100 nM and 1 µM ($N = 2$ isolations, 3 measurements per isolation). **(F)** Pyruvate+Glucose and subsequent Iso stimulus induces more mitochondrial respiration in Cav3 OE CMs ($N = 2$ isolations, 3 measurements per isolation). *p<0.05, **p<0.01, ***p<0.001 compared to TGneg at same dose Iso **(A-E)** or same treatment **(F)**. Data are represented as mean ± SEM.

(6, 72) = 0.828, p = 0.552). Sidak's multiple comparisons post-hoc test revealed no significant differences between TGneg and Cav3 OE at any dose of Iso.

For the measurement of Iso-induced changes in heart rate **(Figure 2.1D)**, we found a significant effect of dose (F (6, 72) = 122.9, p < 0.001) and subject matching (F (12, 72) = 15.71, p < 0.001), but not for genotype (F (1, 12) = 0.131, p = 0.72). There was no significant interaction between dose and genotype (F (6, 72) = 1.001, p = 0.43). Sidak's multiple comparisons post-hoc test revealed no significant differences between TGneg and Cav3 OE at any dose of Iso.

Data for each physiological parameter was adjusted to represent the results as percent of maximal response and was then analyzed using a best-fit curve to calculate the EC50 values of the responses. Using this approach, we found no significant effect of genotype in the EC50 values for contractility (p = 0.87), relaxation (p = 0.56), LVDP (p = 0.52), or heart rate (p = 0.91).

Taken together, these data show that, when compared with results for TGneg mice, Cav3 OE in CMs increases the amplitude of Iso dose-dependent contractile and relaxation responses but not LVDP or heart rate responses. Additionally, the potency of Iso is not different between the two genotypes in contractility, relaxation, LVDP, or heart rate.

Cav3 OE CMs produce more cAMP in response to Iso than TGneg CMs

The contractile response to βAR stimulation is modulated through the second messenger cAMP, so I tested whether Cav3 OE alters physiological responses by modulating cAMP production by treating CMs isolated from Cav3 OE and TGneg

mice to 1 nM – 10 μM Iso and evaluated cAMP accumulation in the presence of the phosphodiesterase inhibitor IBMX ($N = 2$ isolations with 3 measurements each). Cav3 OE myocytes produced more cAMP in response to Iso than did TGneg myocytes **(Figure 2.1E)**. I found a significant effect of dose ($F(5, 69) = 165.2$, $p < 0.001$) and genotype ($F(1, 69) = 11.95$, $p < 0.001$) on Iso-promoted cAMP accumulation. There was a significant interaction between dose and genotype, indicating that Cav3 OE and TGneg CMs responded differently to increasing Iso doses ($F(5, 69) = 2.483$, $p = 0.040$); therefore, I performed Sidak's multiple comparisons post-hoc test, which revealed that Cav3 OE CMs have increases in Iso-induced cAMP of 4.51 pmoles cAMP/μg protein at 100 nM ($p = 0.015$) and 4.02 pmoles cAMP/μg protein at 300 nM ($p = 0.001$).

Adjustment of the dose-response data to percent of maximal response and then applying a best-fit curve to calculate EC50 of response revealed no significant difference between the genotypes in the EC50 values for Iso- stimulated cAMP production ($p = 0.556$).

Cav3 OE CMs demonstrate increased mitochondrial respiration in response to pyruvate + glucose and pyruvate + glucose + Iso than TGneg

To ascertain the effects of Iso stimulation on mitochondrial respiration, CMs from Cav3 OE and TGneg hearts ($N = 2$ isolations with 7 replicates each) were incubated with the substrates glucose + pyruvate, then treated with 100 nM Iso and the oxygen consumption rate (OCR) was recorded (Seahorse XF Analyzer). Analysis was performed for a mean of three measurements after glucose + pyruvate addition

(baseline) and after Iso **(Figure 2.1F)**. I found a significant effect of Iso treatment ($F(1, 26) = 74.15$, $p < 0.001$), subject matching ($F(26, 26) = 6.55$, $p < 0.001$), and genotype ($F(1, 26) = 11.5$, $p = 0.002$), but did not find a significant interaction between Iso and genotype ($F(1, 26) = 2.467$, $p = 0.13$). Use of Sidak's multiple comparisons post-hoc test revealed that Cav3 OE CMs have elevated respiration compared with TGneg CMs at baseline of 23.56 pmol O_2/min ($p = 0.025$) and 33.98 pmol O_2/min after addition of 100 nM Iso ($p < 0.001$). These data demonstrate CMs from Cav3 OE myocytes have elevated mitochondrial respiration at baseline and after addition of Iso.

Prolonged Iso stimulus does not differentially desensitize the βAR response in TGneg or Cav3 OE hearts

As Iso stimulation can desensitize the response of βARs, I determined whether, compared with TGneg hearts, Cav3 OE hearts desensitized at different rates or to a different extent in terms of functional responses to infusion of Iso. I observed no differences in response of the genotypes to a 30 min infusion of Iso **(Figure 2.2)** (N = 5 TGneg, 3 Cav3 OE). Although there were significant effects of time ($F(6, 36) > 4.7$, $p < 0.001$ for contractility, relaxation, and heart rate; $p = 0.001$ for LVDP) and subject matching ($F(6, 36) > 11.99$, $p < 0.001$ for contractility, relaxation, LVDP and heart rate), I found no significant effect of genotype ($F(1, 6) < 1.247$, $p > 0.31$ for all parameters) or interaction between genotype and time ($F(6, 36) < 0.7855$, $p > 0.59$ for all parameters). In summary, TGneg and Cav3 OE hearts respond similarly over a 30 min period of stimulation with Iso, implying that increased expression of Cav3 in CMs

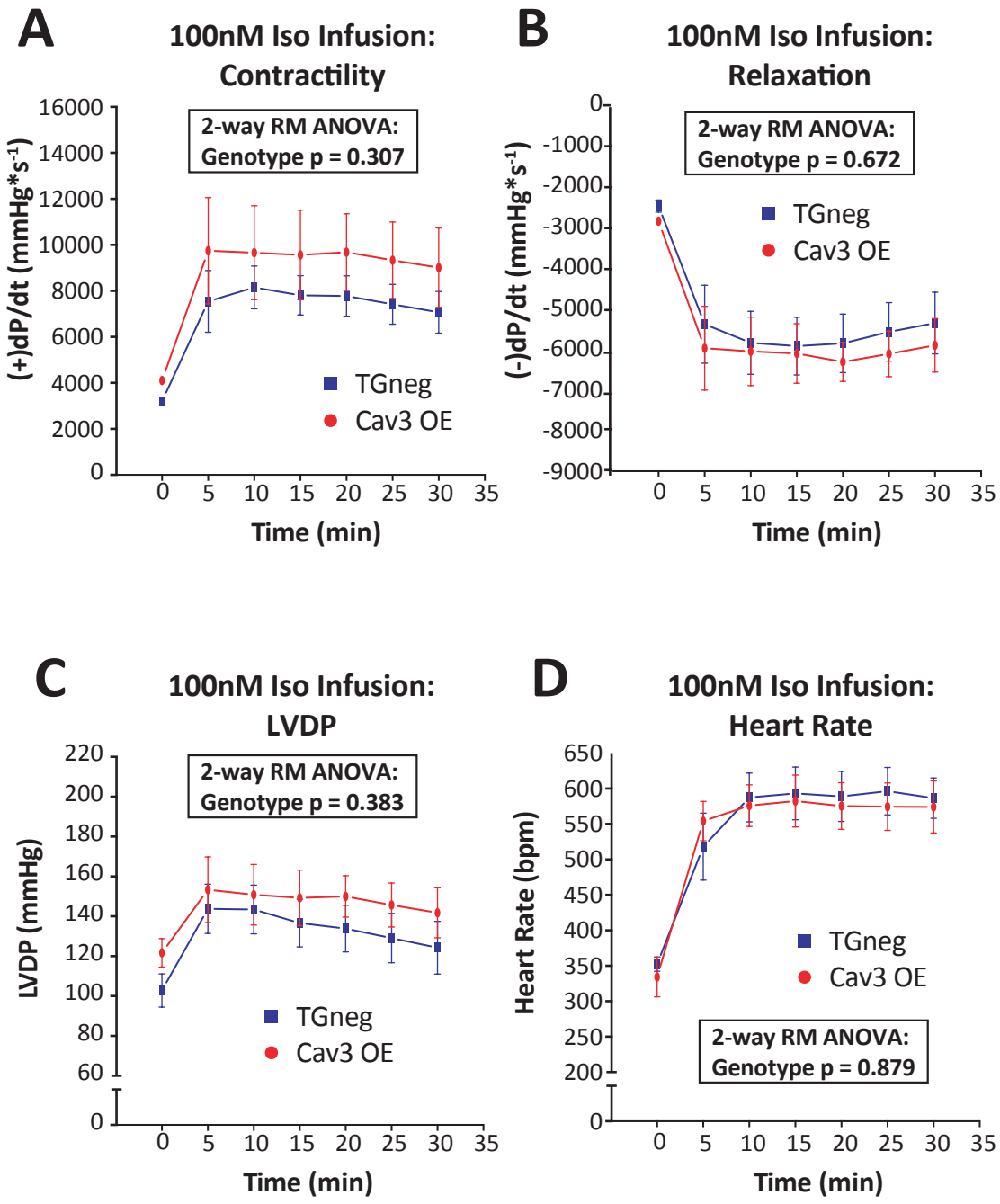

Figure 2.2: Cav3 OE and TGneg hearts do not exhibit differential desensitization in response to Iso. Cav3 OE and TGneg hearts administered with a 30 min infusion of 100 nM Iso do not demonstrate differential responses or desensitization rates in **(A)** contractility, **(B)** relaxation, **(C)** LVDP, or **(D)** heart rate. *N* = 5 TGneg, 3 Cav3 OE. Data are represented as mean ± SEM.

does not alter changes in functional responses that might undergo rapid desensitization to βAR activation.

Cav3 OE does not alter phosphorylation of phospholamban or troponin I in response to Iso

To ascertain whether the differences in cAMP production between Cav3 OE and TGneg result in differences in phosphorylation of the cAMP-activated protein kinase A (PKA) substrates phospholamban (PLB) and troponin I (TropI), I exposed hearts on the Langendorff apparatus to 20 min of acclimatization followed by a 5-min infusion of 100 nM Iso (N = 3/group). Both Cav3 OE and TGneg hearts exhibited enhanced Iso-stimulated TropI and PLB phosphorylation, but there were no differences between the genotypes **(Figure 2.3A)**. Total PLB (relative to the β-actin loading control) had a significant effect of Iso ($F(1, 8) = 34.36$, $p < 0.001$) but not genotype ($F(1, 8) = 0.4708$, $p = 0.51$) and no significant interaction between Iso and genotype ($F(1, 8) = 1.956$, $p = 0.200$). Tukey's multiple comparisons post hoc analysis revealed that Iso decreased total PLB in TGneg by about 36% ($p = 0.0039$) but the 24% decrease in total PLB in Cav3 OE was not significantly different from baseline ($p = 0.053$). The decrease in total PLB is likely due to Iso/cAMP/PKA-induced phosphorylation-dependent degradation of monomeric PLB.

For the measurement of Iso-induced changes in phospho-PLB (p-PLB) over total PLB **(Figure 2.3A)**, we found a significant effect of Iso ($F(1, 8) = 43$, $p < 0.001$) but not for genotype ($F(1, 8) = 0.3252$, $p = 0.58$), or for interaction between Iso and genotype ($F(1, 8)$ 0.1155, $p = 0.74$). Tukey's multiple comparisons post hoc analysis

revealed that Iso significantly increased p-PLB / total PLB by 11-fold in TGneg ($p = 0.010$) and by about 9-fold in Cav3 OE ($p = 0.005$) hearts, but that there was no significant difference between the genotypes in unstimulated or Iso-stimulated p-PLB/total PLB.

Assessment of Iso-induced changes in total TropI **(Figure 2.3B)** revealed a significant effect of genotype ($F (1, 8) = 8.215$, $p = 0.021$) but not Iso ($F (1, 8) = 0.6140$, $p = 0.61$) nor for interaction between Iso and genotype ($F (1, 8) = 0.1659$, $p = 0.70$). Tukey's multiple comparisons post hoc analysis revealed no differences between genotypes or Iso exposure in total TropI. The effect of genotype, therefore, was only apparent when TGneg and Cav3 OE hearts were compared without considering Iso treatment, indicating that Cav3 OE hearts have a slight increase in their amount of total TropI.

Assessment of Iso-induced changes in phospho-TropI (p-TropI)/total TropI **(Figure 2.3B)** revealed a significant effect of Iso ($F (1, 8) = 103.8$, $p < 0.001$) but not genotype ($F (1, 8) = 1.687$, $p = 0.23$) nor for the interaction between Iso and genotype ($F (1, 8) = 3.679$, $p = 0.091$). Tukey's multiple comparisons post hoc analysis revealed that Iso significantly increased p-TropI/r total TropI by 2.4-fold in TGneg ($p = 0.0017$) and by 3.3-fold in Cav3 OE ($p < 0.001$), but that there were no significant differences between TGneg and Cav3 OE hearts with respect to p-TropI in stimulated or unstimulated conditions.

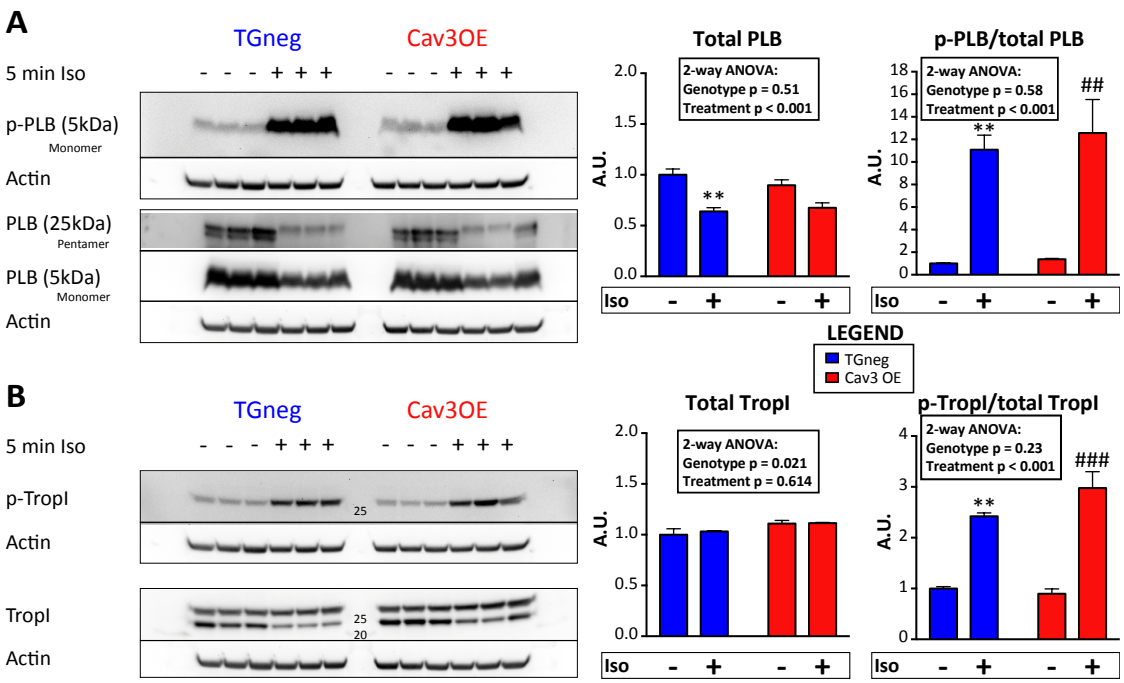

Figure 2.3: Cav3 OE does not alter phosphorylation of PLB and TropI after Iso stimulation. (A) TGneg and Cav3 OE hearts exhibit similar reductions in total PLB and increases in p-PLB/total PLB after 5 min Iso stimulation. Qualitative analysis of PLB and p-PLB normalized to loading control and p-PLB normalized to total PLB. **(B)** TGneg and Cav3 OE hearts exhibit similar p-TropI/total TropI after 5 min Iso stimulation. Qualitative analysis of total TropI (top band) and p-TropI normalized to loading control followed by p-TropI normalization to total TropI. $N = 3$/group $^{**}p<0.01$ compared with TGneg -Iso, $\#\#p<0.01$ compared with Cav3 OE -Iso. Data are represented as mean ± SEM.

Aged Cav3 OE hearts exhibit Iso responsivity that is absent in aged TGneg hearts

Because aging can alter Cav3 expression levels and βAR expression levels, I assessed the dose-response to Iso of 20-24 month-old Cav3 OE and TGneg mouse hearts (*N* = 2 TGneg, 5 Cav3 OE) **(Figure 2.4)**. We found that aged TGneg hearts have severely blunted contractile and relaxation responses to Iso. Importantly, aged Cav3 OE mice have contractile and relaxation responses that are similar to young TGneg even though aged Cav3 OE hearts exhibited reduction in contractile and relaxation responses when compared with young Cav3 OE hearts. Aged TGneg hearts exhibited significant reductions in relaxation and LVDP responses to Iso and showed a trend for reductions in contractile responses when compared with young TGneg hearts. Aged Cav3 OE hearts exhibited significant increases in relaxation compared with aged TGneg hearts. Detailed analyses of the results are presented below and are organized by physiological parameter.

Contractility

Assessment of Iso-induced changes in contractility in young and aged TGneg and Cav3 OE hearts **(Figure 2.4A)** revealed significant overall effects in dose ($F(6, 102) = 40.76$, $p < 0.001$), subject matching ($F(17, 102) = 13.79$, < 0.001), and group (genotype x age) ($F(3, 17) = 6.081$, $p = 0.005$). There was a significant interaction between dose and group ($F(18, 102) = 5.147$, $p < 0.001$); therefore, we performed Tukey's multiple comparisons post-hoc tests, which revealed that between young TGneg and young Cav3 OE hearts, there is a significant effect in Iso-induced contractility at 30 nM ($p = 0.033$), 100 nM ($p = 0.009$), 300 nM ($p < 0.001$), and 1 μM

($p = 0.0014$). The difference in p values between this comparison and those presented for **Figure 2.1A** are a result of the increased multiplicity of comparisons when analyzed in conjunction with the aging Iso dose response data. Post-hoc tests also revealed that between young Cav3 OE hearts and aged Cav3 OE hearts, there is a significant decrease of 5317 $mmHg*s^{-1}$ in Iso-induced contractility at 30 nM ($p = 0.002$), 5865 $mmHg*s^{-1}$ at 100 nM ($p < 0.001$), 6429 $mmHg*s^{-1}$ 300 nM ($p < 0.001$), and 5906 $mmHg*s^{-1}$ 1 μM ($p < 0.001$). Additionally, between young TGneg and aged TGneg hearts, there was a trend indicating a decrease in contractility of 4691 $mmHg*s^{-1}$ at 1 μM Iso ($p = 0.085$). Tukey's multiple comparisons post-hoc test revealed that between young TGneg x aged Cav3 OE hearts, and aged Cav3 OE hearts and aged TGneg hearts there was not a significant effect in Iso-induced contractility at any dose.

Relaxation

Analysis of Iso-induced changes in relaxation in young and aged TGneg and Cav3 OE hearts **(Figure 2.4B)** indicated significant overall effects in dose ($F (6, 102) = 47.99$, $p < 0.001$), subject matching ($F (17, 102) = 10.41$, $p < 0.001$), and group (genotype x age) ($F (3, 17) = 6.279$, $p = 0.005$) and significant interaction between dose and group ($F (18, 102) = 4.371$, $p < 0.001$). Therefore, Tukey's multiple comparisons post hoc tests were performed and revealed a significant effect in Iso-induced relaxation at 100 nM ($p = 0.010$), 300 nM ($p < 0.001$), and 1 μM ($p = 0.004$) between young TGneg and young Cav3 OE hearts. The difference in p values between this comparison and those presented for **Figure 2.1B** are a result of the increased multiplicity of comparisons and increased standard error of the difference when

analyzed in conjunction with the aging Iso dose-response data. Post-hoc tests also revealed significant effects in multiple groups: in aged Cav3 OE hearts compared with young Cav3 OE, there was a decrease in magnitude of relaxation of 1794 $mmHg*s^{-1}$ at 30 nM ($p = 0.010$), 1638 $mmHg*s^{-1}$ at 100 nM ($p = 0.002$), 1742 $mmHg*s^{-1}$ at 300 nM ($p = 0.013$), and 1509 $mmHg*s^{-1}$ at 1 μM ($p = 0.041$); aged TGneg hearts had a 2080 $mmHg*s^{-1}$ reduction in magnitude versus young TGneg at 1 μM ($p = 0.040$); and aged TGneg had a 2279 $mmHg*s^{-1}$ reduction in magnitude of relaxation versus aged Cav3 OE at 300 nM ($p = 0.027$) and 2356 $mmHg*s^{-1}$ reduction at 1 μM (0.021). Of note, there were no significant differences between young TGneg and aged Cav3 OE hearts at any dose.

LVDP

Assessment of Iso-induced changes in LVDP in young and aged TGneg and Cav3 OE hearts **(Figure 2.4C)** revealed significant overall effects in dose ($F (6, 102) = 17.03$, $p < 0.001$), subject matching ($F (17, 102) = 8.84$, $p < 0.001$), but not group (genotype x age) ($p = 0.066$). There was a significant interaction between dose and group ($F (3, 17) = 2.888$, $p < 0.001$). Therefore, Tukey's multiple comparisons post-hoc tests were performed and revealed no significant effect between young TGneg and young Cav3 OE hearts, with respect to Iso-induced LVDP. Post-hoc tests revealed significant reduction in aged TGneg hearts from young TGneg hearts of 58.6 mmHg at 100 nM ($p = 0.032$), 59.0 mmHg at 300 nM ($p = 0.031$), and 65.6 mmHg at 1 μM ($p = 0.013$). Also, there were significant decreases in aged TGneg compared with aged Cav3 OE of 60.1 mmHg at 300 nM ($p = 0.037$) and 66.3 mmHg at 1μM (0.017). As with the

relaxation response to Iso, there were no significant differences between young TGneg x aged Cav3 OE hearts at any dose of Iso.

Heart Rate

Analysis of the Iso-induced changes in heart rate in young and aged TGneg and Cav3 OE hearts **(Figure 2.4D)** revealed significant overall effects in dose ($F(6, 102) = 181.4$, $p < 0.001$) and subject matching ($F(17, 102) = 13.02$, $p < 0.001$), but not group (genotype x age) ($F(3, 17) = 1.072$, $p = 0.39$). There was a significant interaction between dose and group ($F(18, 102) = 2.477$, $p < 0.001$) and thus, Tukey's multiple comparisons post-hoc tests were performed. Post-hoc tests revealed significant reduction between young TGneg and aged TGneg hearts of 89.0 bpm at 3 nM ($p = 0.047$) and 99.4 at 10 nM ($p = 0.021$), but no differences between any other groups.

EC50 values of Iso responses

We adjusted the results to percent of maximal response, then applied a best-fit curve to calculate the EC50 values of each physiological response. For the measurement of age-dependent changes in Iso dose-response EC50 values, we found a significant effect of genotype on contractility **(Figure 2.4E)** ($F(1, 17) = 6.312$, $p = 0.022$), no significant effects of age ($F(1, 17) = 0.2377$, $p = 0.632$), but did see a significant interaction between age and genotype ($F(1, 17) = 6.977$, $p = 0.017$), which Tukey's post-hoc tests revealed to be a 28.5 nM decrease in the EC50 of aged TGneg mice compared with aged Cav3 OE mice ($p = 0.033$).

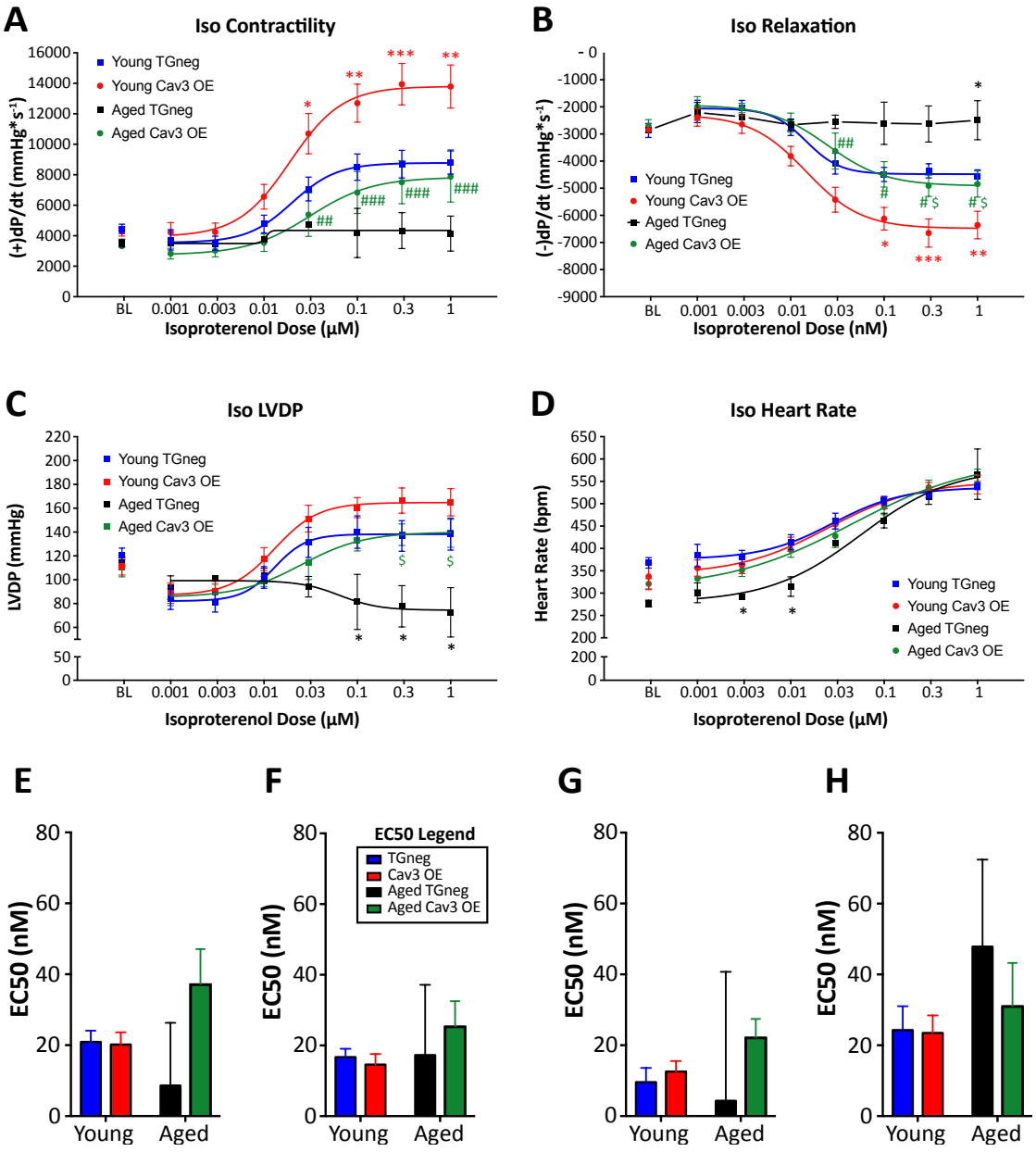

Figure 2.4: Aged Cav3 OE hearts exhibit preserved responsivity to Iso. 20-24 month-old TGneg and Cav3 OE hearts have differential responses to Iso than young hearts, but Cav3 OE hearts demonstrate responses similar to young TGneg hearts in **(A)** contractility, **(B)** relaxation, **(C)** LVDP, and **(D)** heart rate. Aged TGneg hearts have severely blunted responses in **(B)** relaxation, **(C)** LVDP, and at low doses of Iso in **(D)** heart rate. *p<0.05, **p<0.01, ***p<0.001 versus Young TGneg; #p<0.05, ##p<0.01, ###p<0.001 versus Young Cav3 OE; \$$p$<0.05 versus aged TGneg. N = 7/group young, 2 Aged TGneg, 5 Aged Cav3 OE. Data are represented as mean ± SEM.

Analysis of age-dependent changes in Iso dose response relaxation EC50 values **(Figure 2.4F)** indicated no significant effect of genotype ($F(1, 17) = 0.2194$, $p = 0.65$), age ($F(1, 17) = 1.262$, $p = 0.28$), or interaction between age and genotype ($F(1, 17) = 0.9829$, $p = 0.34$).

Similarly, there were no significant effects of genotype ($F(1, 17) = 3.461$, $p = 0.080$), age ($F(1, 17) = 0.05287$, $p = 0.82$), or interaction between age and genotype ($F(1, 17) = 1.759$, $p = 0.20$) with respect to age-dependent changes in EC50 values for LVDP EC50 values **(Figure 2.4G).** The EC50 values for heart rate **(Figure 2.4H)** also showed no significant effect of genotype ($F(1, 17) = 0.5748$, $p = 0.46$), age ($F(1, 17) = 2.363$, $p = 0.14$), or interaction between age and genotype ($F(1, 17) = 0.4184$, $p = 0.53$).

Discussion

Activation of the sympathetic nervous system in cardiac myocytes (CMs) is predominantly mediated through the βARs, which activate downstream mediators to increase contractility, relaxation, and heart rate. β_1ARs and β_2ARs, the two principal βARs expressed in CMs, differentially localize to sarcolemmal caveolae and Cav3 and cholesterol-rich t-tubules: β_2ARs are primarily present in caveolae, whereas β_1ARs are distributed to caveolar and non-caveolar membranes (2). The importance of the βAR caveolar distribution is shown by the disparate signaling profiles of β_1ARs and β_2ARs. β_1AR activation promotes positive inotropic and chronotropic responses via the stimulatory heterotrimeric G protein (Gs) that activates adenylyl cyclases (ACs,

predominantly AC5 and AC6), generating cAMP that activates protein kinase A (PKA). PKA phosphorylates a number of substrates that increase cardiomyocyte inotropy, including phospholamban (PLB), troponin I (TropI), and the L-type calcium channel (LTCC) (3-5). β_2ARs transiently stimulate compartmentalized cAMP production, primarily within cardiac T-tubules, which are enriched in Cav3 and contain LTCCs that help mediate PKA-dependent positive inotropic responses through $G_{\alpha s}$, followed by a negative chronotropic response that has been attributed to β_2AR phosphorylation by PKA followed by coupling to $G_{\alpha i}$ (2, 6, 7). The β_2AR response produces smaller inotropic and relaxation responses than the β_1AR, an observation that has been attributed to regulation by PDEs that hydrolyze cAMP and protein phosphatases that halt PKA activity and PKA substrate activity (8, 9).

The deleterious cardiac effects of persistent βAR activation by increased circulating and neuronally-released catecholamines are thought to result primarily from β_1AR activation, whereas activation of β_2ARs may produce beneficial effects that ameliorate heart failure (reviewed in (10))(11). The differential localization of βARs also has implications for cell death responses and loss of CMs that occur with advancing age: β_1AR stimulation can induce myocyte apoptosis while β_2AR activation protects CMs from apoptosis via a Gi-phosphatidylinositol 3-kinase (PI3K)-Akt pathway (11, 12). However, in the failing heart, the system that regulates and compartmentalizes βAR activity in the young heart is dysfunctional, redistributing β_2ARs from t-tubules to the cell crest, resulting in β_2AR-mediated diffuse cAMP production and phsophorylation of PLB, TropI, and C-protein, as well as increased contractile force (13, 14). Interestingly, disruption of caveolar domains by cholesterol

removal, Cav3 downregulation with siRNA, and cytoskeletal disruption can result in similar β_2AR redistribution and changes in cAMP compartmentation (3). Therefore, the distribution and activity of βARs in the sarcolemma are intrinsically linked to caveolae and cardiac health.

Cav3 expression and caveolae are also critical for cardiac health. Studies from our laboratory have described how ischemic, volatile anesthetic, and opioid-induced preconditioning, a protective phenomenon that improves recovery from subsequent lethal stress, is dependent upon Cav3 expression (15-17). The CM-specific Cav3 overexpressing (Cav3 OE) mouse model used in this study has also been used to probe the consequences of an increased number of caveolar compartments. The protective effects of cardiac-specific Cav3 OE have been assessed in several settings and show improved functional recovery in *ex vivo* hearts subjected to ischemia/reperfusion, attenuate pressure-overload hypertrophic remodeling *in vivo*, and interaction with regulators of autophagy, decrease cell death, and preservation of mitochondrial function in models of simulated ischemia and ischemia/reperfusion (1, 18, 19). Other studies have revealed increased lifespan and preserved caveolar numbers in aged mice that overexpress Cav3. No information is available regarding the connection between Cav3 OE and the βAR system (20). In this chapter, I have investigated the impact of Cav3 OE on cardiac physiological and biochemical responses to βAR stimulation with the agonist Iso.

Sympathetic responsivity plays a major role in cardiovascular homeostasis. Left ventricular contractility (aka inotropy, dP/dt_{max}) is the measure of the steepest upward slope of the left ventricular (LV) pressure-time curve, indicating the maximal

increase of pressure as the LV contracts. Likewise, LV relaxation (aka lusitropy, dP/dt_{min}) is the steepest downward slope of the LV pressure-time curve as the LV relaxes. Contractility is a major determinant of cardiac output and is a commonly-used parameter for assessing disease- or drug-induced changes in cardiac response (21). Relaxation regulates ventricular filling function and also affects cardiac output (22). Both of these parameters are related to heart rate and can reveal changes in cardiac function in different experimental environments (23).

Cav3 OE hearts produce more contractility and relaxation in response to βAR stimulation

The results here reveal that Cav3 OE amplifies βAR responsivity in hearts and isolated CMs. In **Figure 2.1A-D**, I evaluated functional responses of TGneg and Cav3 OE hearts to varying doses of Iso, which has similar affinities for activation of β_1ARs and β_2ARs. Cav3 OE CMs increased the amplitude of Iso-promoted contractility and relaxation without altering LVDP or heart rate. The lack of difference in EC50 values between the genotypes implies that Iso is acting with similar potency on βARs in Cav3 OE and TGneg hearts. The amplification of contractility and relaxation responses in Cav3 OE mice does not appear to depend on increases in heart rate or LVDP. Taken together, the data in **Figure 2.1** strongly suggest that the greater βAR responses of Cav3 OE mice is likely mediated by events that are distal to ligand-receptor interactions.

βARs activate ACs to produce cAMP, which drives subsequent PKA-mediated phosphorylation and activation of Ca^{2+} handling and sarcomeric proteins to increase contractility and relaxation. The results shown in **Figure 2.1E** demonstrate that the

increase in cAMP production with 100 nM and 1 μM Iso is greater in Cav3 OE CMs, perhaps because βARs activate AC more strongly. The potency of Iso in increasing cAMP production in isolated CMs is less than in the physiological responses (cf. **Figure 2.1E** and **Figure 2.1A-D**). That both the physiological responses and cAMP production are elevated in Cav3 OE in response to Iso implicates cAMP production as a mechanism for the increase in physiological response. However, the cAMP accumulation assays were performed in the presence of the PDE inhibitor IBMX (to increase the dynamic range of cAMP production) and isolated CMs are deloaded and contract freely in culture, therefore the two experimental systems are not identical.

Cav3 OE CMs have increased mitochondrial respiration in response to βAR stimulation

The heart predominantly produces ATP via oxidative phosphorylation, a process modulated by βAR signaling (24), which also stimulates myocardial glucose uptake through translocation of the glucose transporter GLUT4 from intracellular vesicles to the plasma membrane (25-27). β_2ARs appear to mediate this process by activating PI3K through $G_{\alpha i}$ and $G_{\beta\gamma}$, which activates Akt to perform inhibitory phosphorylation of the GLUT4 translocation inhibitor TBC1D4 (28-30). β_1ARs are involved in cardiac metabolism. The β_1AR antagonist metoprolol improves myocardial efficiency of failing hearts, prevents hypermetabolic lipolysis and fatty acid oxidation induced by norepinephrine stimulation and increases carbohydrate utilization (31-33). To support the enhanced physiological response to βAR activation, the heart consumes oxygen for mitochondrial respiration.

To test the hypothesis that Cav3 OE alters mitochondrial respiration in CMs, I used the Seahorse Extracellular Flux Analyzer to measure mitochondrial respiration at baseline (after glu + pyr addition) and after addition of 100 nM Iso **(Figure 2.1F)**. I found that mitochondrial respiration at baseline is elevated in CMs from Cav3 OE hearts compared with CMs from TGneg hearts. Iso increased respiration in CMs of both genotypes; however, Cav3 OE CMs showed a larger increase in OCR. Thus, Cav3 OE CMs have a greater increase in mitochondrial respiration in response to Iso than do TGneg CMs. Research from our laboratory has found that delayed anesthetic preconditioning increases Cav3 expression, caveolae formation, and GLUT4/Cav3 co-localization, which indicates that increased Cav3 increases glucose uptake in the myocardium (17). However, since isolated CMs are not load-bearing, the respiration data may not accurately reflect the metabolism of an intact heart. Accordingly, we have acquired equipment to measure the oxygen content of the Langendorff system before and after the heart; these experiments will be performed to evaluate the physiological importance of Iso-stimulated changes in respiration in intact hearts.

Cav3 OE hearts do not demonstrate increased desensitization in response to constant Iso stimulation

Cardiac βARs are subject to activation-dependent desensitization through various mechanisms. Phosphorylation of β_2ARs, in particular by GRK2 (aka β-ARK1) but perhaps also by PKA, or other associated kinases near the Type-1 PDZ binding sequence on the C-terminus of β_2ARs lead to β-Arrestin 2 (β-AAR2) association, G protein uncoupling, and caveolae-independent, clathrin-coated pit-mediated receptor sequestration and endocytosis (34, 35), which results in a rapid loss of hydrophobic

ligand binding to receptors (36-39). The β_1AR is less sensitive to desensitization, possibly due to enhanced binding to PDZ domain proteins such as SAP97 that attenuate β-ARR2 binding (40). To evaluate a role for Cav3 in desensitization, I exposed Cav3OE and TGneg hearts to a 30 min infusion of Iso and evaluated the loss of contractility over time **(Figure 2.2)**. The results show that neither genotype demonstrates substantial desensitization over that period. Thus, the amplified responses **(Figure 2.1A-D)** do not result from less desensitization in Cav3 OE hearts.

Cav3 OE hearts do not demonstrate increased PKA substrate phosphorylation in response to βAR stimulation

The stimulatory effect of cAMP on cardiac contraction involves PKA activation and the phosphorylation of a number of substrates, including PLB, the inhibitor of sarcoplasmic endoplasmic reticulum Ca^{2+}-ATPase (SERCA) and the myofilament regulatory protein TropI (41). I tested whether exposure to 5 min of 100nM Iso in the Langendorff preparation changes the extent of phosphorylation of these substrates in Cav3 OE and TGneg hearts **(Figure 2.3A-B)**. Although I detected Iso-dependent phosphorylation of PLB and TropI in both genotypes, the amplitude of each phosphorylation response was similar in TGneg and Cav3 OE hearts. Thus, although hearts and CMs of Cav3 OE mice show increased contractility and cAMP production, respectively, cAMP-mediated phosphorylation responses are not generally increased in these mice. Of note, prior data indicate that β_2AR-promoted increase in cAMP can be dissociated from PLB phosphorylation, Ca^{2+} current, and contractility (42).

Cav3 OE hearts are resistant to age-related loss of βAR responsivity

The deleterious cardiac effects of persistent βAR activation by increased catecholamines in disease and advanced age are thought to result primarily from β_1AR activation (10). The sequelae of chronic hyper adrenergic signaling include: β_1AR downregulation, uncoupling of β_2ARs mediated via $G_{\alpha i}$ and GRK2 upregulation, and downregulation of ACs (43-47). These losses blunt βAR responses in patients with heart failure and have led to the use of βAR (especially β_1AR blockers, such as metoprolol) to blunt maladaptive βAR responses (48-53). Accordingly, βAR blocker therapy is a standard-of-care treatment for patients with heart failure as it improves mortality, morbidity, and LV ejection fraction (54-58).

Because of this dysregulation of βARs, the differential responses to βAR stimulation in Cav3 OE hearts **(Figure 2.1A-D)** have implications for aging-related cardiac dysfunction. Expression of Cav3 and caveolar number decrease in the aged heart (59, 60). Studies of caveolae-resident receptors, G-proteins, kinases, and channels have identified aging-related changes in many components of this pathway, including $G_{\alpha s}$, ACs, and LTCCs; but previous work has not linked these changes to alterations in the membrane domain that localizes such components (61-65). In CMs from young animals, redistribution of β_2ARs from Cav3-rich domains prevents coupling to $G_{\alpha i}$ and PDE activity, resulting in an elevated diffuse cAMP pool similar to β_1AR signaling (8, 14, 66). Therefore, altered Cav3 expression in aged animals and changes in expression and caveolar localization of βAR pathway components may contribute to the loss of function in aged and failing hearts. Since hearts from young Cav3OE mice have elevated contractile response **(Figure 2.1A-B)**, one might expect

that age-dependent changes in βAR response would be more detrimental in these mice than in TGneg mice. However, aged Cav3 OE hearts show greater increases in Iso-induced contractility than aged TGneg hearts, which exhibit a blunted ability to increase contractility or relaxation **(Figure 2.4A-B)**. Since cardiac β_1AR expression is predictive of the maximal exercise response of heart failure, these data suggest that Cav3OE "protects" the heart from aging-induced changes, such as decreased expression of β_1ARs (50).

Conclusions

The roles of the two major cardiac βAR isoforms and their differences in localization and regulatory pathways are of interest as targets for therapeutic intervention, currently directly with β-blockers. Our findings are the first to implicate Cav3 OE as an amplifier of βAR responsivity in young and aged hearts, however, the detailed mechanisms and effects of Cav3 OE on βARs and their signaling remain unclear; although young Cav3 OE hearts produce greater contractility and relaxation, aged Cav3 OE hearts also show resistance to certain aging-related losses in cardiac function. Importantly, the activation of major mediators of contractility and relaxation is not different between genotypes and we found no differential βAR desensitization in rate or level of response in Cav3 OE hearts. Taken together, the results in this study demonstrate that the increase in caveolae and Cav3 expression in Cav3 OE hearts enable enhanced βAR-dependent contractility into old age, marking Cav3 as a target for modulation of this vital cardiac signaling pathway which may contribute to the improved lifespan of Cav3 OE mice (unpublished Patel lab data).

Chapter 2 is being prepared for submission for publication; authors include Busija, Anna R; Schilling, Jan M.; Roth, David M.; Insel, Paul A.; and Patel, Hemal H. The dissertation author was the primary investigator of these studies.

REFERENCES

1. Tsutsumi YM, Horikawa YT, Jennings MM, Kidd MW, Niesman IR, Yokoyama U, Head BP, Hagiwara Y, Ishikawa Y, Miyanohara A, Patel PM, Insel PA, Patel HH, Roth DM. Cardiac-specific overexpression of caveolin-3 induces endogenous cardiac protection by mimicking ischemic preconditioning. Circulation. 2008;118(19):1979-88.

2. Xiang Y, Rybin VO, Steinberg SF, Kobilka B. Caveolar localization dictates physiologic signaling of beta 2-adrenoceptors in neonatal cardiac myocytes. J Biol Chem. 2002;277(37):34280-6.

3. Balijepalli RC, Foell JD, Hall DD, Hell JW, Kamp TJ. Localization of cardiac L-type Ca(2+) channels to a caveolar macromolecular signaling complex is required for beta(2)-adrenergic regulation. Proc Natl Acad Sci U S A. 2006;103(19):7500-5.

4. Ballard-Croft C, Locklar AC, Kristo G, Lasley RD. Regional myocardial ischemia-induced activation of MAPKs is associated with subcellular redistribution of caveolin and cholesterol. Am J Physiol Heart Circ Physiol. 2006;291(2):H658-67.

5. Li L, Desantiago J, Chu G, Kranias EG, Bers DM. Phosphorylation of phospholamban and troponin I in beta-adrenergic-induced acceleration of cardiac relaxation. Am J Physiol Heart Circ Physiol. 2000;278(3):H769-79.

6. Freedman NJ, Lefkowitz RJ. Desensitization of G protein-coupled receptors. Recent Prog Horm Res. 1996;51:319-51; discussion 52-3.

7. Hausdorff WP, Bouvier M, O'Dowd BF, Irons GP, Caron MG, Lefkowitz RJ. Phosphorylation sites on two domains of the beta 2-adrenergic receptor are involved in distinct pathways of receptor desensitization. J Biol Chem. 1989;264(21):12657-65.

8. Chen-Izu Y, Xiao RP, Izu LT, Cheng H, Kuschel M, Spurgeon H, Lakatta EG. G(i)-dependent localization of beta(2)-adrenergic receptor signaling to L-type Ca(2+) channels. Biophys J. 2000;79(5):2547-56.

9. Macdougall DA, Agarwal SR, Stopford EA, Chu H, Collins JA, Longster AL, Colyer J, Harvey RD, Calaghan S. Caveolae compartmentalise beta2-adrenoceptor signals by curtailing cAMP production and maintaining phosphatase activity in the sarcoplasmic reticulum of the adult ventricular myocyte. J Mol Cell Cardiol. 2012;52(2):388-400.

10. Xiao RP, Zhu W, Zheng M, Chakir K, Bond R, Lakatta EG, Cheng H. Subtype-specific beta-adrenoceptor signaling pathways in the heart and their potential clinical implications. Trends Pharmacol Sci. 2004;25(7):358-65.

11. Communal C, Singh K, Sawyer DB, Colucci WS. Opposing effects of beta(1)- and beta(2)-adrenergic receptors on cardiac myocyte apoptosis : role of a pertussis toxin-sensitive G protein. Circulation. 1999;100(22):2210-2.

12. Jo SH, Leblais V, Wang PH, Crow MT, Xiao RP. Phosphatidylinositol 3-kinase functionally compartmentalizes the concurrent G(s) signaling during beta2-adrenergic stimulation. Circ Res. 2002;91(1):46-53.

13. Kaumann A, Bartel S, Molenaar P, Sanders L, Burrell K, Vetter D, Hempel P, Karczewski P, Krause EG. Activation of beta2-adrenergic receptors hastens relaxation and mediates phosphorylation of phospholamban, troponin I, and C-protein in ventricular myocardium from patients with terminal heart failure. Circulation. 1999;99(1):65-72.

14. Nikolaev VO, Moshkov A, Lyon AR, Miragoli M, Novak P, Paur H, Lohse MJ, Korchev YE, Harding SE, Gorelik J. Beta2-adrenergic receptor redistribution in heart failure changes cAMP compartmentation. Science. 2010;327(5973):1653-7.

15. See Hoe LE, Schilling JM, Tarbit E, Kiessling CJ, Busija AR, Niesman IR, Du Toit E, Ashton KJ, Roth DM, Headrick JP, Patel HH, Peart JN. Sarcolemmal cholesterol and caveolin-3 dependence of cardiac function, ischemic tolerance, and opioidergic cardioprotection. Am J Physiol Heart Circ Physiol. 2014;307(6):H895-903.

16. Tsutsumi YM, Kawaraguchi Y, Niesman IR, Patel HH, Roth DM. Opioid-induced preconditioning is dependent on caveolin-3 expression. Anesth Analg. 2010;111(5):1117-21.

17. Tsutsumi YM, Kawaraguchi Y, Horikawa YT, Niesman IR, Kidd MW, Chin-Lee B, Head BP, Patel PM, Roth DM, Patel HH. Role of caveolin-3 and glucose transporter-4 in isoflurane-induced delayed cardiac protection. Anesthesiology. 2010;112(5):1136-45.

18. Kassan A, Pham U, Nguyen Q, Reichelt ME, Cho E, Patel PM, Roth DM, Head BP, Patel HH. Caveolin-3 plays a critical role in autophagy after ischemia-reperfusion. Am J Physiol Cell Physiol. 2016;311(6):C854-C65.

19. Horikawa YT, Panneerselvam M, Kawaraguchi Y, Tsutsumi YM, Ali SS, Balijepalli RC, Murray F, Head BP, Niesman IR, Rieg T, Vallon V, Insel PA, Patel HH, Roth DM. Cardiac-specific overexpression of caveolin-3 attenuates cardiac hypertrophy and increases natriuretic peptide expression and signaling. J Am Coll Cardiol. 2011;57(22):2273-83.

20. Wang J, Schilling JM, Niesman IR, Headrick JP, Finley JC, Kwan E, Patel PM, Head BP, Roth DM, Yue Y, Patel HH. Cardioprotective trafficking of caveolin to mitochondria is Gi-protein dependent. Anesthesiology. 2014;121(3):538-48.

21. Guth BD, Chiang AY, Doyle J, Engwall MJ, Guillon JM, Hoffmann P, Koerner J, Mittelstadt S, Ottinger S, Pierson JB, Pugsley MK, Rossman EI, Walisser J, Sarazan RD. The evaluation of drug-induced changes in cardiac inotropy in dogs: Results from a HESI-sponsored consortium. J Pharmacol Toxicol Methods. 2015;75:70-90.

22. Zile MR, Gaasch WH. Load-dependent left ventricular relaxation in conscious dogs. Am J Physiol. 1991;261(3 Pt 2):H691-9.

23. Pugsley MK, Guth B, Chiang AY, Doyle JM, Engwall M, Guillon JM, Hoffmann PK, Koerner JE, Mittelstadt SW, Pierson JB, Rossman EI, Sarazan DR, Parish ST. An evaluation of the utility of LVdP/dt40, QA interval, LVdP/dtmin and Tau as indicators of drug-induced changes in contractility and lusitropy in dogs. J Pharmacol Toxicol Methods. 2017;85:1-21.

24. Stanley WC, Recchia FA, Lopaschuk GD. Myocardial substrate metabolism in the normal and failing heart. Physiol Rev. 2005;85(3):1093-129.

25. Egert S, Nguyen N, Schwaiger M. Contribution of alpha-adrenergic and beta-adrenergic stimulation to ischemia-induced glucose transporter (GLUT) 4 and GLUT1 translocation in the isolated perfused rat heart. Circ Res. 1999;84(12):1407-15.

26. Rattigan S, Edwards SJ, Hettiarachchi M, Clark MG. The effects of alpha- and beta-adrenergic agents, Ca2+ and insulin on 2-deoxyglucose uptake and phosphorylation in perfused rat heart. Biochim Biophys Acta. 1986;889(2):225-35.

27. Rattigan S, Appleby GJ, Clark MG. Insulin-like action of catecholamines and Ca2+ to stimulate glucose transport and GLUT4 translocation in perfused rat heart. Biochim Biophys Acta. 1991;1094(2):217-23.

28. Nevzorova J, Bengtsson T, Evans BA, Summers RJ. Characterization of the beta-adrenoceptor subtype involved in mediation of glucose transport in L6 cells. Br J Pharmacol. 2002;137(1):9-18.

29. Zhang W, Yano N, Deng M, Mao Q, Shaw SK, Tseng YT. beta-Adrenergic receptor-PI3K signaling crosstalk in mouse heart: elucidation of immediate downstream signaling cascades. PLoS One. 2011;6(10):e26581.

30. Sakamoto K, Holman GD. Emerging role for AS160/TBC1D4 and TBC1D1 in the regulation of GLUT4 traffic. Am J Physiol Endocrinol Metab. 2008;295(1):E29-37.

31. Eichhorn EJ, Heesch CM, Barnett JH, Alvarez LG, Fass SM, Grayburn PA, Hatfield BA, Marcoux LG, Malloy CR. Effect of metoprolol on myocardial function and energetics in patients with nonischemic dilated cardiomyopathy: a randomized, double-blind, placebo-controlled study. J Am Coll Cardiol. 1994;24(5):1310-20.

32. Lommi J, Kupari M, Yki-Jarvinen H. Free fatty acid kinetics and oxidation in congestive heart failure. Am J Cardiol. 1998;81(1):45-50.

33. From AH. Should manipulation of myocardial substrate utilization patterns be a component of the congestive heart failure therapeutic paradigm? J Card Fail. 1998;4(2):127-9.

34. Mukherjee S, Tessema M, Wandinger-Ness A. Vesicular trafficking of tyrosine kinase receptors and associated proteins in the regulation of signaling and vascular function. Circ Res. 2006;98(6):743-56.

35. Marchese A, Paing MM, Temple BR, Trejo J. G protein-coupled receptor sorting to endosomes and lysosomes. Annu Rev Pharmacol Toxicol. 2008;48:601-29.

36. Hausdorff WP, Campbell PT, Ostrowski J, Yu SS, Caron MG, Lefkowitz RJ. A small region of the beta-adrenergic receptor is selectively involved in its rapid regulation. Proc Natl Acad Sci U S A. 1991;88(8):2979-83.

37. Hertel C, Coulter SJ, Perkins JP. A comparison of catecholamine-induced internalization of beta-adrenergic receptors and receptor-mediated endocytosis of epidermal growth factor in human astrocytoma cells. Inhibition by phenylarsine oxide. The Journal of biological chemistry. 1985;260(23):12547-53.

38. Mahan LC, Motulsky HJ, Insel PA. Do agonists promote rapid internalization of beta-adrenergic receptors? Proc Natl Acad Sci U S A. 1985;82(19):6566-70.

39. Wang HY, Berrios M, Malbon CC. Localization of beta-adrenergic receptors in A431 cells in situ. Effect of chronic exposure to agonist. The Biochemical journal. 1989;263(2):533-8.

40. He J, Bellini M, Inuzuka H, Xu J, Xiong Y, Yang X, Castleberry AM, Hall RA. Proteomic analysis of beta1-adrenergic receptor interactions with PDZ scaffold proteins. The Journal of biological chemistry. 2006;281(5):2820-7.

41. Bean BP, Nowycky MC, Tsien RW. Beta-adrenergic modulation of calcium channels in frog ventricular heart cells. Nature. 1984;307(5949):371-5.

42. Xiao RP, Hohl C, Altschuld R, Jones L, Livingston B, Ziman B, Tantini B, Lakatta EG. Beta 2-adrenergic receptor-stimulated increase in cAMP in rat heart cells is not coupled to changes in Ca2+ dynamics, contractility, or phospholamban phosphorylation. J Biol Chem. 1994;269(29):19151-6.

43. Bristow MR. Mechanism of action of beta-blocking agents in heart failure. Am J Cardiol. 1997;80(11A):26L-40L.

44. Bristow MR, Minobe W, Rasmussen R, Larrabee P, Skerl L, Klein JW, Anderson FL, Murray J, Mestroni L, Karwande SV, Fowler M, Ginsburg R. Beta-adrenergic neuroeffector abnormalities in the failing human heart are produced by local rather than systemic mechanisms. J Clin Invest. 1992;89(3):803-15.

45. Feldman AM, Cates AE, Veazey WB, Hershberger RE, Bristow MR, Baughman KL, Baumgartner WA, Van Dop C. Increase of the 40,000-mol wt pertussis toxin substrate (G protein) in the failing human heart. J Clin Invest. 1988;82(1):189-97.

46. Ungerer M, Bohm M, Elce JS, Erdmann E, Lohse MJ. Altered expression of beta-adrenergic receptor kinase and beta 1-adrenergic receptors in the failing human heart. Circulation. 1993;87(2):454-63.

47. Chen LA, Vatner DE, Vatner SF, Hittinger L, Homcy CJ. Decreased Gs alpha mRNA levels accompany the fall in Gs and adenylyl cyclase activities in compensated left ventricular hypertrophy. In heart failure, only the impairment in adenylyl cyclase activation progresses. J Clin Invest. 1991;87(1):293-8.

48. Fowler MB, Laser JA, Hopkins GL, Minobe W, Bristow MR. Assessment of the beta-adrenergic receptor pathway in the intact failing human heart: progressive receptor down-regulation and subsensitivity to agonist response. Circulation. 1986;74(6):1290-302.

49. Colucci WS, Denniss AR, Leatherman GF, Quigg RJ, Ludmer PL, Marsh JD, Gauthier DF. Intracoronary infusion of dobutamine to patients with and without severe congestive heart failure. Dose-response relationships, correlation with circulating catecholamines, and effect of phosphodiesterase inhibition. J Clin Invest. 1988;81(4):1103-10.

50. White M, Yanowitz F, Gilbert EM, Larrabee P, O'Connell JB, Anderson JL, Renlund D, Mealey P, Abraham WT, Bristow MR. Role of beta-adrenergic receptor downregulation in the peak exercise response in patients with heart failure due to idiopathic dilated cardiomyopathy. Am J Cardiol. 1995;76(17):1271-6.

51. Heilbrunn SM, Shah P, Bristow MR, Valantine HA, Ginsburg R, Fowler MB. Increased beta-receptor density and improved hemodynamic response to catecholamine stimulation during long-term metoprolol therapy in heart failure from dilated cardiomyopathy. Circulation. 1989;79(3):483-90.

52. Hall JA, Kaumann AJ, Brown MJ. Selective beta 1-adrenoceptor blockade enhances positive inotropic responses to endogenous catecholamines mediated through beta 2-adrenoceptors in human atrial myocardium. Circ Res. 1990;66(6):1610-23.

53. Gilbert EM, Abraham WT, Olsen S, Hattler B, White M, Mealy P, Larrabee P, Bristow MR. Comparative hemodynamic, left ventricular functional, and antiadrenergic effects of chronic treatment with metoprolol versus carvedilol in the failing heart. Circulation. 1996;94(11):2817-25.

54. Sabbah HN, Shimoyama H, Kono T, Gupta RC, Sharov VG, Scicli G, Levine TB, Goldstein S. Effects of long-term monotherapy with enalapril, metoprolol, and digoxin on the progression of left ventricular dysfunction and dilation in dogs with reduced ejection fraction. Circulation. 1994;89(6):2852-9.

55. Morita H, Suzuki G, Mishima T, Chaudhry PA, Anagnostopoulos PV, Tanhehco EJ, Sharov VG, Goldstein S, Sabbah HN. Effects of long-term monotherapy with metoprolol CR/XL on the progression of left ventricular dysfunction and remodeling in dogs with chronic heart failure. Cardiovasc Drugs Ther. 2002;16(5):443-9.

56. Waagstein F, Caidahl K, Wallentin I, Bergh CH, Hjalmarson A. Long-term beta-blockade in dilated cardiomyopathy. Effects of short- and long-term metoprolol treatment followed by withdrawal and readministration of metoprolol. Circulation. 1989;80(3):551-63.

57. Eichhorn EJ, Bristow MR. Medical therapy can improve the biological properties of the chronically failing heart. A new era in the treatment of heart failure. Circulation. 1996;94(9):2285-96.

58. Bristow MR, Gilbert EM, Abraham WT, Adams KF, Fowler MB, Hershberger RE, Kubo SH, Narahara KA, Ingersoll H, Krueger S, Young S, Shusterman N. Carvedilol produces dose-related improvements in left ventricular function and

survival in subjects with chronic heart failure. MOCHA Investigators. Circulation. 1996;94(11):2807-16.

59. Kawabe JI, Grant BS, Yamamoto M, Schwencke C, Okumura S, Ishikawa Y. Changes in caveolin subtype protein expression in aging rat organs. Mol Cell Endocrinol. 2001;176(1-2):91-5.

60. Ratajczak P, Damy T, Heymes C, Oliviero P, Marotte F, Robidel E, Sercombe R, Boczkowski J, Rappaport L, Samuel JL. Caveolin-1 and -3 dissociations from caveolae to cytosol in the heart during aging and after myocardial infarction in rat. Cardiovasc Res. 2003;57(2):358-69.

61. Kandilci HB, Tuncay E, Zeydanli EN, Sozmen NN, Turan B. Age-related regulation of excitation-contraction coupling in rat heart. J Physiol Biochem. 2011;67(3):317-30.

62. Xiao RP, Tomhave ED, Wang DJ, Ji X, Boluyt MO, Cheng H, Lakatta EG, Koch WJ. Age-associated reductions in cardiac beta1- and beta2-adrenergic responses without changes in inhibitory G proteins or receptor kinases. J Clin Invest. 1998;101(6):1273-82.

63. Kilts JD, Akazawa T, Richardson MD, Kwatra MM. Age increases cardiac Galpha(i2) expression, resulting in enhanced coupling to G protein-coupled receptors. J Biol Chem. 2002;277(34):31257-62.

64. Kilts JD, Akazawa T, El-Moalem HE, Mathew JP, Newman MF, Kwatra MM. Age increases expression and receptor-mediated activation of G alpha i in human atria. J Cardiovasc Pharmacol. 2003;42(5):662-70.

65. Juhaszova M, Rabuel C, Zorov DB, Lakatta EG, Sollott SJ. Protection in the aged heart: preventing the heart-break of old age? Cardiovasc Res. 2005;66(2):233-44.

66. Horikawa YT, Patel HH, Tsutsumi YM, Jennings MM, Kidd MW, Hagiwara Y, Ishikawa Y, Insel PA, Roth DM. Caveolin-3 expression and caveolae are required for isoflurane-induced cardiac protection from hypoxia and ischemia/reperfusion injury. J Mol Cell Cardiol. 2008;44(1):123-30.

CHAPTER 3: ALTERED ISOPROTERENOL RESPONSE OF CARDIAC MYOCYTE-SPECIFIC CAVEOLIN-3 OVEREXPRESSION IS NOT MEDIATED INDEPENDENTLY VIA ADENYLYL CYCLASES, β_1-ADRENERGIC RECEPTORS, OR β_2-ADRENERGIC RECEPTORS

Abstract

The differential localization of βAR isoforms within and outside caveolae has been implicated in the compartmentation of β_2AR-mediated signaling whereas β_1ARs contribute to global upregulation of cAMP. However, the influence of altered expression of Cav3 on compartmentation of βARs has not been defined. In this study, I tested the hypotheses that 1) the increased expression of Cav3 and number of caveolae in the sarcolemmal membrane of Cav3 OE cardiac myocytes (CMs) would alter the distribution of βARs and effectors of cAMP signals, and 2) Cav3 OE βAR responses would be biased toward β_2AR activation. I found that neither β_1ARs nor β_2ARs, nor phosphodiesterase 4 (PDE4) isoforms are disparately aggregated within Cav3 OE caveolae. Additionally, although expression of major adenylyl cyclase isoforms is increased in Cav3 OE caveolar fractions, stimulation of adenylyl cyclase, or selective activation of β_1ARs or β_2ARs did not induce greater physiological or cAMP response in Cav3 OE hearts or CMs, respectively. In Cav3 OE CMs, inhibition of PDEs had a disparate effect on cAMP production by Iso but not forskolin, results that implicate PDE compartmentation of caveolar cAMP signal in the regulation of PDE activity and cAMP concentrations in CMs and the intact heart.

Experimental procedures

Animals

Laboratory Animals were maintained as described in Chapter 2.

Langendorff isolated perfused heart model and Iso administrations

Hearts were isolated and perfused on the Langendorff apparatus as described in Chapter 2. βAR antagonists (for β_2ARs, 100 nM ICI18, 551: Tocris; for β_1ARs, 30 nM CGP20712a: Tocris) were introduced after 10 min of cardiac acclimatization at 100 times the applicable dose at 0.01x flow rate via a syringe driver (Harvard Apparatus) into perfusion buffer proximal to the heart and continued throughout the Iso bolus administration protocol (total volume after injection port = 500 μl). Dose-response curves of Iso (Isuprel: Hospira, Inc.) were performed after 10 min of antagonist treatment by bolus injection of 250 μl of the lowest concentration of Iso (1 nM) into the perfusion system proximal to the cardiac cannula. After a 10 min wash-out period, the serial doses of Iso were delivered. Peak LVDP, ±dP/dt, and heart rate were measured after each dose. Norepinephrine (NE) and zinterol dose-responses were administered similarly to Iso. Forskolin (10 μM) was also used to activate AC.

Adult mouse cardiac myocyte isolation

Adult mouse CM isolation was performed as described in Chapter 2.

Measurement of cAMP production in adult mouse CMs

Adult CMs were plated on 24-well laminin-coated cell culture plates for 1 h, then media was exchanged for Joklik without BDM supplemented with 1.2 mM $CaCl_2$. Cells were prepared for cAMP accumulation by incubation with media or 200 μM IBMX: Sigma for 10 min with antagonists 100 nM ICI118,551 or 3 nM CGP20712. Media, DMSO, or agonists were introduced after 10 min incubation ± IBMX and antagonists: Forskolin (1 and 10 μM, Tocris) was administered ± IBMX and in conjunction with 1 μM Iso ± IBMX. 1 μM Iso was administered to IBMX + ICI- and CGP-incubated wells. Dobutamine and zinterol (both at 10 μM, Tocris) were used as β_1AR- and β_2AR-selective agonists, respectively. Assay medium was aspirated after 10 min of stimulation. Cells were washed once with ice-cold PBS; 50 μl of ice-cold 7.5% w/v trichloroacetic acid (TCA: Ricca Chemical Co.) was then immediately added to each well.

TCA extracts were assayed for cAMP content via competitive radioimmunoassay as described in Chapter 2.

Caveolar fractionation

Hearts from 2-4 month-old Cav3 OE and TGneg mice were excised by thoracotomy and flash-frozen in liquid nitrogen, then pulverized on dry ice before lysis in high-pH lysis buffer (500 mM Na_2CO_3 pH 11, 5 mM EDTA, Halt protease inhibitor cocktail (Thermo Scientific), PMSF, pepstatin, and leupeptin (Sigma)) in a Dounce glass-glass homogenizer, then drawn through a 23g needle 10 times. Samples were sonicated five times for 10 sec each at 40% amplitude (Sonics VibraCell) on ice,

then centrifuged for 10 min at 1000xg and 4ºC. Bradford assay was performed and protein content normalized between samples to 15 µg protein/ml, then mixed with 90% sucrose at the bottom of a Beckman 12 mL ultraclear ultracentrifuge tube and layered with 35% and 5% sucrose concentrations. Discontinuous sucrose gradients were centrifuged in a Beckman Ultracentrifuge SW41 swinging bucket rotor at 175,000xg for 18 h at 4ºC, then the gradients were separated into 12 1-mL fractions, mixed well, and aliquoted into a 50:50 mix of LDS loading buffer (Bio-Rad) and 20% SDS loading buffer in the presence of 100 mM dithiothreitol. The whole heart lysates used to make the fractions were also aliquoted and stored at -80ºC.

De-glycosylated buoyant fractions

Pooled caveolar fractions (CFs) from caveolar fractionation were incubated at equal volumes with a PNGase F deglycosylation kit (P0704S: New England Biolabs) for 2 h at 37ºC to remove carbohydrate modifications prior to immunoblot analysis of βAR expression.

Immunoblots

Whole lysates and buoyant fractions (pooled from the 4-6 mL fractions of the discontinuous sucrose gradient) were subjected to sodium dodecyl sulfate polyacrylamide gel electrophoresis (SDS-PAGE) as in Chapter 2. Antibodies used were against ACV/VI (1:50 sc-590, Santa Cruz Biotech), β_1AR (1:1000 ab3442, Abcam, 40-50 kDa glycosylated, ~30 kDa de-glycosylated), β_2AR (1:100 sc-570 Santa Cruz Biotech, 40-50 kDa glycosylated, ~30 kDa de-glycosylated), β_2AR (1:1000

NBP2-15564 Novus Biologicals, 40-50 kDa glycosylated, ~30 kDa de-glycosylated), Cav1 (1:200 sc-894 Santa Cruz Biotech, 20 kDa), PDE4 (1:500 PD4-101AP FabGennix, predominant isoform PDE4D4 at 120 kDa), GAPDH-HRP (1:500 sc-25778, Santa Cruz Biotech, 37 kDa), Cav3 (1:1000 BD610421, BD Bioscience, 13 kDa major, 18 kDa minor, ~40 kDa dimer bands), $G_{\alpha s}$ (1:200 sc-823 Santa Cruz Biotech, 43 kDa detected band), PKAc-α (1:1000 #4782S Cell Signaling, ~40 kDa detected band), and Ryr (1:1000 ab2868 Abcam, detected >300 kDa). Blots were washed thrice for 10 min in TBST at room temperature, then incubated at room temperature with 3% BSA-TBST containing horseradish peroxide-conjugated (HRP) secondary antibodies raised in mouse against rabbit (Santa Cruz Biotechnology sc-2357), in donkey against goat (Santa Cruz Biotechnology sc-2020), and in goat against mouse (Santa Cruz Biotechnology sc-2004) at 1:1000 dilutions. After three more washes with TBST, HRP activity was detected using SuperSignal West Dura chemiluminescence reagent (Thermo Scientific) or Lumigen Ultra TMA-6 (Lumigen) and recorded using a UVP exposure box and CCD camera (UVP, LLC). Intensity values were measured with Image Studio Lite and signal measured in whole cell lysates (WCL) normalized to GAPDH signal. Caveolar fractions were added to SDS-PAGE gels by volume and were not normalized.

Statistical analysis

All data analysis and statistics were performed with GraphPad Prism 7 software (GraphPad Software Inc., La Jolla, CA). All data are expressed as means ± S.E.M. Significant differences were accepted for α when $p < 0.05$ for all statistical tests.

2-way ANOVA of repeated measures

Peak responses after bolus for each agonist dose from Langendorff studies were analyzed by 2-way repeated measures analysis of variance (ANOVA: genotype x dose Iso) with subject matching, followed by the indicated multiple comparisons post-hoc tests on individual doses.

Ordinary 2-way ANOVA of isolated responses

Peak responses after bolus for 1 μM Iso ± antagonist groups or single agonists for functional responses and cAMP accumulation were analyzed by 2-way ANOVA.

Assessment of EC50 values and 2-way ANOVA

Due to a slight depression in LVDP, contractility, and relaxation at the smallest dose of Iso and because the similarities in baseline measurements in both genotypes, dose-response curve fitting was performed with the unstimulated values excluded to provide accurate EC50 values. Dose-response data from all experiments were normalized to 0%-100% of response and fitted to a four-parameter dose-response curve with variable slope, from which LogEC50 values were calculated. LogEC50 values from Iso ± inhibitors were compared by 2-way ANOVA (genotype x inhibitor) with the indicated post-hoc multiple comparisons tests. LogEC50 values were transformed to EC50 for graphical presentation and are presented as ± S.E.M.

3-way ANOVA of 1 μM or 10 μM Iso ± IBMX or 1 μM or 10 μM forskolin ± IBMX

Responses across two Iso or two forskolin doses in the presence and absence of IBMX were analyzed by 3-way ANOVA to characterize the relationship between the interactions of genotype and IBMX across different doses of agonist.

Results

Cav3 OE hearts do not express different amounts or caveolar localization of βAR pathway proteins with the exception of ACV/VI, which is increased within caveolae

To test the hypothesis that Cav3 OE alters distribution of βAR pathway proteins to caveolae, I compared TGneg and Cav3 OE hearts (n=6/group) for the expression of proteins in the βAR signal transduction pathway in WCL **(Figure 3.1A)**. Cav3 was increased by 3.1 fold in Cav3 OE ($p < 0.001$) but I detected no significant differences in expression of ACV/VI, Cav1, β_1AR, PDE4, or β_2AR **(Figure 3.1A)**.

A sucrose gradient fractionation technique was used to isolate caveolar fractions (CFs), fractions 4-6, from WCL **(Figure 3.1B)** to evaluate CFs for differences in βAR signal transduction pathway protein localization in TGneg and Cav3 OE hearts ($N = 3$/group) **(Figure 3.1C)**. CFs from Cav3OE hearts had a 3.5-fold increase in Cav3 protein ($p = 0.002$) and a 1.4-fold increase in expression of ACV/VI compared with CFs from TGneg hearts ($p = 0.030$).

CFs were de-glycosylated with PNGase F to reduce the molecular mass of glycosylated βAR isoform proteins in CFs. β_1ARs and β_2ARs were reduced to ~30 kDa after deglycosylation. Neither β_1AR nor β_2AR expression was increased in Cav3 OE CFs.

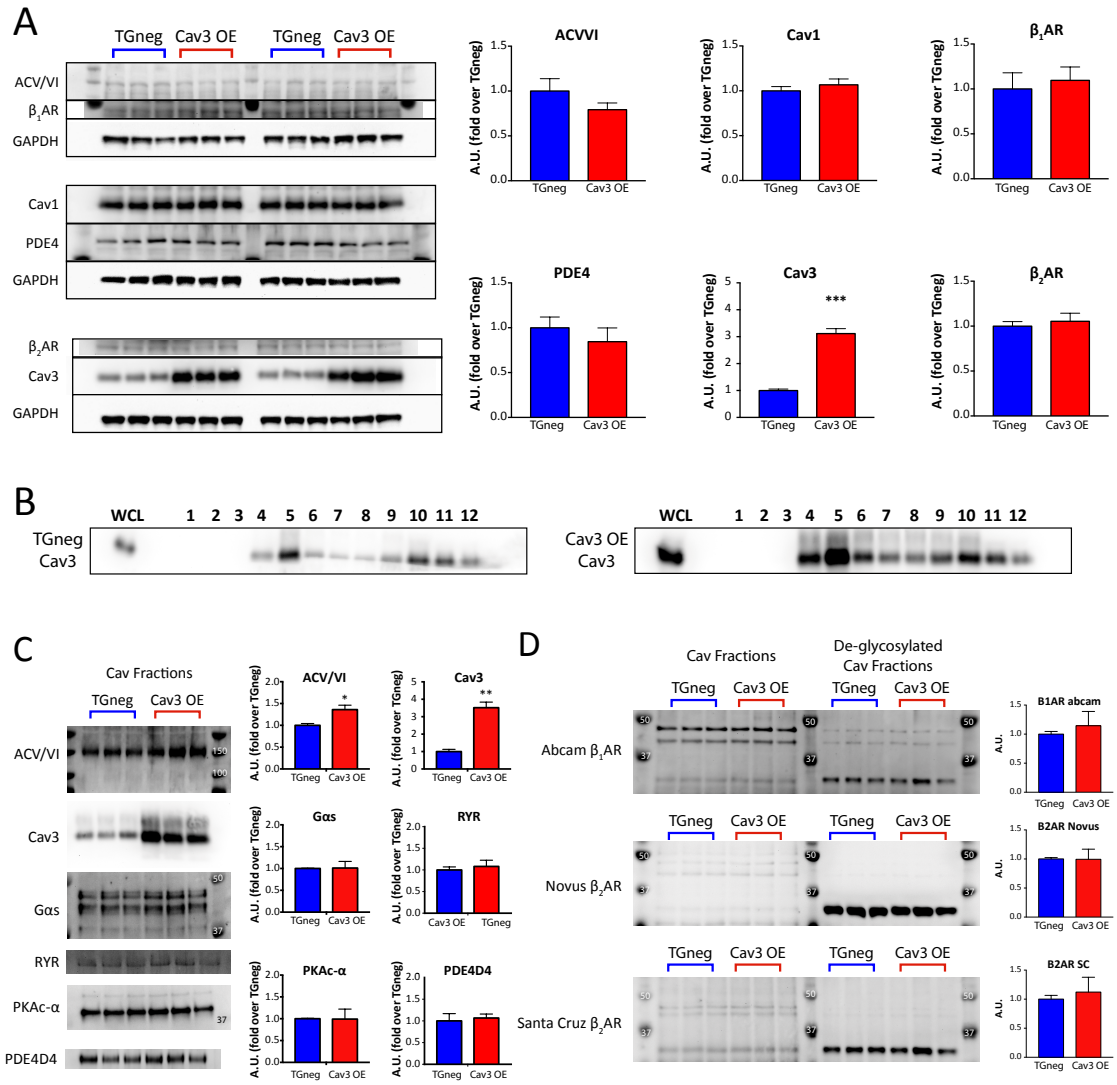

Figure 3.1: Cav3 OE does not alter expression or distribution of βAR pathway proteins except for increased compartmentation of ACV/VI. (A) Qualitative analysis of ACV/VI, β_1AR, β_2AR, PDE4D4, Cav1, and Cav3 expression in whole cell lysates of TGneg and Cav3 OE hearts. **(B)** Distribution of caveolar fractions in the 12 fractions from a discontinuous sucrose gradient. **(C)** Qualitative analysis of ACV/VI, Gas, Ryr, PKAc-α, and PDE4D4 localization to caveolar fractions. **(D)** Qualitative analysis of de-glycosylated β_1AR and β_2AR protein in caveolar fractions. *p<0.05, *p<0.01, *p<0.001 versus TGneg. N = 6/group whole heart lysate, 3/group cav fractions. Data are represented as mean + SEM.

AC activation with forskolin does not yield different responses in Cav3 OE hearts or CMs compared with TGneg hearts and CMs

As shown in Chapter 2, functional and cAMP responses to Iso-stimulated βAR activation were greater in Cav3 OE than in TGneg hearts and CMs. To test if direct activation of AC would yield similar results, we evaluated the effects of 10 μM forskolin (a non-selective stimulant of ACs) on hearts from Cav3 OE and TGneg mice **(Figure 3.2)** ($N = 6$). Both genotypes had increased contractility, relaxation, LVDP, and heart rate in response to forskolin, but the genotypes yielded similar responses. Forskolin increased contractility **(Figure 3.2A)** ($F(1, 12) = 111.4$, $p < 0.001$) but no significant difference was found between genotype ($F(1, 12) = 0.2836$, $p = 0.60$), with subject matching ($F(12, 12) = 0.6562$, $p = 0.76$) or interaction between dose and genotype ($F(1, 12) < 0.001$, $p = 0.99$). Sidak's multiple comparisons post-hoc tests revealed significant forskolin-induced increases of 4015 $mmHg*s^{-1}$ and 4016 $mmHg*s^{-1}$ in TGneg hearts and Cav3 OE mice (both $p < 0.001$), respectively.

Forskolin increased relaxation **(Figure 3.2B)** ($F(1, 12) = 136.2$, $p < 0.001$) but without significant effect between the genotypes ($F(1, 12)$ 0.3084, $p = 0.59$), with subject matching ($F(12, 12) = 1.016$, $p = 0.49$ or significant interaction between dose and genotype ($F(1, 12)$ 0.01052, $p = 0.92$). Sidak's multiple comparisons post hoc tests yielded forskolin-induced decreases of 2097 $mmHg*s^{-1}$ and 2060 $mmHg*s^{-1}$in TGneg and Cav3 OE hearts (both $p < 0.001$), respectively.

Forskolin increased LVDP **(Figure 3.2C)** ($F(1, 12) = 46.04$, $p < 0.001$) but without significant effect of genotype ($F(1, 12) = 0.1562$, $p = 0.70$) or subject matching ($F(12, 12) = 2.386$, $p = 0.07$) and no significant interaction between dose

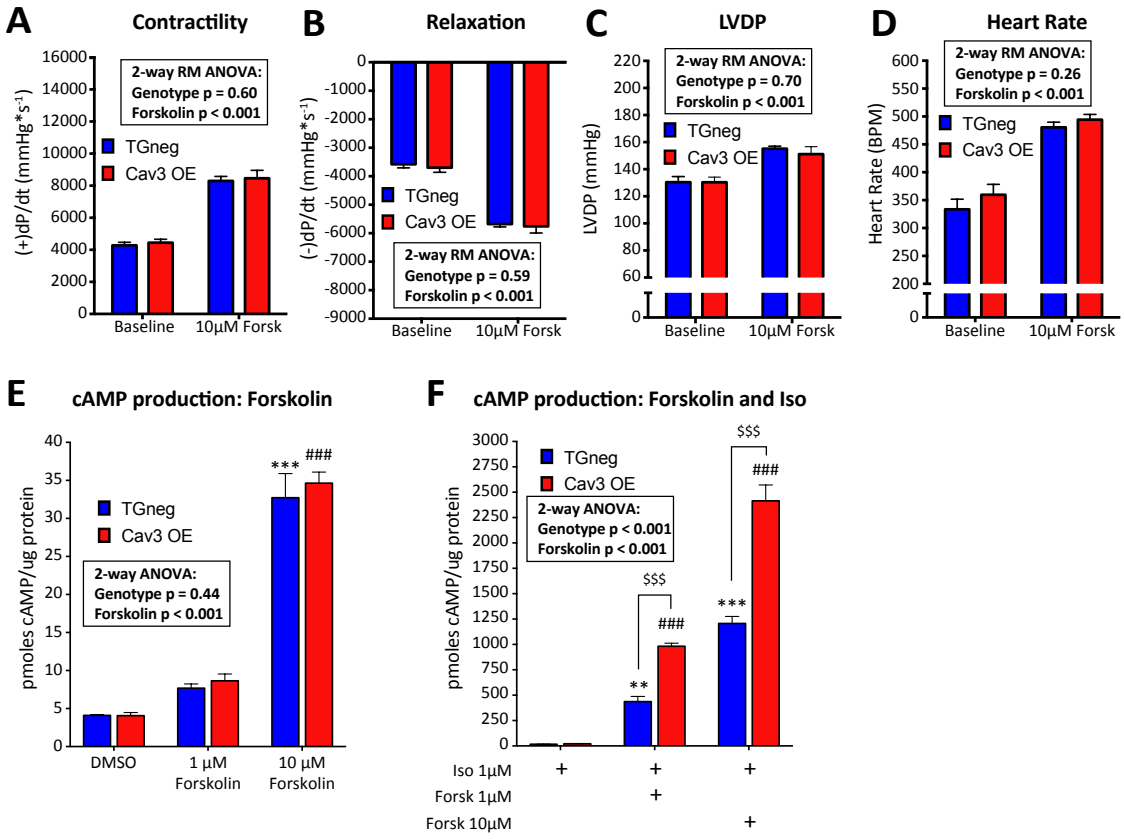

Figure 3.2: Forskolin does not differentially activate physiological responses or cAMP production in Cav3 OE hearts and CMs in the absence of Iso. Forskolin induces similar increase in physiological responses of Cav3 OE and TGneg hearts in **(A)** contractility, **(B)** relaxation, **(C)** LVDP, and **(D)** heart rate. **(E)** cAMP responses to forskolin in the presence of IBMX are similar between genotypes. **(F)** In the presence of Iso and IBMX, forskolin amplifies Cav3 OE cAMP production over TGneg. **p<0.01, ***p<0.001 versus TGneg in DMSO **(E)** or with Iso only **(F)**; ###p<0.001 versus Cav3 OE in DMSO **(E)** or with Iso only **(F)**; $$$$p$<0.001 versus TGneg at bracketed dosage. N = 6/group **(A-D)**, 2 isolations with 3 measurements/isolation **(E-F)**. Data are represented as mean ± SEM.

and genotype (F (1, 12) = 0.3489, p = 0.57). Sidak's multiple comparisons post hoc test revealed forskolin-induced increases of 24.7 mmHg and 20.8 mmHg in TGneg < 0.001) and Cav3 OE hearts (p = 0.001), respectively.

Forskolin increased heart rate **(Figure 3.2D)** (F (1, 12) = 116.9, p < 0.001) but without significant effect of genotype (F (1, 12) = 1.414, p = 0.26) or subject matching (F (12, 12) = 1.657, p = 0.20) and no significant interaction between genotype and dose (F (1, 12) = 0.2269, p = 0.65). Sidak's multiple comparisons post-hoc tests revealed that forskolin increased heart rate 147 bpm in TGneg and 135 bpm in Cav3 OE mice (both p < 0.001).

Cav3 OE and TGneg CMs produce similar amounts of cAMP in response to forskolin

Two doses (1 and 10 μM) of forskolin were used to stimulate CMs isolated from Cav3 OE and TGneg mouse hearts (*N* = 2 isolations, 3 measurements each). 10 μM Forskolin increased cAMP generation in CMs from TGneg and Cav3 OE **(Figure 3.2E)** (F (2, 30) = 228.2, p < 0.001) with similar responses in the two genotypes (F (1, 30) = 0.6024, p = 0.44). There was no significant interaction between dose and genotype (F (2, 30) = 0.2122, p = 0.81). Sidak's multiple comparisons post-hoc test revealed significant 10 μM forskolin-induced increases of 28.6 pmoles cAMP/μg protein in CMs from TGneg hearts (p < 0.001) and 28.7 pmoles cAMP/μg protein in CMs from Cav3 OE hearts (p = 0.001). No significant differences between cAMP responses of the genotypes occurred with DMSO, 1 μM forskolin, or 10 μM forskolin.

Treatment with both forskolin and Iso unmasks increased cAMP production in Cav3 OE CMs

Addition of forskolin together with a GPCR agonist engenders a synergistic effect on cAMP accumulation (1). Treating CMs from Cav3 OE and TGneg hearts with forskolin and Iso **(Figure 3.2F)** (N = 2 isolations, 3 measurements per isolation) significantly increased cAMP levels ($F(2, 30) = 298.9$, $p < 0.001$) with a significant effect of genotype ($F(1, 30) = 94.24$, $p < 0.001$). There was significant interaction between dose and genotype ($F(2, 30) = 33.3$, $p < 0.001$). Tukey's multiple comparisons post-hoc test revealed significant differences within genotypes in multiple treatment groups: a 420 pmol cAMP/μg protein increase in TGneg CMs between 1 μM Iso and 1 μM Iso+1 μM forskolin ($p = 0.005$); a 961 pmol cAMP/μg protein increase between Cav3 OE CMs by 1 μM Iso and 1 μM Iso+1 μM forskolin ($p = 0.005$); a 1190 pmol cAMP/μg protein increase in TGneg CMs between 1 μM Iso and 1 μM Iso+10 μM forskolin ($p < 0.001$); and a 2394 pmol cAMP/μg protein increase in Cav3 OE CMs between 1 μM Iso and 1 μM Iso+10 μM forskolin ($p < 0.001$). Between genotypes, there was a significant effect in two comparisons: a 545 pmol cAMP/μg protein increase in Cav3 OE CMs compared with TGneg CMs by 1 μM Iso+1 μM forskolin ($p < 0.001$) and a 1209 pmol cAMP/μg protein increase in Cav3 OE CMs compared with TGneg by 1 μM Iso + 10 μM forskolin ($p < 0.001$).

In summary, Cav3 OE and TGneg hearts respond similarly to forskolin with respect to contractility, relaxation, LVDP, and heart rate. Additionally, CMs from TGneg and Cav3 OE hearts produce similar amounts of cAMP in response to forskolin. However, when Iso is added with either 1 μM or 10 μM forskolin, cAMP

production is enhanced in both genotypes, but Cav3 OE CMs produce more cAMP than TGneg CMs.

Cav3 OE hearts treated with the β_2AR antagonist ICI118,551 show no enhancement in Iso dose-dependent contractility or relaxation

Iso activates both β_1ARs and β_2ARs; therefore, to discern the potential roles of the β_1AR in increased Cav3 OE contractility and relaxation, we exposed Cav3 OE and TGneg hearts (N = 7/group) to ICI118,51 (ICI), a β_2AR-selective antagonist, and then performed the dose response of Iso. Cav3 OE and TGneg hearts responded similarly in amplitude and in the EC50's of Iso response in the presence of ICI. Iso-induced changes in contractility with ICI **(Figure 3.3A)** showed a significant effect of dose ($F(6, 72) = 59.57$, $p < 0.001$) and subject matching ($F(12, 72) = 22.26$, $p < 0.001$) but not genotype ($F(1, 12) = 0.096$, $p = 0.76$). There was not a significant interaction between dose and genotype ($F(6, 72) = 0.569$, $p = 0.75$); therefore, post-hoc tests were not performed.

Measurement of Iso-induced changes in relaxation with ICI **(Figure 3.3B)** revealed a significant effect of dose ($F(6, 72) = 44.84$, $p < 0.001$) and subject matching ($F(12, 72) = 22.26$, $p < 0.001$), but not genotype ($F(1, 12) = 0.123$, $p = 0.73$). There was not a significant interaction between dose and genotype ($F(6, 72) = 0.320$, $p = 0.93$); therefore, post-hoc tests were not performed.

Iso + ICI induced dose-dependent increases in LVDP **(Figure 3.3C)** with a significant effect of dose ($F(6, 72) = 15.99$, $p < 0.001$) and subject matching ($F(12, 72) = 8.037$, $p < 0.001$) but not genotype ($F(1, 12) = 0.203$, $p = 0.66$). Because there

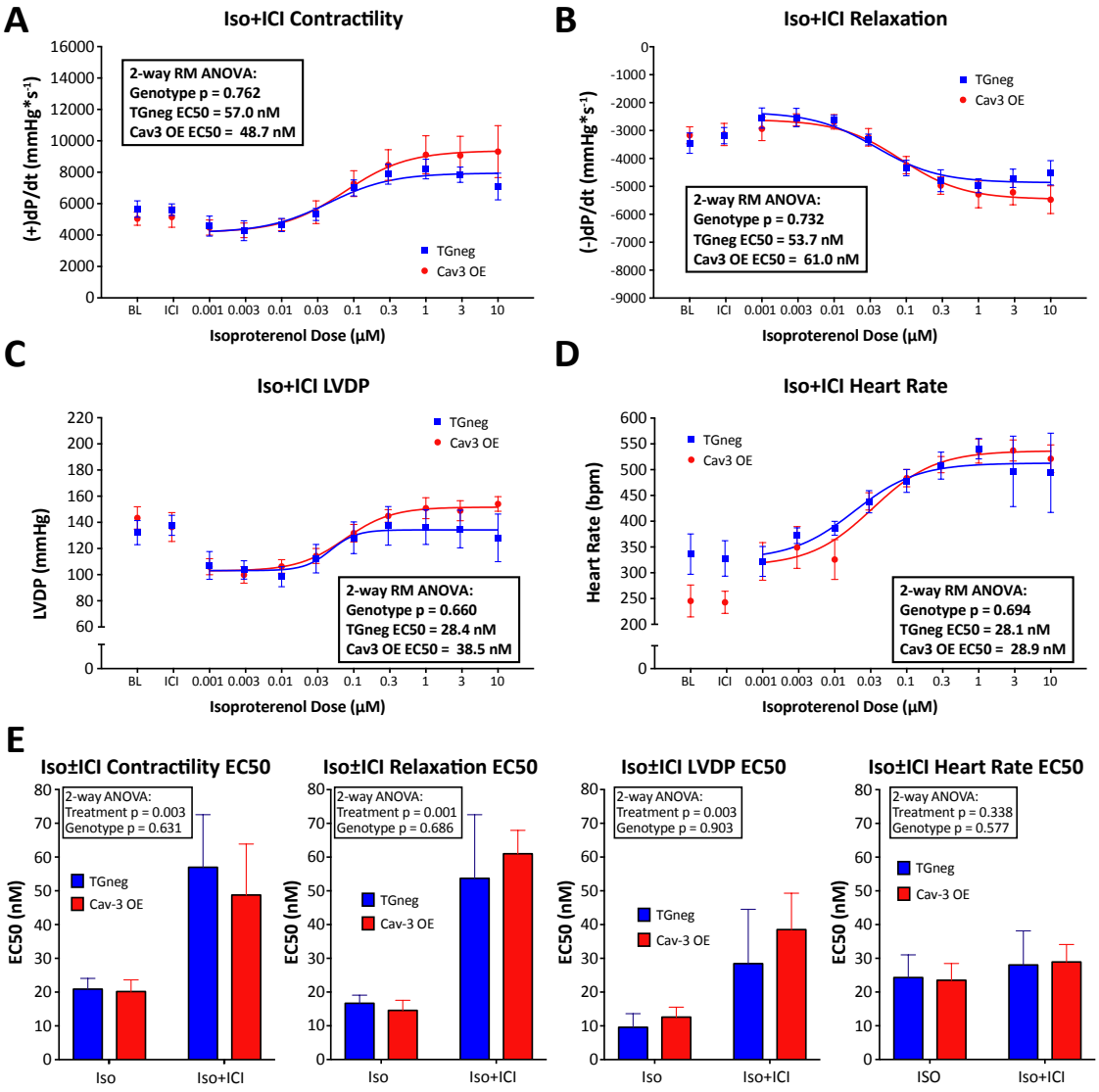

Figure 3.3: Cav3 OE and TGneg hearts demonstrate similar physiological responses to Iso with the β_2AR antagonist ICI118,551. Cav3 OE and TGneg hearts show no differences between genotypes in Iso+ICI responses **(A-D)** or EC50s of response **(E)**. ICI decreases potency of Iso **(E).** *N* = 7/group. Data are represented as mean ± SEM.

was not a significant interaction between dose and genotype ($F(6, 72) = 0.455$, $p = 0.84$), post-hoc tests were not performed.

Measurement of Iso-induced increases in heart rate with ICI **(Figure 3.3D)** revealed a significant effect of dose ($F(6, 72) = 48.19$, $p < 0.001$) and subject matching ($F(12, 72) = 9.52$, $p < 0.001$) but not genotype ($F(1, 12) = 0.163$, $p = 0.69$). There was not a significant interaction between dose and genotype ($F(6, 72) = 0.946$, $p = 0.47$); therefore, post-hoc tests were not performed.

The β_2AR antagonist ICI does not alter EC50 values between genotypes

For each physiological parameter, the data were plotted as percent of maximal response, then analyzed with a best-fit curve to calculate the EC50 values of the responses. ICI produced no significant effect on the EC50 values **(Figure 3.3E)** for effect of genotype in contractility ($p = 0.68$), relaxation ($p = 0.70$), LVDP ($p = 0.49$), or heart rate ($p = 0.94$). Thus, Cav3 OE and TGneg hearts respond similarly to Iso at all doses when treated with ICI with no change in EC50 between the genotypes.

The potency of Iso is decreased in Cav3 OE and TGneg hearts treated with the β_2AR antagonist ICI

To evaluate the effects of ICI as a competitive antagonist for the cardiac β_2ARs, I compared EC50 values for Iso alone and Iso+ICI **(Figure 3.3E)** and found a significant effect of Iso+ICI vs Iso on contractility ($F(1, 24) = 20.16$, $p < 0.001$), relaxation ($F(1, 24) = 43.55$, $p < 0.001$), and LVDP ($F(1, 24) = 9.94$, $p = 0.004$) but not heart rate ($F(1, 24) = 0.56$, $p = 0.46$). Sidak's multiple comparisons post-hoc tests

revealed that ICI significantly increased the EC50 for Iso by 36.1 nM, and 37.0 in TGneg CMs for contractility ($p = 0.005$) and relaxation ($p < 0.001$), respectively but produced no significant change in the EC50 for LVDP ($p = 0.089$). Post-hoc tests also revealed that ICI significant increased the EC50 for Iso in Cav3 OE CMs by 28.6 nM in contractility ($p = 0.013$) and 46.4 nM in relaxation ($p < 0.001$) studies but did not produce a statistically significant change in the LVDP EC50 ($p = 0.054$). There was no significant effect of genotype or interaction between genotypes and treatment on contractility, relaxation, LVDP, or heart rate.

These data show that ICI has a similar effect on the EC50 of Iso dose response in both Cav3 OE and TGneg hearts, are consistent with the ability of ICI to act as a competitive βAR antagonist, with no difference between genotypes.

Cav3 OE, but not TGneg, hearts have a decreased response to 1 μM Iso in the presence of ICI

As a further comparison, TGneg and Cav3 OE hearts were compared for their response to Iso or Iso+ICI ($N = 7$/group) at 1 μM Iso, a maximally effective dose in both groups **(Figure 3.4A)**. As shown in prior experiments in Chapter 2, Iso increased contractility and relaxation to a greater extent in Cav3 OE hearts. Moreover, addition of ICI yielded a significantly greater decrease in the contractility response in Cav3 OE hearts than in TGneg hearts, but this was not observed for the other responses.

ICI significantly reduced the effect of Iso on contractility ($F (1, 24) = 6.264$, $p = 0.020$) in a genotype-selective manner ($F (1, 24) = 7.666$, $p = 0.011$) but with no significant interaction between ICI and genotype ($F (1, 45\ 3.662$, $p = 0.068$). Tukey's

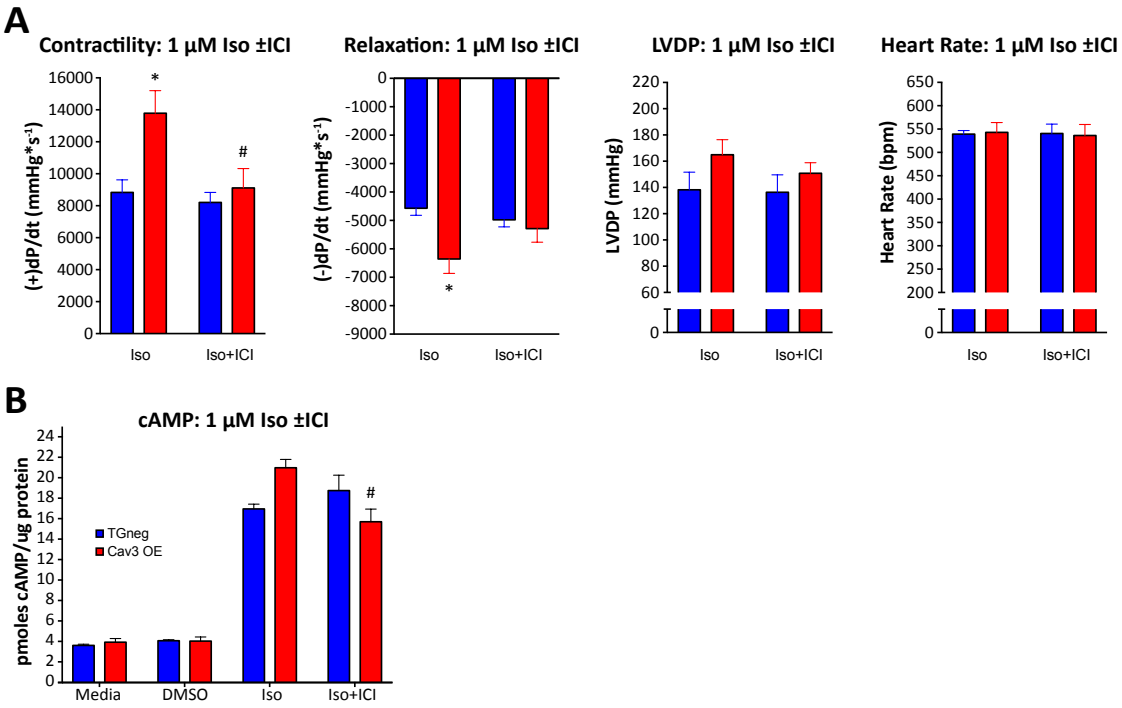

Figure 3.4: The β_2AR antagonist ICI118,551 decreases response to 1 µM Iso in Cav3 OE hearts and CMs. (A) Cav3 OE hearts increase contractility and relaxation versus TGneg in response to 1 µM Iso which is ablated in contractility with ICI. **(B)** Cav3 OE CMs, but not TGneg CMs, reduce Iso-induced cAMP accumulation with ICI treatment. *p<0.05 versus TGneg at 1 µM Iso; #p<0.05 versus Cav3 OE at 1 µM Iso. N =7/group **(A)**, 2 isolations with 3 measurements/isolation **(B)**. Data are represented as mean ± SEM.

multiple comparisons post-hoc tests revealed significant effects between multiple groups: Iso increased Cav3 OE contractility by 4955 $mmHg*s^{-1}$ compared with TGneg ($p = 0.015$), Iso+ICI decreased the Cav3 OE contractility compared with Iso by 4674 $mmHg*s^{-1}$ ($p = 0.024$), and Iso + ICI yielded no significant differences in TGneg hearts compared with Iso alone ($p = 0.99$) or between TGneg and Cav3 OE hearts ($p = 0.99$).

ICI reduced Iso-induced changes in relaxation **(Figure 3.4A)** with an effect of genotype ($F (1, 24) = 7.212$, $p = 0.013$) but not ICI ($F (1, 24) = 0.7162$, $p = 0.41$). There was no significant interaction between ICI and genotype ($F (1, 24) = 3.566$, $p = 0.071$). Tukey's multiple comparisons post-hoc tests revealed a significant 1786 $mmHg*s^{-1}$ increase in Cav3 OE relaxation in response to Iso compared with that of TGneg ($p = 0.021$). No significant differences were found in several comparisons of relaxation: Iso+ICI compared with Iso alone in TGneg ($p = 0.98$), effect of ICI on Cav3 OE Iso-dependent relaxation ($p = 0.33$), and difference between TGneg and Cav3 OE hearts when both were exposed to Iso+ICI ($p = 0.99$).

Assessment of Iso-induced changes in LVDP by Iso only and Iso+ICI **(Figure 3.4A)** revealed no significant effect of genotype ($F (1, 24) = 0.3078$, $p = 0.091$) or ICI ($F (1, 24) = 0.4672$, $p = 0.50$) nor significant interaction between ICI and genotype ($F (1, 24) = 0.2732$, $p = 0.61$). Tukey's multiple comparisons post-hoc tests revealed no significant effect between several groups: TGneg and Cav3 OE exposed to Iso alone ($p = 0.54$), effect of ICI on TGneg response to Iso ($p > 0.99$) or Cav3 OE response to Iso ($p = 0.95$), or differences in Iso+ICI responses between the genotypes ($p = 0.95$).

Assessment of Iso-induced changes in heart rate by Iso only and Iso+ICI **(Figure 3.4A)** also revealed no significant effect of genotype ($F(1, 24) = 0.00042$, $p = 0.98$) or ICI ($F(1, 24) = 0.01914$, $p = 0.89$) and no significant interaction between ICI and genotype ($F(1, 24) = 0.0439$, $p = 0.83$). Tukey's multiple comparison post-hoc test revealed no significant effect between multiple groups: TGneg and Cav3 OE exposed to Iso alone ($p > 0.99$), effect of ICI on response to Iso in TGneg hearts ($p > 0.99$) or Cav3 OE hearts ($p > 0.99$), or Iso+ICI responses of the genotypes ($p > 0.99$).

Cav3 OE, but not TGneg, CMs have decreased cAMP production to 1 μM Iso in the presence of ICI

To define the impact of β_1ARs on cAMP accumulation, I treated CMs isolated from TGneg and Cav3 OE hearts ($N = 2$ isolations, 3 measurements each) with Iso in the presence and absence of ICI and assessed cAMP production **(Figure 3.4B).** The findings indicated that ICI decreased cAMP production by Cav3 OE, but not the TGneg CMs. There was no significant effect of genotype ($F(1, 20) = 0.2045$, $p = 0.66$) or overall of ICI ($F(1, 20) = 2.596$, $p = 0.12$), but the results revealed a significant interaction between ICI and genotype ($F(1, 20) = 10.7$, $p = 0.0038$); therefore, Tukey's multiple comparisons post-hoc tests were performed. Post-hoc tests revealed that in Cav3 OE CMs, ICI significantly reduced cAMP production (by 5.27 pmoles cAMP/μg protein compared with treatment with Iso alone, $p = 0.012$). Cav3 OE CMs produced 4.02 pmoles cAMP/μg protein more than TGneg CMs ($p = 0.07$). ICI did not significantly change TGneg cAMP production ($p = 0.65$) and yielded no difference between TGneg and Cav3 OE CMs ($p = 0.22$).

Cav3 OE hearts have an increased contractile response to the AR agonist norepinephrine

Norepinephrine (NE), the key catecholamine produced by sympathetic nerves and which selectively activates β_1AR, was tested for its effect on contractility and relaxation and to compare responses in Cav3 OE and TGneg hearts (N = 4/group). Cav3 OE hearts treated with 3 nM – 3 μM NE had greater contractility than did TGneg hearts **(Figure 3.5A)** but there were no significant differences in relaxation, LVDP, heart rate **(Figure 3.5B-D)**, or EC50's were found in any of the responses.

For contractility **(Figure 3.5A)**, there was a significant effect of dose ($F(6, 36) = 58.36$, $p < 0.001$) and genotype ($F(1, 6) = 7.006$, $p = 0.038$) but not subject matching ($F(6, 36), = 1.031$, $p = 0.42$) nor was there a significant interaction between dose and genotype ($F(6, 36) = 1.516$, $p = 0.20$). Sidak's multiple comparison post-hoc test revealed no significant difference between Cav3 OE and TGneg at any individual NE dose.

The NE-induced increase in relaxation **(Figure 3.5B)** showed a significant effect of dose ($F(6, 36) = 42.68$, $p < 0.001$) and subject matching ($F(6, 36) = 19.23$, $p < 0.001$), but not genotype ($F(1, 6) = 0.3902$, $p = 0.56$), and a significant interaction between dose and genotype ($F(6, 36) = 4.092$, $p = 0.003$). However, Sidak's multiple comparison post-hoc test revealed no significant difference between Cav3 OE and TGneg at any individual NE dose.

The NE increase in LVDP **(Figure 3.5C)** showed a significant effect of dose ($F(6, 36) = 19.57$, $p < 0.001$) and subject matching ($F(6, 36) = 11.54$, $p < 0.001$) but

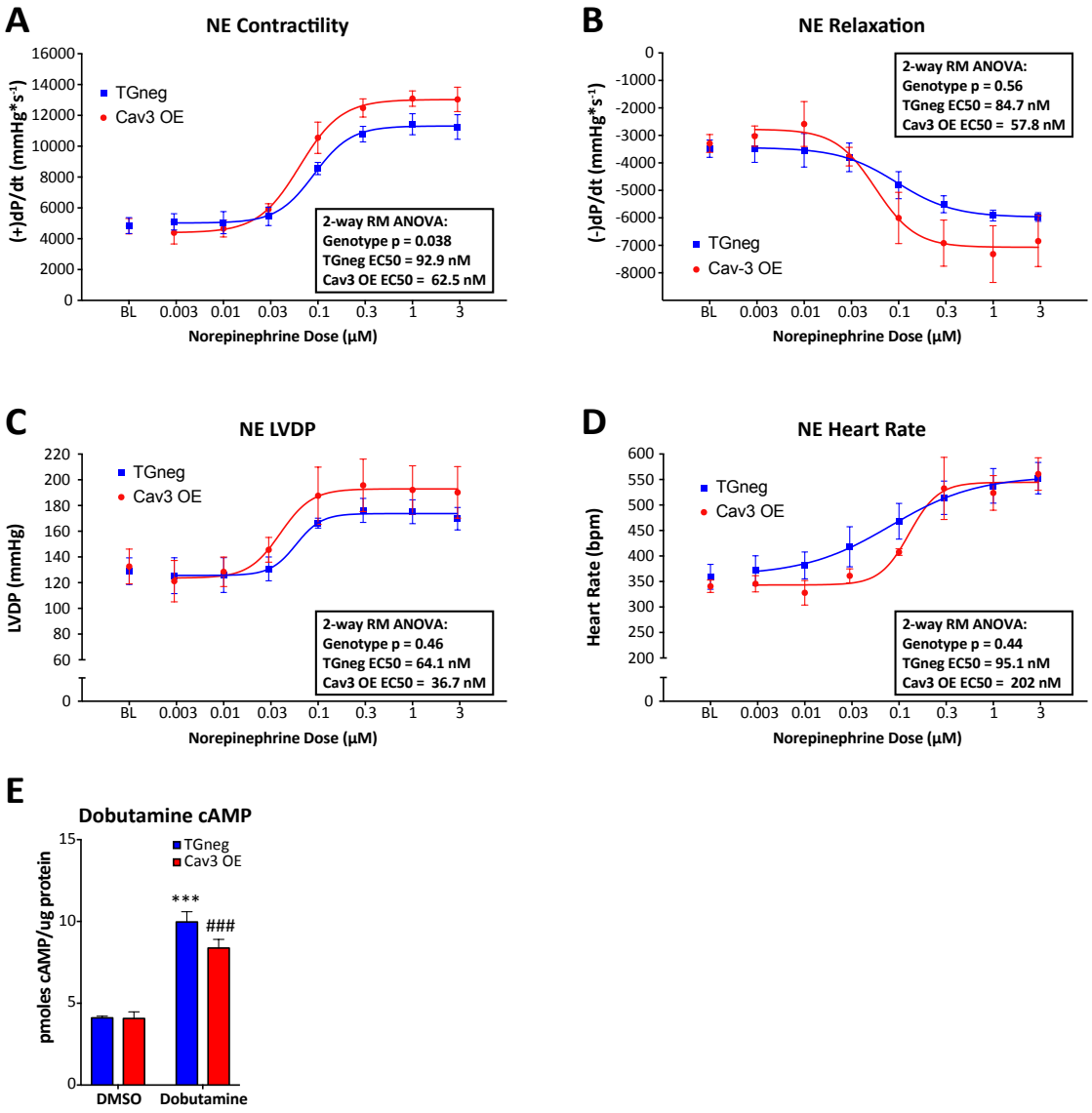

Figure 3.5: Cav3 OE hearts show a slight increase in contractility with the β_1AR > β_2AR selective agonist, norepinephrine. (A) Cav3 OE hearts exhibit a slight increase in contractility versus TGneg in response to NE, but no differences in **(B-D)** relaxation, LVDP, or heart rate. **(E)** Cav3 OE CMs do not produce more cAMP in response to dobutamine than TGneg CMs. ***p<0.001 versus TGneg with DMSO; ###p<0.001 versus Cav3 OE with DMSO. N = 4/group **(A-D)**, 2 isolations with 3 measurements/isolation **(E).** Data are represented as mean ± SEM.

not genotype ($F(1, 6) = 0.6297$, $p = 0.46$). There was not a significant interaction between dose and genotype ($F(6, 36) = 0.6022$, $p = 0.73$).

NE increased heart rate **(Figure 3.5D)** with a significant effect of dose ($F(6, 36) = 24.63$, $p < 0.001$) and subject matching ($F(6, 36) = 6.006$, $p < 0.001$) but not genotype ($F(1, 6) = 0.6733$, $p = 0.44$). There was no significant interaction between dose and genotype ($F(6, 36) = 0.8559$, $p = 0.54$).

Cav3OE and TGneg hearts have a similar EC50 of response to NE

For each physiological response, we adjusted the data as percent maximal response, then applied a best-fit curve to the data to calculate the EC50 values. We found no significant effect on EC50 for genotype in contractility ($p = 0.24$), relaxation ($p = 0.52$), LVDP ($p = 0.15$), or heart rate ($p = 0.20$).

Cav3 OE and TGneg CMs have similar responses to the partial β_1AR agonist dobutamine

Dobutamine, a partial β_1AR agonist, was used as a further means to evaluate β_1ARs by testing its effect on CMs isolated from TGneg and Cav3 OE hearts ($N = 2$ isolations, 3 measurements each). Cav3 OE and TGneg CMs showed similar cAMP production in response to dobutamine **(Figure 3.5E)**. TGneg and Cav3OE CMs produced 5.8 and 4.3 pmol cAMP/μg protein more in response to dobutamine than did the DMSO controls and there were no differences between TGneg and Cav3 OE responses to DMSO ($p > 0.99$) or dobutamine ($p = 0.097$).

The β_1AR antagonist CGP20712a suppresses most of the contractile response to Iso in TGneg and Cav3 OE hearts

To reveal the potential roles of β_2ARs in the increased Iso-induced contractility and relaxation in Cav3OE hearts, the β_1AR-selective antagonist CGP20712a (CGP) was used to block β_1ARs and the effect of Iso was tested in Cav3 OE and TGneg hearts (N = 7/Iso groups, 4 TGneg, 3 Cav3 OE+CGP). Except for an increase in heart rate, Cav3 OE and TGneg hearts did not significantly respond to Iso when CGP was present **(Figure 3.6A-D)**. As a result, the dose-response analyses are not reported in detail for contractility, relaxation, or LVDP.

The heart rate response with Iso+CGP **(Figure 3.6D)** showed a significant effect of dose ($F(8, 30) = 12.74$, $p < 0.001$) and subject matching ($F(5, 40) = 10.6$, $p < 0.001$), but not genotype ($F(1, 5) = 0.03757$, $p = 0.84$). There was a not a significant interaction between dose and genotype ($F(8, 40) = 1.42$, $p = 0.22$). Fitting the dose-response curve to obtain EC50 revealed no significant effect of genotype ($p = 0.89$).

Cav3 OE and TGneg hearts treated with the β_1AR antagonist CGP show decreased sensitivity to Iso

To evaluate the effects of CGP as a competitive antagonist for the β_1ARs, we compared EC50 values for the heart rate response to Iso alone and Iso+CGP **(Figure 3.6D).** As expected for a competitive antagonist, the EC50's were right-shifted, but we found no differences between the two genotypes. I found a significant effect of Iso+CGP compared with Iso ($F(1, 17) = 33.46$, $p < 0.001$) but no significant effect of genotype ($F(1, 17) = 0.04632$, $p = 0.83$) or interaction between treatment and

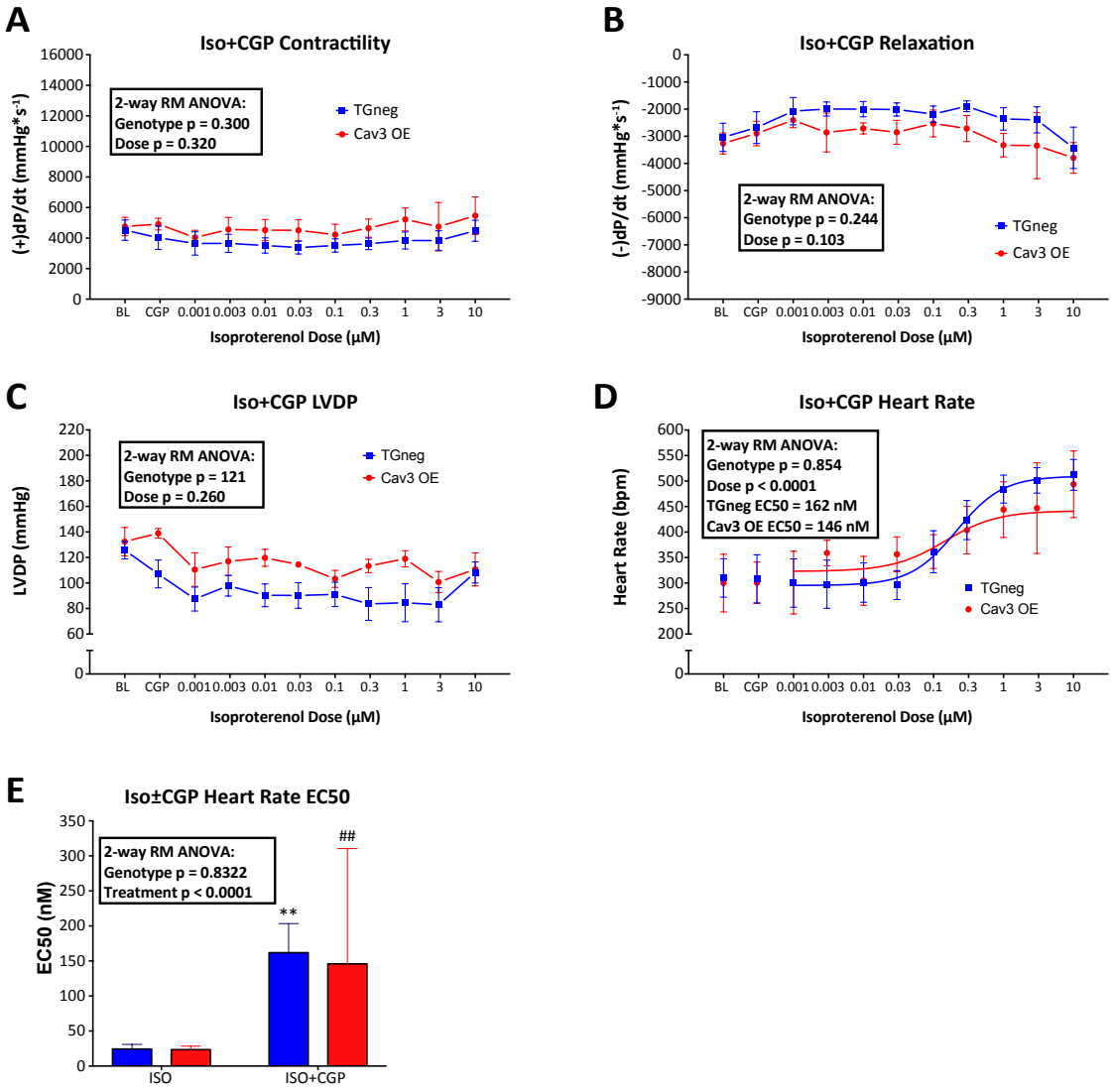

Figure 3.6: The β_1AR antagonist CGP20712a reduces response to Iso in Cav3 OE and TGneg hearts. (A-C) Neither Cav3 OE nor TGneg hearts respond positively to Iso when treated with CGP **(D)** CGP does not prevent heart rate response to Iso. **(E)** Cav3 OE versus TGneg demonstrate similar potency of Iso, and CGP decreases the potency of Iso in both genotypes. $^{**}p<0.01$ versus TGneg with Iso only; $\#\#p<0.01$ Cav3 OE with Iso only. $N = 4$ TGneg, 3 Cav3 OE **(A-D)**, 7/group Iso only, 4 TGneg, 3 Cav3 OE Iso+CGP **(E)**. Data are represented as mean ± SEM.

genotype (F (1, 17)= 0.01163, p = 0.92). Tukey's multiple comparisons post hoc tests revealed significant differences in two groups: a 137 nM increase in the Iso EC50 for TGneg hearts exposed to Iso+CGP (p = 0.0021) and a 122 nM increase in Iso EC50 for OE hearts exposed to Iso+CGP (p = 0.0066). There was no significant difference between genotypes with either treatment (p = 0.99 for Iso and Iso+CGP in both genotypes).

Cav3 OE and TGneg hearts treated with 1μM CGP have reduced, similar responses to Iso

Using CGP at 30nM produced variable responses that made it impossible to fit sigmoidal dose response curves for contractility, relaxation, or LVDP. However, since experiments with Iso alone or with CGP were performed similarly, a comparison of Iso and Iso+CGP at a single dose of Iso was possible. The EC50 of the heart rate response to Iso+CGP was 175 nM for TGneg and 259 nM for Cav3 OE hearts. Therefore, the 1μM dose of Iso was chosen to compare Iso alone and Iso+CGP in the contractility, relaxation, and LVDP responses. The results revealed that CGP reduced the contractility and relaxation responses of both genotypes and that the responses to Iso+CGP were similar for Cav3 OE and TGneg hearts.

Analysis of the differences in contractility between Iso only and Iso+CGP **(Figure 3.7A)** revealed a significant effect of CGP (F (1, 17) = 30.67, p < 0.001) and genotype (F (1, 17) = 6.698, p = 0.019) but no significant interaction between CGP and genotype (F (1, 17) = 2.141, p = 0.17). Tukey's multiple comparisons post-hoc tests revealed a significant effect of several groups: In Cav3 OE hearts, Iso increased

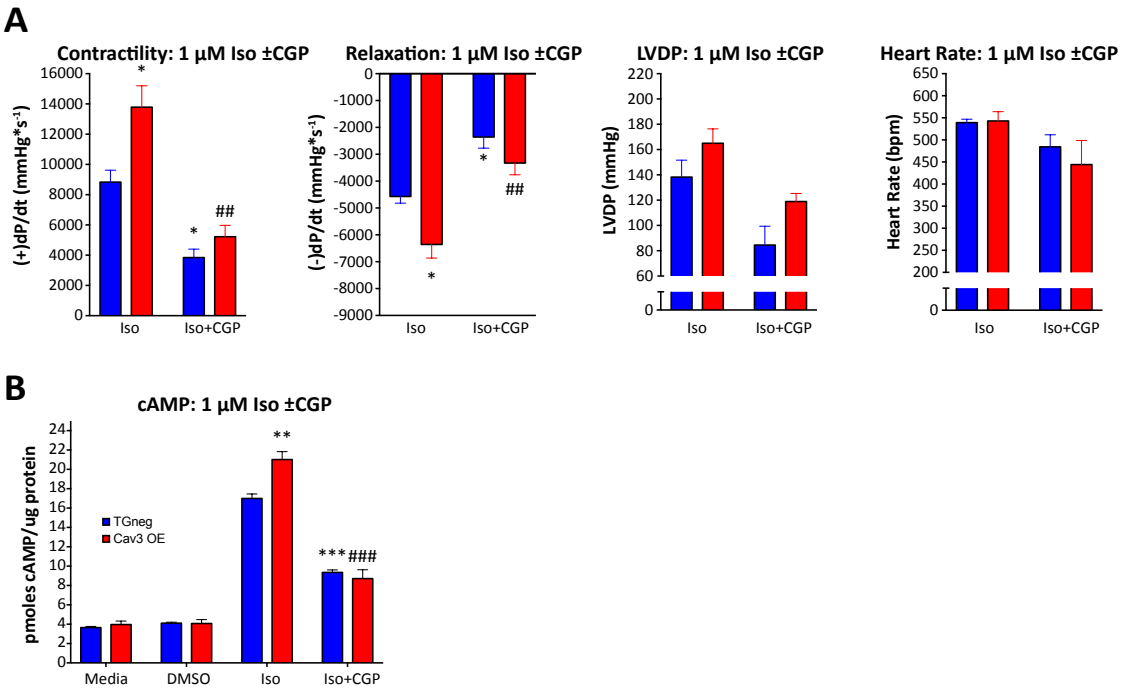

Figure 3.7: Cav3 OE and TGneg cardiac responses to Iso are suppressed at 1 µM Iso with the β_1AR antagonist CGP20712a. (A) Cav3 OE hearts exhibit increased contractility and relaxation in response to Iso that is suppressed to similar levels as TGneg when CGP is administered. **(B)** Cav3 OE hearts exhibit increased cAMP accumulation in response to Iso in the presence of IBMX that is suppressed to similar levels as TGneg when CGP is administered. **p*<0.05, ***p*<0.01, ****p*<0.001 versus TGneg with Iso only; ##*p*<0.01, ###*p*<0.001 versus Cav3 OE with Iso only. *N* = 7/group Iso only, 4 TGneg, 3 Cav3 OE Iso +CGP. Data are represented as mean ± SEM.

Cav3 OE contractility by 4955 mmHg*s^{-1} more than TGneg hearts ($p = 0.018$); compared with Iso, Iso+CGP reduced TGneg contractility by 4985 mmHg*s^{-1} ($p = 0.044$); and the Cav3 OE Iso response by 8564 mmHg*s^{-1} ($p = 0.027$). No significant differences were found between genotypes with Iso+CGP ($p = 0.99$).

For Iso-induced changes in relaxation between Iso only and Iso+CGP **(Figure 3.7A)** there was a significant effect of CGP ($F (1, 17) = 32.35$, $p < 0.001$) and genotype ($F (1, 17) = 8.955$, $p = 0.0082$) but no significant interaction between CGP and genotype ($F (1, 17) = 0.7836$, $p = 0.39$). Tukey's multiple comparisons post-hoc tests revealed significant effects for several groups: Iso alone increased Cav3 OE relaxation by 1786 mmHg*s^{-1} ($p = 0.021$), CGP reduced the TGneg response to Iso by 2212 mmHg*s^{-1} ($p = 0.014$), and Cav3 OE response to Iso by 3027 mmHg*s^{-1} ($p = 0.0022$). The difference between TGneg and Cav3 OE hearts exposed to CGP was not significant ($p = 0.99$).

Analysis of Iso-induced changes in LVDP by Iso alone and Iso+CGP **(Figure 3.7A)** revealed a significant effect of CGP ($F (1, 17) = 12.25$, $p = 0.0027$) and genotype ($F (1, 17) = 4.601$, $p = 0.047$) but no significant interaction between CGP and genotype ($F (1, 17) = 0.07355$, $p = 0.79$). Tukey's multiple comparisons post-hoc tests revealed no significant effect between TGneg and Cav3 OE exposed to Iso alone ($p = 0.54$). CGP did not significantly alter the TGneg response to Iso ($p = 0.071$) or the Cav3 OE response to Iso ($p = 0.23$). TGneg and Cav3 OE the Iso+CGP responses were not significantly different ($p = 0.65$).

The Iso-induced increases in heart rate between Iso only and Iso+CGP **(Figure 3.7A)** showed a significant effect of CGP ($F (1, 17) = 9.623$, $p = 0.0065$) but not

genotype (F (1, 17) = 0.5448, p = 0.47) and no significant interaction between CGP and genotype (F (1, 17) = 0.7801, p = 0.39). Tukey's multiple comparisons post-hoc tests revealed no significant effect between several groups: TGneg and Cav3 OE exposed to Iso alone (p > 0.99), CGP did not alter the TGneg response (p = 0.53) or Cav3 OE response to Iso (p = 0.089), and the Iso+CGP responses were not different between genotypes (p = 0.92).

CGP reduces 1 μM-stimulated cAMP accumulation in Cav3 OE and TGneg CMs

I compared the role of β_2ARs in stimulating AC in isolated CMs from TGneg and Cav3 OE hearts by assessing cAMP accumulation to Iso in the presence and absence of CGP. Because 30 nM CGP suppressed most of the contractile responses of the hearts in **Figure 3.7A**, 3 nM CGP was used for the cAMP study to prevent the total suppression of cAMP production (N = 2 isolations with three measurements per isolation) **(Figure 3.7B)**. The results indicated that Cav3 OE myocytes produce more cAMP in response to Iso (as in **Figure 2.1E**) and that CGP reduces cAMP accumulation of both genotypes to similar levels. There was a significant effect of CGP (F (1, 20) = 221.5, p < 0.001) and genotype (F (1, 20 = 6.365), p = 0.020); also a significant interaction between CGP and genotype (F (1, 20) = 12.08, p = 0.0024). Therefore, Tukey's multiple comparisons post-hoc tests were performed. Post-hoc tests revealed significant effects between multiple groups: Iso increased the Cav3 OE cAMP production by 4.02 pmol cAMP/μg protein compared with TGneg (p = 0.0021), CGP reduced TGneg cAMP production by 7.65 pmol cAMP/μg protein compared with TGneg with Iso (p < 0.001), and CGP reduced Cav3 OE cAMP production by

12.3 pmol cAMP/μg protein ($p < 0.001$). There were no significant differences between TGneg and Cav3 OE CMs treated with CGP ($p = 0.91$).

The β_2AR agonist zinterol does not differentially affect Cav3 OE and TGneg hearts

Zinterol increased contractility ($N = 3$/group) **(Figure 3.8A)** with a significant effect of dose ($F (8, 32) = 28.83$, $p < 0.001$) and subject matching ($F (4, 32 = 8.273$, $p < 0.001$), but not genotype ($F (1, 4) = 0.06031$, $p = 0.82$). No significant interaction occurred between dose and genotype ($F (8, 32) = 0.757$, $p = 0.642$). Sidak's multiple comparison post-hoc test revealed that Cav3 OE does not significantly change Zinterol-induced contractility at any dose.

Zinterol also increased relaxation **(Figure 3.8B)** with a significant effect of dose ($F (8, 32) = 16.35$, $p < 0.001$) and subject matching ($F (4, 32) = 5.707$, $p = 0.0014$), but not genotype ($F (1, 4) = 0.7379$, $p = 0.44$). There was no significant interaction between dose and genotype ($F (8, 32) = 0.2095$, $p = 0.987$). Sidak's multiple comparison post-hoc test revealed that Cav3 OE does not significantly change Zinterol-induced relaxation at any dose.

Zinterol increased LVDP **(Figure 3.8C)**, with a significant effect of dose ($F (8, 32) = 16.82$, $p < 0.001$) and subject matching ($F (4, 32) = 11.89$, $p < 0.001$) but not genotype ($F (1, 4) = 0.7883$, $p = 0.88$). No significant interaction occurred between dose and genotype ($F (8, 32) = 1.003$, $p = 0.398$). Sidak's multiple comparison post-hoc test revealed that Cav3 OE does not significantly change Zinterol-induced LVDP at any dose.

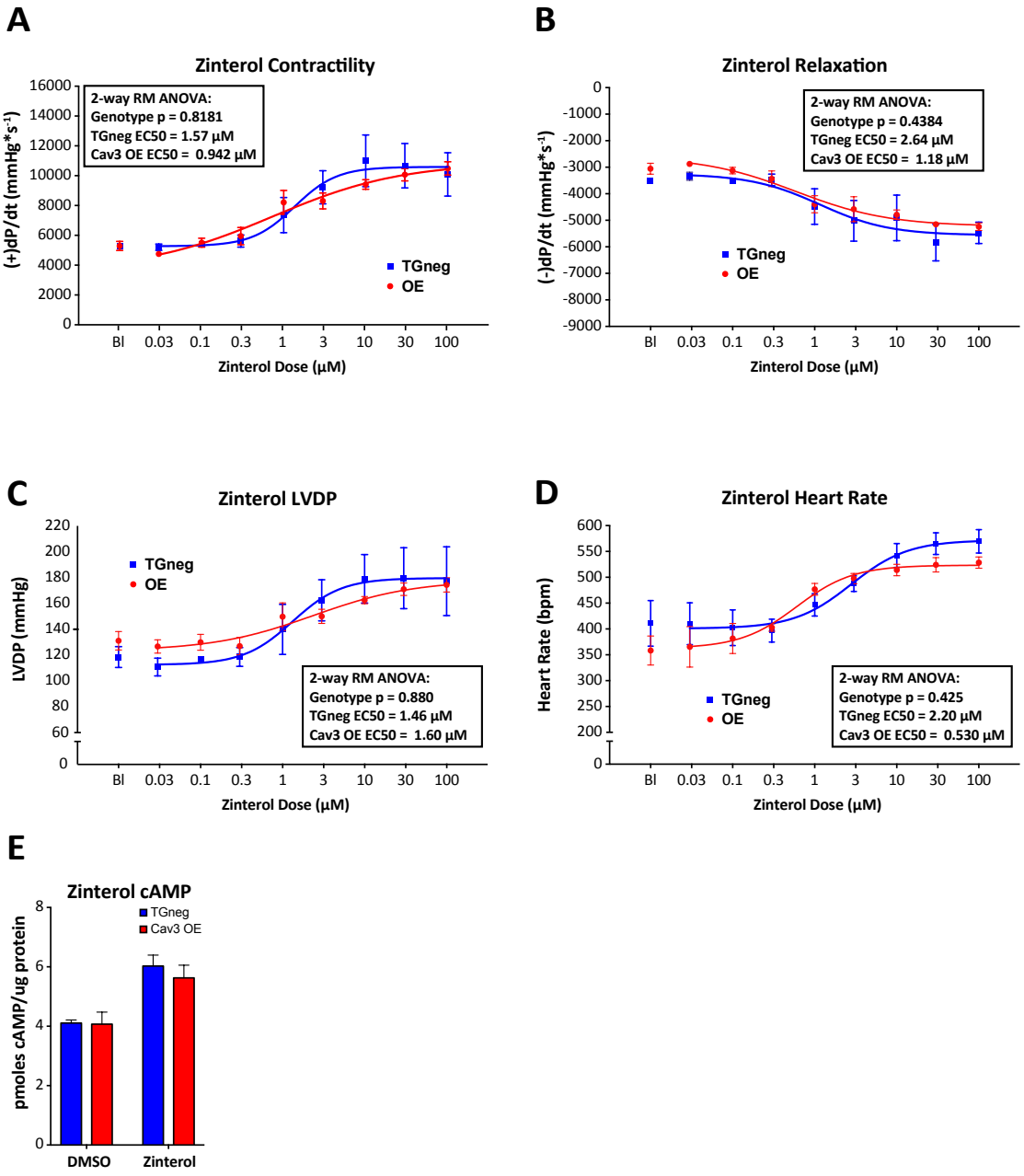

Figure 3.8: Cav3 OE and TGneg hearts have similar responses to the β_2AR agonist zinterol. (A-D) Cav3 OE and TGneg showed no significant differences in response or EC50 except in **(D)** where Cav3 OE exhibit increased potency of zinterol. **(E)** Cav3 OE and TGneg CMs accumulated similar amounts of cAMP in response to zinterol. *N* = 3/group. Data are represented as mean ± SEM.

Zinterol increased heart rate **(Figure 3.8D)** with a significant effect of dose ($F(8, 32 = 23.94$, $p < 0.001$) and subject matching ($F(4, 32)$ 5.604, $p < 0.001$) but not genotype ($F(1, 4) = 0.7883$, $p = 0.82$). There was no significant interaction between dose and genotype ($F(8, 32) = 1.003$, $p = 0.642$). Sidak's multiple comparison post-hoc test revealed that Cav3 OE does not significantly change Zinterol-induced contractility at any dose.

The EC50 for Zinterol was similar between TGneg and Cav3 OE hearts **(Figure 3.8A-D)** for contractility ($p = 0.37$), relaxation ($p = 0.30$), and LVDP ($p = 0.90$); but the EC50 for heart rate was 1.6 μM lower in Cav3 OE hearts ($p = 0.045$).

In summary, Cav3 OE and TGneg hearts respond similarly to Zinterol in terms of contractility, relaxation, LVDP, and heart rate. Additionally, there were no significant differences in the EC50 of zinterol between genotypes except for heart rate, in which Cav3 OE hearts had increased potency of Zinterol.

Cav3 OE and TGneg CMs respond similarly to 10 μM zinterol

The ability of 10 μM Zinterol to increase cAMP production was compared in CMs isolated from TGneg and Cav3 OE hearts ($N = 2$ isolations with 3 measurements per isolation) **(Figure 3.8E)**. The increase in cAMP was significant ($F(1, 20) = 24.43$, $p < 0.001$) but showed no differences as a function of genotype ($F(1, 20) = 0.3877$, $p = 0.86$) and with no significant interaction between genotype and Zinterol ($F(1, 20) = 0.2695$, $p = 0.61$). Tukey's multiple comparison post-hoc test revealed significant effect between multiple groups: Zinterol increased TGneg and Cav3OE CM cAMP production by 1.92 pmol and 1.56 pmol cAMP/μg protein, respectively, compared

with addition of DMSO ($p = 0.0049$ and 0.025, respectively). No significant effect was found between TGneg and Cav3 OE CMs treated with DMSO ($p = 0.99$) or Zinterol ($p = 0.85$).

Cav3 OE and TGneg hearts respond differently to PDE inhibition with IBMX

Due to the high PDE activity in CMs, we used the non-selective PDE inhibitor IBMX for most of the cAMP accumulation experiments to prevent cAMP degradation and amplify cAMP levels to have a larger dynamic range of response. However, certain PDEs are compartmentalized in caveolae and regulate caveolar cAMP pools (2-4). Therefore, we performed cAMP accumulation studies with Iso and forskolin in the absence of IBMX **(Figure 3.9A-B)** ($N = 2$ isolations with 3 measurements per isolation) to test whether PDE inhibition by IBMX differentially affects Cav3 OE and TGneg cAMP accumulation in response to Iso and forskolin. The results indicate that the response to Iso, but not forskolin, is differentially regulated in Cav3 OE CMs by PDE inhibition. For each drug, a 3-way ANOVA was used to evaluate the interactions between genotype, drug dose, and/or IBMX.

Analysis of Iso responses **(Figure 3.9A)** revealed a significant effect of genotype ($F(1, 1) = 5.829$, $p = 0.020$), IBMX ($F(1, 1) = 755.1$, $p < 0.001$), but not dose of Iso ($F(1, 1) = 1.554$, $p = 0.22$) on cAMP production. Two-factor interactions analysis identified significant interaction between genotype and IBMX ($F(1, 1) = 4.856$, $p = 0.033$), genotype and doses of Iso ($F(1, 1) = 8.05$, $p = 0.0071$), but not IBMX and doses of Iso ($F(1, 1) = 2.25$, $p = 0.14$). The three-factor analysis identified a significant effect between TGneg and Cav3 OE in response to IBMX that differed

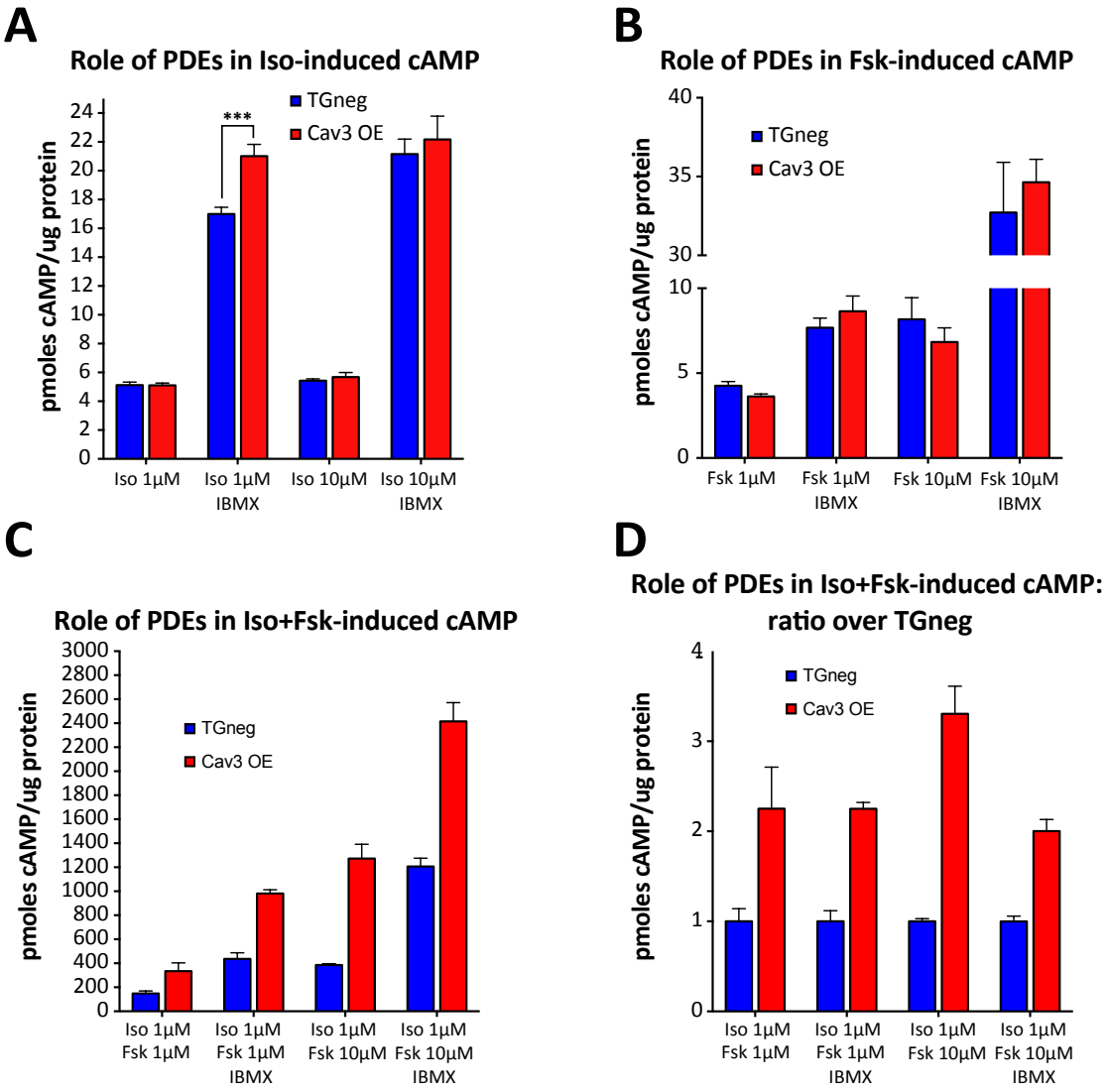

Figure 3.9: Cav3 OE myocytes exhibit βAR, but not AC, regulation by PDEs. (A) Increased Iso-induced cAMP accumulation in Cav3 OE CMs is unmasked by PDE inhibition, but **(B)** PDE inhibition does not alter cAMP accumulation in the presence of Fsk. **(C)** Synergistic cAMP production with Iso+Fsk is increased in the presence of IBMX, but the ratio between TGneg and Cav3 OE remains similar in different treatment groups (visualized by normalizing to TGneg in **(D)**). ***p<0.001. N = 2 isolations with 3 measurements/isolation. Data are represented as mean ± SEM.

for the two Iso doses ($F(1, 1) = 4.113$, $p = 0.049$). These data show there is a greater increase of Iso-induced cAMP production in Cav3 OE versus TGneg CMs in the presence of IBMX than in its absence but that the interaction with IBMX also depends upon the dose of Iso used. Sidak's post hoc multiple comparisons revealed significant effects between cAMP accumulation of Cav3 OE and TGneg CMs at 1 μM Iso +IBMX ($p < 0.001$), but no significant differences between genotypes in the 1 μM – IBMX ($p = 0.98$), 10 μM –IBMX ($p > 0.99$), or 10 μm +IBMX ($p > 0.99$) groups.

Analysis of forskolin responses **(Figure 3.9B)** showed a significant effect of IBMX ($F(1, 1) = 234.4$, $p < 0.001$) and the forskolin dose ($F(1, 1) = 214.6$, $p < 0.001$) but not of genotype ($F(1, 1) = 0.05444$, $p = 0.82$). Two-factor interactions occurred between IBMX and forskolin dose ($F(1, 1) = 122.4$, $p < 0.001$), but not between genotype and forskolin dose ($F(1, 1) = 0.003645$, $p = 0.95$) or between genotype and IBMX ($F(1, 1) = 1.496$, $p = 0.23$). The three factor analysis yielded no significant difference between interactions of genotype and IBMX across forskolin doses. Thus, forskolin-induced cAMP accumulation did not differ between the genotypes in the presence or absence of IBMX, and differences between the genotypes were not present if different doses of forskolin were used with or without IBMX.

Analyses of Iso+Forskolin responses **(Figure 3.9C-D)** were performed separately for 1 μM and 10 μM Forskolin due to differing n values, which condition excludes the possibility of a 3-way ANOVA. For 1 μM Iso + 1 μM Forskolin responses, we found a significant effect of IBMX ($F(1, 20) = 100.6$, $p < 0.001$), genotype ($F(1, 20) = 61.54$, $p < 0.001$), and an interaction between genotype and IBMX ($F(1, 20) = 14.86$, $p = 0.001$). Sidak's multiple comparisons post-hoc tests

found significant IBMX-induced increases in cAMP accumulation in TGneg CMs of 287.9 and Cav3 OE CMs of 647.3 pmoles cAMP/μg protein ($p = 0.002$ and $p < 0.001$, respectively). Additionally, post-hoc tests found that in the absence of IBMX, Cav3 OE CMs did not show a significant increase in cAMP accumulation over TGneg CMs ($p = 0.062$) but that in the presence of IBMX, Cav3 OE CMs had a 545.4 pmoles cAMP/μg protein increase versus TGneg CMs ($p < 0.001$).

For 1 μM Iso + 10 μM Forskolin responses, we found a significant effect of IBMX ($F (1, 18) = 88.25$, $p < 0.001$) and genotype differences ($F (1, 18) = 100.5$, $p < 0.001$) but no significant interaction between IBMX and genotype ($F (1, 18) = 2.359$, $p = 0.14$). Sidak's multiple comparisons post-hoc tests found significant IBMX-induced increases in both TGneg and Cav3 OE cAMP accumulation of 821.5 and 1143 pmoles cAMP/μg protein, respectively (both $p < 0.001$). Additionally, in the absence of IBMX, Cav3 OE CMs produced 887.5 pmoles cAMP/μg protein more than TGneg CMs ($p < 0.001$) and, in the presence of IBMX, Cav3 OE CMs produced 1209 pmoles cAMP/μg protein more than TGneg CMs ($p < 0.001$).

Discussion

βAR pathway proteins in caveolae

Studies in various tissue types have reported that caveolae compartmentalize signaling proteins through interactions with caveolins, membrane lipids, cytoskeletal components, and scaffolding proteins among other mechanisms (reviewed in (5-11)). Caveolae protect Cavs (Cav1 $t_{1/2} > 24$ hr, Cav3 $t_{1/2} = 5.5$-7 hr) and cavins (t/1/2 5-8 hr)

from premature degradation by internalization and ubiquitination (12-18). The relationship between β_2ARs and lipids concentrated within cholesterol-rich lipid rafts and caveolae alters G-protein affinity and activation, changes the conformational stability and plasticity of the transmembrane domains, and can act as allosteric modifiers of β_2AR activity (19-22). After activation, β_2ARs dissociate from caveolar domains to undergo degradation through β-arrestin and clathrin-mediated endocytosis (22-24). In addition, binding to Cavs can inhibit AC activity as well as that of other enzymes, such as eNOS (25-28). Therefore, I hypothesized that Cav3 OE, which increases sarcolemmal caveolae and has been shown to alter global expression of voltage-gated ion channels, may alter the distribution of βARs and their effectors (29, 30). However, with one exception (increased AC V/VI), I found no differences in the expression or distribution of βAR signaling proteins in Cav3 OE hearts **(Figure 3.1)**.

A randomized clinical trial evaluating the therapeutic potential and safety of adenoviral administration of ACVI to heart failure patients revealed an increase in cardiac relaxation at baseline, but differences between groups disappeared with administration of intravenous dobutamine (31). Notably, preliminary reports using pigs with heart failure have reported a preservation of contractility and relaxation responses to Iso and increased Iso-stimulated cAMP production with ACVI gene transfer (32). Thus, dobutamine does not appear to stimulate an ACVI increase-dependent effect, by contrast with basal neurohormonal activation of cardiac contractility in patients or Iso administered to pigs. In this study, I hypothesized that the increased compartmentation of ACV/VI may increase the impact of the β_2AR

response and thus I tested if Iso-induced increases in Cav3 OE responses result from AC activation and via β_1ARs, β_2ARs or both βAR subtypes**.**

ACs are increased in caveolae of Cav3 OE hearts but do not have increased physiological response or cAMP production in the absence of activation

ACV and ACVI are the predominant mediators of βAR-dependent cAMP generation in CMs (25). ACV is primarily localized within Cav3-positive t-tubules in close approximation with β_1/β_2ARs and L-type Ca^{2+} channels (LTCCs), where its influence on Ca^{2+} currents is restricted by PDE activity, while ACVI is primarily localized outside of T-tubules and associates primarily with β_1ARs (25, 33). Overexpression of ACVI in neonatal cardiomyocytes increases the ACV/VI content of CFs and increases forskolin-induced cAMP formation (34). Additionally, basal AC activity and responsivity to Iso or forskolin is increased in Cav3 immunoprecipitates of ACVI OE CMs, which demonstrates that signaling complexes formed by Cav3 may enhance cAMP generation by AC with and without $G_{\alpha s}$ stimulation (34). Enzymatic activity of the ACs is inhibited by the addition of Cav1 scaffolding domain (CSD) peptides and Cav3 CSD peptides also modulate ACV activity, unmasking the stimulatory effect of Iso on LTCCs in a manner similar to the actions of PDE3/4 inhibitors (25, 26). Therefore, differential compartmentation of ACV/VI in Cav3 OE CMs may be an important regulator of βAR responsivity.

I found that compartmentation of ACV/VI within caveolae is increased in Cav3 OE CFs but that forskolin does not increase cardiac contraction, relaxation, or cAMP production between genotypes **(Figure 3.2A-E)**. Forskolin activates ACs

independently of receptors but can be influenced by basal Gi or Gs tone, which respectively reduce or increase forskolin responses. Data acquired in Langendorff *ex vivo* hearts or isolated adult CMs have little, if any, influence of systemic neurohormonal adrenergic signaling. The relationship between βARs and ACs can be considered two components in series, with the catalytic action of ACs distal to the receptors. Stimulation at the receptors can be amplified by stimulation of AC to produce a supra-additive or synergistic effects (1, 35). The current results imply that forskolin does not differentially stimulate cAMP production in Cav3 OE compared with TGneg hearts so I assessed the synergistic effects of forskolin + Iso and found a greater increase in cAMP formation in Cav3 OE myocytes with PDE inhibition **(Figure 3.2F)**. Forskolin has the capacity to potentiate receptor interactions with Iso; further studies with forskolin and βAR subtype-selective agonists may provide more information as to whether Cav3 OE CMs have altered receptor-AC interaction (1, 36). Interestingly, forskolin can help restore desensitized responses to Iso (1). β_2ARs in caveolae are susceptible to agonist-induced, GRK2-dependent desensitization while β_1ARs are not; perhaps differential modulation of GRK2 activity or β_2AR recycling occurs when Iso and forskolin are administered in combination and contributes to forskolin-Iso synergy in Cav3 OE CMs (34). However, the current data implies that direct activation of ACs is not significantly altered in Cav3 OE hearts. This result led to studies to evaluate if increases in response to Iso in Cav3 OE hearts result from β_1AR or β_2AR effects.

βARs in the heart

A recent study using mRNA gene array analysis of CMs and nonspecific radio-ligand binding in β_1-KO and $\beta_{1/2}$-KO mouse CMs found that β_2AR and β_3ARs are mostly absent in ventricular CMs (37). However, other radioligand binding studies have found β_2ARs in CMs (38-41). Additionally, previous studies have noted that isolation of adult CMs may lead to proteolysis and truncation of βARs and in turn, to aberrant detection or signaling (42). If β_2ARs are not present in adult mouse ventricular myocytes, we would expect that the adrenergic agents used in this study (namely Iso, NE, Iso+CGP, Iso+ICI, and zinterol) would induce positive inotropic responses only through the β_1ARs, and thus that the enhanced responses of Cav3 OE hearts with Iso would be β_1AR-specific. If so, Cav3 OE hearts would be expected to have increased response irrespective of the drugs used, which was not the case. It is important to note that non-myocytes in the heart secrete exosomes that contain microRNAs and even intact GPCRs, which may explain how myocytes could gain βAR function even if they lack receptor mRNA (43, 44). Therefore, it seems reasonable that adult mouse ventricular myocytes express both β_1ARs and β_2ARs.

β_1ARs do not demonstrate differential responses in Cav3 OE versus TGneg hearts

Studies reporting compartmentation of βARs within caveolae have focused on β_2ARs; however, β_1ARs are present in and signal through caveolae. Notably, studies on AC compartmentation in ventricular myocytes have identified two separate pools of β_1ARs: in t-tubules, signaling primarily through ACV and restricted by PDE activity; and in the sarcolemma, activating ACVI and less susceptible to PDE

regulation (25, 34, 45). This idea is in accordance with findings in CFs where β_1ARs are found both within and without caveolae **(Figure 3.1D)** (33, 34, 46). Overexpression of ACVI increases Iso response primarily, but not exclusively, through the β_1AR (34).

My results show that Cav3 OE does not alter the Iso response if β_2ARs are inhibited with ICI, which implicates β_2ARs as potentially mediating the enhanced Iso response in Cav3 OE hearts and CMs. Comparison of Iso and Iso+ICI reveals that ICI reduces the contractility and cAMP production response to Iso in Cav3 OE but not TGneg hearts, implying that Cav3 OE hearts accomplish enhanced Iso-stimulated contractility, relaxation, and cAMP production through β_2AR activation. ICI can exhibit inverse agonism against Iso in tissues that express high levels of β_2ARs (47) so an alternative approach, administration of NE, which has a much higher affinity for β_1ARs, was used. NE produced similar relaxation in LVDP and heart rate responses in TGneg and Cav3 OE hearts but a slightly greater contractility without significant effects was revealed by post-hoc analysis at each dose point. Studies in CMs with the partial agonist dobutamine, which has higher selectivity for β_1ARs, revealed no differences between genotypes in cAMP production.

β_2ARs do not demonstrate differential responses in Cav3 OE versus TGneg hearts

Compartmentation of the β_2AR has been extensively studied, but cardiac contractile response to β_2AR activation is not well understood (48, 49). Positive inotropic effects of β_2AR activation can be opposed by $G_{\alpha s}/G_{\alpha i}$ dual specificity and

phosphodiesterases and β_1AR knockout mice demonstrate a lack of contractile response to β_2-agonists (3, 4, 50, 51).

The current studies show that β_2AR-promoted inotropic responses (1 μM Iso in the presence of 30 nM CGP) were negligibly different from baseline in both TGneg and Cav3 OE hearts **(Figure 3.6)**. These findings are similar to what occurs in right ventricular myocardium with 1 μM CGP in the presence to the β_2AR-selective agonist salbutamol (4). Therefore, β_1ARs appear to mediate the majority of the inotropic response to Iso in both Cav3 OE and TGneg hearts. This concept is consistent with data showing that β_2AR stimulation is uncoupled from contraction in ventricular CMs (52). The heart rate response from Iso+CGP experiments was slightly (not significantly) decreased compared with Iso alone and the EC50 was right-shifted. Thus, β_1AR blockade did not have as strong an effect on heart rate as on the contractile parameters and is consistent with prior data indicating a role for β_2ARs in chronotropy (53-55).

The current data imply that activity of β_2AR is not a major contributor to the enhanced responsivity of Cav3 OE hearts to Iso. β_1AR blockade with CGP reduced Iso-promoted effects on contractility, relaxation, and cAMP production of TGneg and Cav3OE mice. Due to the enhanced Iso response of Cav3 OE hearts and CMs, the amplitude of these decreases was greater in the Cav3 OE, a result similar to the selective decrease in Cav3 OE response by the β_2AR antagonist ICI **(Figure 3.4)**. The lack of a role for β_2ARs is supported by findings with Zinterol, a selective β_2AR agonist (K_d = 9 nM [β_2AR], 1096 nM [β_1AR]), that produces strong inotropic and

relaxation responses in both TGneg and Cav3 OE hearts **(Figure 3.8)** (56). The EC50s of our physiological responses to zinterol are in the μM range, indicating that β_1ARs are also likely activated by the doses used in these experiments. Studies in isolated rat ventricular myocytes have shown maximal zinterol-induced contraction at 100 μM; contraction at 100 nM is abolished by β_2AR inhibition with ICI but not β_1AR inhibition with CGP (52). In preliminary testing in WT hearts for the current studies, 1 μM ICI completely abrogated the inotropic response to 10 μM zinterol and 100 nM ICI inhibited the response to about 60% of initial zinterol response. The selectivity of ICI for the β_2AR at doses > 30 nM is not clear, just as for the selectivity of zinterol (56, 57) Thus, higher doses of zinterol and ICI may also be working on the β_1AR.

This potential β_1AR activity of zinterol may explain why data from the zinterol and Iso+CGP dose-response studies are contradictory. If CGP only inhibits the β_1AR, as implied by its selectivity (Kd = 1.55 nM [β_1AR]; 776 nM [β_2AR]), then β_2ARs may not to be involved in inotropy or relaxation without PDE inhibition or caveolae disruption, an idea suggested by prior data (3, 4, 52, 58). Conversely, if zinterol only activates β_2ARs one might conclude that β_2ARs can enhance inotropy and relaxation without PDE inhibitors, as has also been reported (59). These conflicting results are perhaps one reason why zinterol and CGP+nonselective agonist data are not often reported together in cardiac studies, although they have been shown to produce similar effects (42, 60, 61). CGP can show inverse agonist activity, which correlates with β_2AR expression levels in CHO cells (47). Another potential explanation is that zinterol may activate cardiac β_3ARs, which activate $G_{\alpha s}$ and $G_{\alpha i/o}$ in CMs and are an emerging target in cardiac research (62). In light of these discrepancies between β_2AR

stimulation paradigms used here, further work is required to clarify the role of β_2ARs in Cav3 OE hearts. One approach may be to use zinterol along with CGP (58).

The EC50 of zinterol-induced changes in heart rate is significantly lower in Cav3 OE, and no other dose-response experiments yielded EC50 differences in heart rate **(Figure 3.8D)**. Previous data indicate that Cav3 OE mice have lower 24-hr *in vivo* heart rates than do TGneg mice. *In vivo* responses to dobutamine do not differ between genotypes, but Cav3 OE show a faster recovery to baseline and if treated with the non-selective β-blocker propranolol, Cav3 OE mice heart rates had a longer recovery period (29). The current *ex vivo* experiments did not show a significant effect of genotype on maximal heart rate of TGneg or Cav3 OE mice when exposed to boluses of the agonists Iso, zinterol, or NE or to the antagonists ICI or CGP with Iso. Further, analysis of the duration of response to an Iso bolus at 100 nM Iso did not show differences in the decay of heart rate in TGneg and Cav3 OE hearts (data not shown). However, dominant-negative mutations in Cav3 can create a longer Q-T interval in human patients through gain-of-function of voltage-gated sodium channels (Na_v) and the hearts of Cav3 OE mice have shorter QTcB intervals and prolonged PR intervals along with increased expression of $K_v1.4$, $K_v4.3$, and $Na_v1.5$ channels and the gap junction protein connexin 43 (29, 63-65). The heart rate effects of Cav3 OE or mutants may be linked to the increased β_2AR/β_1AR ratios in the sinoatrial node of the heart that unmask effects not apparent in contractile myocytes (66). Although this study was designed to determine differences in the amplitude of contractile responses between genotypes, further work is needed to clarify the impact of Cav3 OE on heart rate.

Differential responses of Cav3 OE hearts may be regulated by increased PDE activity

The role of PDEs in compartmentation of localized cAMP pools in CMs is regulated by Cav3 (58, 67) and PDE inhibition can unmask positive inotropic effects of β_2AR stimulation (3, 4). Immunoblotting **(Figure 3.1)** did not detect differences in PDE4 expression or localization to caveolae of Cav3 OE hearts; however, activity of PDEs may be modulated without changes in protein expression. In the cAMP accumulation experiments with Iso, Iso+ICI, Iso+CGP, and forskolin, 200 μM IBMX was used to prevent degradation of cAMP. If the increased ACV/VI observed in the CFs of Cav3 OE hearts is restricted by PDE activity or Cav3 binding, addition of a PDE inhibitor might help unmask AC-dependent increases in cAMP production. IBMX increases cAMP accumulation in both genotypes so there are no unmasked differences between genotypes in the forskolin response **(Figure 3.9B)** (25). In the absence of IBMX, Iso does not stimulate Cav3 OE CMs to produce more cAMP but in the presence of IBMX, and only at 1 μM Iso, do Cav3 OE CMs produce more cAMP **(Figure 3.9A).** Additionally, Iso+Fsk, in the presence or absence of IBMX, exhibit differential increases in the amplitude of cAMP production; however, the ratios between Cav3 OE and TGneg cAMP production remain similar in the presence and absence of IBMX **(Figure 3.9C-D)**. Together, these data demonstrate that the cAMP response mediated by direct AC activation is likely not influenced by PDEs, whereas, when βARs are activated, PDEs have greater impact on cAMP accumulation in Cav3 OE.

In light of the role of PDEs in Iso-only amplification of Cav3 OE cAMP generation, the similar responses from βAR subtype-selective cAMP experiments may

not represent the effects of only the individual receptors. The cAMP studies were all performed in the presence of IBMX, so one cannot compare the actions of PDEs against the βAR subtype-selective actions. IBMX, CGP+Iso, ICI+Iso, dopamine, and zinterol stimulated similar cAMP production in the genotypes, but perhaps PDEs have differential effects on the βAR sub-types. However, our data from whole *ex vivo* hearts, which were obtained in the absence of PDE inhibition, show that βAR isoforms are not independently mediating the enhanced Iso effect in Cav3 OE hearts.

Conclusions

These studies showed that the enhanced Iso responses of Cav3 OE hearts are associated with increased compartmentation of ACV/VI and greater stimulation with Iso of cAMP (in the presence of a PDE inhibitor). Testing of individual receptor and AC components of these responses in isolation, however, decreases the difference between the genotypes. Increased ACV/VI compartmentation may amplify the contractility and relaxation responses by increasing caveolar accessibility of AC to βARs, and PDEs may be compartmentalizing the cAMP response without inhibiting contractility. Studies of PDE restriction of cAMP signaling isolate the β_2AR response that predominantly localizes to caveolae whereas β_1ARs are not restricted to caveolae. Collectively, the data show that both βAR subtypes contribute to the Cav3 OE-mediated increases in contractility and relaxation.

Chapter 3 is currently being prepared for submission for publication of the material with authors, Busija, Anna R; Schilling, Jan M.; Roth, David M.; Insel, Paul A.; Patel, and Hemal H. The dissertation author was the primary investigator and author of this material.

REFERENCES

1. Darfler FJ, Mahan LC, Koachman AM, Insel PA. Stimulation of forskolin of intact S49 lymphoma cells involves the nucleotide regulatory protein of adenylate cyclase. J Biol Chem. 1982;257(20):11901-7.

2. Nilsson R, Ahmad F, Sward K, Andersson U, Weston M, Manganiello V, Degerman E. Plasma membrane cyclic nucleotide phosphodiesterase 3B (PDE3B) is associated with caveolae in primary adipocytes. Cell Signal. 2006;18(10):1713-21.

3. Perez-Schindler J, Philp A, Baar K, Hernandez-Cascales J. Regulation of contractility and metabolic signaling by the beta2-adrenergic receptor in rat ventricular muscle. Life Sci. 2011;88(19-20):892-7.

4. Gonzalez-Munoz C, Fuente T, Hernandez-Cascales J. Phosphodiesterases inhibition unmask a positive inotropic effect mediated by beta2-adrenoceptors in rat ventricular myocardium. Eur J Pharmacol. 2009;607(1-3):151-5.

5. Cheng JP, Nichols BJ. Caveolae: One Function or Many? Trends Cell Biol. 2016;26(3):177-89.

6. Cavalli A, Eghbali M, Minosyan TY, Stefani E, Philipson KD. Localization of sarcolemmal proteins to lipid rafts in the myocardium. Cell Calcium. 2007;42(3):313-22.

7. Daniel EE, El-Yazbi A, Cho WJ. Caveolae and calcium handling, a review and a hypothesis. J Cell Mol Med. 2006;10(2):529-44.

8. Epand RM. Proteins and cholesterol-rich domains. Biochim Biophys Acta. 2008;1778(7-8):1576-82.

9. Insel PA, Head BP, Ostrom RS, Patel HH, Swaney JS, Tang CM, Roth DM. Caveolae and lipid rafts: G protein-coupled receptor signaling microdomains in cardiac myocytes. Ann N Y Acad Sci. 2005;1047:166-72.

10. Patel HH, Murray F, Insel PA. Caveolae as organizers of pharmacologically relevant signal transduction molecules. Annu Rev Pharmacol Toxicol. 2008;48:359-91.

11. Busija AR, Patel HH, Insel PA. Hugh Davson Distinguished Lectureship Article Caveolins and cavins in the trafficking, maturation, and degradation of caveolae: implications for cell physiology. Am J Physiol Cell Physiol. 2017:ajpcell 00355 2016.

12. Lim JS, Nguyen KC, Han JM, Jang IS, Fabian C, Cho KA. Direct Regulation of TLR5 Expression by Caveolin-1. Mol Cells. 2015;38(12):1111-7.

13. Parat MO, Fox PL. Palmitoylation of caveolin-1 in endothelial cells is post-translational but irreversible. J Biol Chem. 2001;276(19):15776-82.

14. Hayer A, Stoeber M, Ritz D, Engel S, Meyer HH, Helenius A. Caveolin-1 is ubiquitinated and targeted to intralumenal vesicles in endolysosomes for degradation. J Cell Biol. 2010;191(3):615-29.

15. Galbiati F, Volonte D, Minetti C, Chu JB, Lisanti MP. Phenotypic behavior of caveolin-3 mutations that cause autosomal dominant limb girdle muscular dystrophy (LGMD-1C). Retention of LGMD-1C caveolin-3 mutants within the golgi complex. J Biol Chem. 1999;274(36):25632-41.

16. Sotgia F, Woodman SE, Bonuccelli G, Capozza F, Minetti C, Scherer PE, Lisanti MP. Phenotypic behavior of caveolin-3 R26Q, a mutant associated with hyperCKemia, distal myopathy, and rippling muscle disease. Am J Physiol Cell Physiol. 2003;285(5):C1150-60.

17. Galbiati F, Volonte D, Minetti C, Bregman DB, Lisanti MP. Limb-girdle muscular dystrophy (LGMD-1C) mutants of caveolin-3 undergo ubiquitination and proteasomal degradation. Treatment with proteasomal inhibitors blocks the dominant negative effect of LGMD-1C mutanta and rescues wild-type caveolin-3. The Journal of biological chemistry. 2000;275(48):37702-11.

18. Tillu VA, Kovtun O, McMahon KA, Collins BM, Parton RG. A phosphoinositide-binding cluster in cavin1 acts as a molecular sensor for cavin1 degradation. Mol Biol Cell. 2015;26(20):3561-9.

19. Prasanna X, Sengupta D, Chattopadhyay A. Cholesterol-dependent Conformational Plasticity in GPCR Dimers. Sci Rep. 2016;6:31858.

20. Mancia F, Assur Z, Herman AG, Siegel R, Hendrickson WA. Ligand sensitivity in dimeric associations of the serotonin 5HT2c receptor. EMBO Rep. 2008;9(4):363-9.

21. Laganowsky A, Reading E, Allison TM, Ulmschneider MB, Degiacomi MT, Baldwin AJ, Robinson CV. Membrane proteins bind lipids selectively to modulate their structure and function. Nature. 2014;510(7503):172-5.

22. Dawaliby R, Trubbia C, Delporte C, Masureel M, Van Antwerpen P, Kobilka BK, Govaerts C. Allosteric regulation of G protein-coupled receptor activity by phospholipids. Nat Chem Biol. 2016;12(1):35-9.

23. Zocher M, Zhang C, Rasmussen SG, Kobilka BK, Muller DJ. Cholesterol increases kinetic, energetic, and mechanical stability of the human beta2-adrenergic receptor. Proc Natl Acad Sci U S A. 2012;109(50):E3463-72.

24. Goodman OB, Jr., Krupnick JG, Santini F, Gurevich VV, Penn RB, Gagnon AW, Keen JH, Benovic JL. Beta-arrestin acts as a clathrin adaptor in endocytosis of the beta2-adrenergic receptor. Nature. 1996;383(6599):447-50.

25. Timofeyev V, Myers RE, Kim HJ, Woltz RL, Sirish P, Heiserman JP, Li N, Singapuri A, Tang T, Yarov-Yarovoy V, Yamoah EN, Hammond HK, Chiamvimonvat N. Adenylyl cyclase subtype-specific compartmentalization: differential regulation of L-type Ca2+ current in ventricular myocytes. Circ Res. 2013;112(12):1567-76.

26. Toya Y, Schwencke C, Couet J, Lisanti MP, Ishikawa Y. Inhibition of adenylyl cyclase by caveolin peptides. Endocrinology. 1998;139(4):2025-31.

27. Garcia-Cardena G, Martasek P, Masters BS, Skidd PM, Couet J, Li S, Lisanti MP, Sessa WC. Dissecting the interaction between nitric oxide synthase (NOS) and caveolin. Functional significance of the nos caveolin binding domain in vivo. The Journal of biological chemistry. 1997;272(41):25437-40.

28. Michel JB, Feron O, Sacks D, Michel T. Reciprocal regulation of endothelial nitric-oxide synthase by Ca2+-calmodulin and caveolin. J Biol Chem. 1997;272(25):15583-6.

29. Schilling JM, Horikawa YT, Zemljic-Harpf AE, Vincent KP, Tyan L, Yu JK, McCulloch AD, Balijepalli RC, Patel HH, Roth DM. Electrophysiology and metabolism of caveolin-3-overexpressing mice. Basic Res Cardiol. 2016;111(3):28.

30. Tsutsumi YM, Horikawa YT, Jennings MM, Kidd MW, Niesman IR, Yokoyama U, Head BP, Hagiwara Y, Ishikawa Y, Miyanohara A, Patel PM, Insel PA, Patel HH, Roth DM. Cardiac-specific overexpression of caveolin-3 induces endogenous cardiac protection by mimicking ischemic preconditioning. Circulation. 2008;118(19):1979-88.

31. Hammond HK, Penny WF, Traverse JH, Henry TD, Watkins MW, Yancy CW, Sweis RN, Adler ED, Patel AN, Murray DR, Ross RS, Bhargava V, Maisel A, Barnard DD, Lai NC, Dalton ND, Lee ML, Narayan SM, Blanchard DG, Gao MH. Intracoronary Gene Transfer of Adenylyl Cyclase 6 in Patients With Heart Failure: A Randomized Clinical Trial. JAMA Cardiol. 2016;1(2):163-71.

32. Lai NC, Roth DM, Gao MH, Tang T, Dalton N, Lai YY, Spellman M, Clopton P, Hammond HK. Intracoronary adenovirus encoding adenylyl cyclase VI increases left ventricular function in heart failure. Circulation. 2004;110(3):330-6.

33. Head BP, Patel HH, Roth DM, Lai NC, Niesman IR, Farquhar MG, Insel PA. G-protein-coupled receptor signaling components localize in both sarcolemmal and intracellular caveolin-3-associated microdomains in adult cardiac myocytes. J Biol Chem. 2005;280(35):31036-44.

34. Ostrom RS, Gregorian C, Drenan RM, Xiang Y, Regan JW, Insel PA. Receptor number and caveolar co-localization determine receptor coupling efficiency to adenylyl cyclase. J Biol Chem. 2001;276(45):42063-9.

35. Bristow MR, Ginsburg R, Strosberg A, Montgomery W, Minobe W. Pharmacology and inotropic potential of forskolin in the human heart. J Clin Invest. 1984;74(1):212-23.

36. Morin D, Sapena R, Tillement JP, Urien S. Evidence for different interactions between beta(1)- and beta(2)-adrenoceptor subtypes with adenylyl cyclase in the rat brain: a concentration-response study using forskolin. Pharmacol Res. 2000;41(4):435-43.

37. Myagmar BE, Flynn JM, Cowley PM, Swigart P, Montgomery M, Thai K, Nair DR, Gupta R, Hosoda C, Melov S, Baker AJ, Simpson PC. Adrenergic Receptors in Individual Ventricular Myocytes: The Beta-1 and Alpha-1B Are in All Cells, the Alpha-1A Is in a Subpopulation, and the Beta-2 and Beta-3 Are Mostly Absent. Circ Res. 2017.

38. Kuznetsov V, Pak E, Robinson RB, Steinberg SF. Beta 2-adrenergic receptor actions in neonatal and adult rat ventricular myocytes. Circ Res. 1995;76(1):40-52.

39. Buxton IL, Brunton LL. Beta-adrenergic receptor subtypes and subcellular compartmentation of cyclic AMP and cyclic AMP-dependent protein kinase in rabbit cardiomyocytes. Biochem Int. 1985;11(2):137-44.

40. Zhu WZ, Chakir K, Zhang S, Yang D, Lavoie C, Bouvier M, Hebert TE, Lakatta EG, Cheng H, Xiao RP. Heterodimerization of beta1- and beta2-adrenergic receptor subtypes optimizes beta-adrenergic modulation of cardiac contractility. Circ Res. 2005;97(3):244-51.

41. Zhou YY, Yang D, Zhu WZ, Zhang SJ, Wang DJ, Rohrer DK, Devic E, Kobilka BK, Lakatta EG, Cheng H, Xiao RP. Spontaneous activation of beta(2)- but not beta(1)-adrenoceptors expressed in cardiac myocytes from beta(1)beta(2) double knockout mice. Mol Pharmacol. 2000;58(5):887-94.

42. Rybin VO, Pak E, Alcott S, Steinberg SF. Developmental changes in beta2-adrenergic receptor signaling in ventricular myocytes: the role of Gi proteins and caveolae microdomains. Mol Pharmacol. 2003;63(6):1338-48.

43. Wang Y, Zhang L, Li Y, Chen L, Wang X, Guo W, Zhang X, Qin G, He SH, Zimmerman A, Liu Y, Kim IM, Weintraub NL, Tang Y. Exosomes/microvesicles from induced pluripotent stem cells deliver cardioprotective miRNAs and prevent cardiomyocyte apoptosis in the ischemic myocardium. Int J Cardiol. 2015;192:61-9.

44. Pironti G, Strachan RT, Abraham D, Mon-Wei Yu S, Chen M, Chen W, Hanada K, Mao L, Watson LJ, Rockman HA. Circulating Exosomes Induced by Cardiac Pressure Overload Contain Functional Angiotensin II Type 1 Receptors. Circulation. 2015;131(24):2120-30.

45. Nikolaev VO, Moshkov A, Lyon AR, Miragoli M, Novak P, Paur H, Lohse MJ, Korchev YE, Harding SE, Gorelik J. Beta2-adrenergic receptor redistribution in heart failure changes cAMP compartmentation. Science. 2010;327(5973):1653-7.

46. Head BP, Patel HH, Roth DM, Murray F, Swaney JS, Niesman IR, Farquhar MG, Insel PA. Microtubules and actin microfilaments regulate lipid raft/caveolae localization of adenylyl cyclase signaling components. J Biol Chem. 2006;281(36):26391-9.

47. Hoffmann C, Leitz MR, Oberdorf-Maass S, Lohse MJ, Klotz KN. Comparative pharmacology of human beta-adrenergic receptor subtypes--characterization of stably transfected receptors in CHO cells. Naunyn Schmiedebergs Arch Pharmacol. 2004;369(2):151-9.

48. Brodde OE, Bruck H, Leineweber K. Cardiac adrenoceptors: physiological and pathophysiological relevance. J Pharmacol Sci. 2006;100(5):323-37.

49. Collis LP, Srivastava S, Coetzee WA, Artman M. beta2-Adrenergic receptor agonists stimulate L-type calcium current independent of PKA in newborn rabbit ventricular myocytes. Am J Physiol Heart Circ Physiol. 2007;293(5):H2826-35.

50. He JQ, Balijepalli RC, Haworth RA, Kamp TJ. Crosstalk of beta-adrenergic receptor subtypes through Gi blunts beta-adrenergic stimulation of L-type Ca2+ channels in canine heart failure. Circ Res. 2005;97(6):566-73.

51. Bender AT, Beavo JA. Cyclic nucleotide phosphodiesterases: molecular regulation to clinical use. Pharmacol Rev. 2006;58(3):488-520.

52. Xiao RP, Hohl C, Altschuld R, Jones L, Livingston B, Ziman B, Tantini B, Lakatta EG. Beta 2-adrenergic receptor-stimulated increase in cAMP in rat heart cells is not coupled to changes in Ca2+ dynamics, contractility, or phospholamban phosphorylation. J Biol Chem. 1994;269(29):19151-6.

53. Isidori AM, Cornacchione M, Barbagallo F, Di Grazia A, Barrios F, Fassina L, Monaco L, Giannetta E, Gianfrilli D, Garofalo S, Zhang X, Chen X, Xiang YK, Lenzi A, Pellegrini M, Naro F. Inhibition of type 5 phosphodiesterase counteracts beta2-adrenergic signalling in beating cardiomyocytes. Cardiovasc Res. 2015;106(3):408-20.

54. Hedberg A, Minneman KP, Molinoff PB. Differential distribution of beta-1 and beta-2 adrenergic receptors in cat and guinea-pig heart. J Pharmacol Exp Ther. 1980;212(3):503-8.

55. Stiles GL, Taylor S, Lefkowitz RJ. Human cardiac beta-adrenergic receptors: subtype heterogeneity delineated by direct radioligand binding. Life Sci. 1983;33(5):467-73.

56. Baker JG. The selectivity of beta-adrenoceptor agonists at human beta1-, beta2- and beta3-adrenoceptors. Br J Pharmacol. 2010;160(5):1048-61.

57. Smith C, Teitler M. Beta-blocker selectivity at cloned human beta 1- and beta 2-adrenergic receptors. Cardiovasc Drugs Ther. 1999;13(2):123-6.

58. Macdougall DA, Agarwal SR, Stopford EA, Chu H, Collins JA, Longster AL, Colyer J, Harvey RD, Calaghan S. Caveolae compartmentalise beta2-adrenoceptor signals by curtailing cAMP production and maintaining phosphatase activity in the sarcoplasmic reticulum of the adult ventricular myocyte. J Mol Cell Cardiol. 2012;52(2):388-400.

59. McConville P, Spencer RG, Lakatta EG. Temporal dynamics of inotropic, chronotropic, and metabolic responses during beta1- and beta2-AR stimulation in the isolated, perfused rat heart. Am J Physiol Endocrinol Metab. 2005;289(3):E412-8.

60. Sosunov EA, Gainullin RZ, Moise NS, Steinberg SF, Danilo P, Rosen MR. beta(1) and beta(2)-adrenergic receptor subtype effects in German shepherd dogs with inherited lethal ventricular arrhythmias. Cardiovasc Res. 2000;48(2):211-9.

61. Altschuld RA, Billman GE. beta(2)-Adrenoceptors and ventricular fibrillation. Pharmacol Ther. 2000;88(1):1-14.

62. Michel LY, Balligand JL. New and Emerging Therapies and Targets: Beta-3 Agonists. Handb Exp Pharmacol. 2016.

63. Arnestad M, Crotti L, Rognum TO, Insolia R, Pedrazzini M, Ferrandi C, Vege A, Wang DW, Rhodes TE, George AL, Jr., Schwartz PJ. Prevalence of long-QT syndrome gene variants in sudden infant death syndrome. Circulation. 2007;115(3):361-7.

64. Cronk LB, Ye B, Kaku T, Tester DJ, Vatta M, Makielski JC, Ackerman MJ. Novel mechanism for sudden infant death syndrome: persistent late sodium current secondary to mutations in caveolin-3. Heart Rhythm. 2007;4(2):161-6.

65. Hedley PL, Kanters JK, Dembic M, Jespersen T, Skibsbye L, Aidt FH, Eschen O, Graff C, Behr ER, Schlamowitz S, Corfield V, McKenna WJ, Christiansen M. The role of CAV3 in long-QT syndrome: clinical and functional assessment of a caveolin-3/Kv11.1 double heterozygote versus caveolin-3 single heterozygote. Circulation Cardiovascular genetics. 2013;6(5):452-61.

66. Saito K, Torda T, Potter WZ, Saavedra JM. Characterization of beta 1- and beta 2-adrenoceptor subtypes in the rat sinoatrial node and stellate ganglia by quantitative autoradiography. Neurosci Lett. 1989;96(1):35-41.

67. Calaghan S, Kozera L, White E. Compartmentalisation of cAMP-dependent signalling by caveolae in the adult cardiac myocyte. J Mol Cell Cardiol. 2008;45(1):88-92.

CHAPTER 4: CONCLUSIONS

The studies reported in this dissertation were designed to discover how the localization and signaling of βARs are altered by Cav3 OE and reveal some surprising results. Cav3 OE hearts have a greatly amplified contractile and relaxation response to Iso, although the mechanisms for these increased effects may be multi-factorial. Importantly, the enhanced βAR functionality of Cav3 OE hearts was preserved in aged mice. Multiple studies from the Patel laboratory have reported the protective aspects of Cav3 OE for cardiac health. Together with the increased cardiac βAR response in young and aged hearts, efforts to increase Cav3 expression should be viewed as a therapeutic approach for further study. Investigation of subtype selectivity of βARs for caveolae in the setting of Cav3 OE revealed unexpected findings. Despite the increased number of caveolae in the membrane and thus increase in Cav3 in caveolar fractions, the distribution of βAR pathway proteins remained largely the same in Cav3 OE hearts. These results could mean that previously reported, compartmentalized βAR signaling occurs in t-tubules so that Cav3 OE, despite increasing the number of caveolae, does not greatly alter t-tubules. This possibility is supported by data linking LTCCs and ryanodine receptors to βAR signaling in t-tubules, and indeed increased ryanodine receptor expression was not found in caveolae of Cav3 OE hearts (1-3).

Even though increased localization of β_1ARs or β_2ARs did not occur in Cav fractions from Cav3 OE hearts, Cav3 OE hearts have a prominent increase in βAR response and ACV/ACVI was the only protein exhibiting increased expression in the Cav fractions. Forskolin-stimulated cAMP accumulation was similar in Cav3 OE and

TGneg hearts or myocytes, and PDE inhibition amplified Cav3 OE and TGneg cAMP accumulation without altering the relationship between the genotypes. In isolated CMs, cAMP responses were only elevated in Cav3 OE in three conditions: 1) if βARs were activated by Iso with PDE inhibition, 2) AC activation by forskolin, or 3) forskolin plus PDE inhibition. PDE4D4 was detected in cav fractions but in caveolae, similar to other non-AC components of the βAR compartmentalization pathway, they were not more concentrated in caveolae of Cav3 OE hearts.

These studies performed in whole hearts and isolated adult CMs have limitations that require further investigation. The *ex vivo* dose-response studies enabled evaluation of pharmacological interventions in the whole heart while the cAMP experiments were performed in CMs, which have divergent βAR signaling from CMs in the heart due to proteolytic cleavage and truncation of surface-localized βARs (4). Additionally, to increase the dynamic range of cAMP production, we used the PDE inhibitor, IBMX, in the βAR subtype-selective experiments, which differentially increased cAMP accumulation in Cav3 OE myocytes. There are multiple caveats to the interpretation of these results: 1) cAMP data from CMs may not directly relate to *ex vivo* or *in vivo* cardiac responses; 2) cAMP differences in CMs exposed to βAR subtype-selective stimuli may have been masked by inhibition of PDEs; 3) Global cAMP levels in CMs may be less important for contractility than (unmeasured) localized pools of cAMP; 4) βAR-selective pharmacological agents may have influenced β_1ARs and β_2ARs; and 5) Increased Iso-induced Cav3 OE responsivity may be influenced by factors not studied here, such as $G_{\alpha i}$ localization and activity,

localization and activity of PDE3 and other PDEs, PKA and protein phosphatase activity, Ca^{2+} flux, and channel activity.

Crosstalk among G_{α} protein-mediated signals may increase the complexity of the responses we measured beyond effects on ACs and should be investigated. Protein phosphatases participate in compartmentation of cAMP signals in CMs and may be differentially compartmentalized or activated in Cav3 OE (5). Ca^{2+} signals propagated by activation of T-type and L-type calcium channels, the ryanodine receptor, and SERCA activation may be differentially compartmentalized and regulated by Cav3 OE CMs at baseline and in response to Iso. Therefore, measurement and modulation of these responses would provide useful insight into the complex relationships between βAR activation, Cav3 OE, and contractile responses in the heart.

My findings engender new questions about the role of Cav3 OE in the regulation of βAR signaling. The data reveal that Cav3 OE increases Iso-promoted contractile and relaxation responses in the heart, but our approach to the role of Cav3 OE was informed by studies that can define the actions of β_1ARs and β_2ARs in the heart, based on their compartmentation inside/outside caveolae and differential regulation by a number of factors (e.g., GRK2, PDEs, PPs). However, in the *ex vivo* hearts and isolated CMs used here, the role of Cav3 OE in the amplification of contractile responses appears not to be limited to just one of the βAR subtypes. The contractile response of βARs was only (maximally) elevated when both receptors were activated by Iso.

The study of βARs with two pharmacological approaches—using a nonselective agonist plus selective antagonist or testing a selective agonist—revealed

that Cav3 OE appears not to increase cardiac contractility or cAMP production exclusively through just one of the βAR subtypes. If only ICI or CGP had been used to inhibit βARs with Iso, the conclusions would have been flawed. The ideas were informed by studies with NE and with a selective β_2AR zinterol. Additionally, the use of pharmacological agents in isolated adult CMs to activate ACs directly and inhibit PDE activity led to the discovery that although Cav3 OE hearts have more ACV/VI in caveolae, that compartmentation does not directly result in increased cAMP or contractility and those ACs may not be differentially regulated by PDEs. The results lead to the conclusion that when β_1ARs and β_2ARs are activated together, they develop an increased response in Cav3 OE compared with TGneg CMs. From a different perspective, therefore, Cav3 OE unmasks increased efficacy of both βARs in the heart. Because the physiological agonists for the βARs are not exclusively acting on one or the other receptor, and not just on βARs, it seems unlikely that CMs reserve one or the other isoform for specific, strictly delineated functionality.

If βAR subtypes work together to amplify response in Cav3 OE CMs, a number of possible mechanisms may be involved. β_2AR dimerization may be enabled by cholesterol binding, a feature that may be involved in enhanced conformational plasticity of βARs in cholesterol-containing membranes (6-8). β_1AR-β_2AR heterodimers demonstrate an increase in Iso potency that was not seen in our Cav3 OE hearts (9). Studies from our laboratories have found the μ-opioid receptor in Cav3 immunoprecipitates from CMs and there is recent evidence that β_2ARs can heterodimerize with, and alter the analgesic activity of, μ-ORs in neural cells (10). The oligomeric state of βARs, therefore, remains an interesting possibility.

Other possibilities of βAR signaling modification exist as well. For instance, the β_2AR has been identified as a factor that activates multiple cardiac kinase signaling cascades, including PI3K, Akt, ERK1/2, and GSK-3α/β, among others. Interestingly, PI3K associates with GRK2, which brings it to βARs, after which it generates $PI(3,4,5)P_3$ species that recruit β-arrestin and AP-2, both of which can drive internalization of βARs (11). Disruption of PI3K localization with agonist-activated βARs prevents downregulation of the receptor and preserves cardiac function in mice exposed to chronic catecholamine stress or pressure-overload (12). β_2AR activation of G_i can activate PI3K to increase PDE4 activity, regulating cAMP signal duration and intensity as well as contractility in isolated CMs (13). From the review of the formation, degradation, and relative stability of caveolae in Chapter 1, it may be that having more caveolae in a contractile cell subjected to constant mechanical motion may make each caveola more protected from degradative stimuli. The 30 min exposure of hearts to Iso did not demonstrably alter the βAR response in either genotype but these hearts were removed from mice, indicating that the thoracotomy and loss of blood pressure inundated the heart with catecholamines. I have developed a pan-PKA phospho substrate blot performed on lysates from hearts that were flash frozen right after removal, and found that the signal was both strong and diverse among hearts. Although our interventions were performed in the whole heart and isolated myocytes it is possible that we induced a downregulation of TGneg βARs that was not as strong in Cav3 OE, and this contributed to effects seen in these studies. However, results from caveolar fractionations are reassuring in that respect, as we did

not detect alterations in either βAR's localization in caveolae nor in expression levels, of hearts that removed in the same way.

Thus, it appears that neither βAR subtype nor AC are independently responsible for the Cav3 OE-mediated increases in catecholaminergic cardiac responsivity and preservation of βARs into old age. Instead, the specific, mechanistic roles of Cav3 in βAR regulation may involve multiple aspects of the signaling pathway, for instance: 1) altering activity of PDEs; 2) stoichiometric ratios of AC:receptor within caveolae, glucose and pyruvate-driven, Iso-potentiated mitochondrial respiration; and/or 3) by providing a more sheltered, stabilizing environment for βARs, ACs, PDEs, and other regulatory proteins that localize within and near caveolae. The data in aged mice emphasize that therapeutic potential of increasing Cav3 to benefit the hearts of humans.

REFERENCES

1. Nikolaev VO, Moshkov A, Lyon AR, Miragoli M, Novak P, Paur H, Lohse MJ, Korchev YE, Harding SE, Gorelik J. Beta2-adrenergic receptor redistribution in heart failure changes cAMP compartmentation. Science. 2010;327(5973):1653-7.

2. Balijepalli RC, Kamp TJ. Cardiomyocyte transverse tubule loss leads the way to heart failure. Future Cardiol. 2011;7(1):39-42.

3. Timofeyev V, Myers RE, Kim HJ, Woltz RL, Sirish P, Heiserman JP, Li N, Singapuri A, Tang T, Yarov-Yarovoy V, Yamoah EN, Hammond HK, Chiamvimonvat N. Adenylyl cyclase subtype-specific compartmentalization: differential regulation of L-type Ca2+ current in ventricular myocytes. Circ Res. 2013;112(12):1567-76.

4. Rybin VO, Pak E, Alcott S, Steinberg SF. Developmental changes in beta2-adrenergic receptor signaling in ventricular myocytes: the role of Gi proteins and caveolae microdomains. Mol Pharmacol. 2003;63(6):1338-48.

5. Macdougall DA, Agarwal SR, Stopford EA, Chu H, Collins JA, Longster AL, Colyer J, Harvey RD, Calaghan S. Caveolae compartmentalise beta2-adrenoceptor signals by curtailing cAMP production and maintaining phosphatase activity in the sarcoplasmic reticulum of the adult ventricular myocyte. J Mol Cell Cardiol. 2012;52(2):388-400.

6. Prasanna X, Chattopadhyay A, Sengupta D. Cholesterol modulates the dimer interface of the beta(2)-adrenergic receptor via cholesterol occupancy sites. Biophys J. 2014;106(6):1290-300.

7. Rothberg KG, Heuser JE, Donzell WC, Ying YS, Glenney JR, Anderson RG. Caveolin, a protein component of caveolae membrane coats. Cell. 1992;68(4):673-82.

8. Zocher M, Zhang C, Rasmussen SG, Kobilka BK, Muller DJ. Cholesterol increases kinetic, energetic, and mechanical stability of the human beta2-adrenergic receptor. Proc Natl Acad Sci U S A. 2012;109(50):E3463-72.

9. Zhu WZ, Chakir K, Zhang S, Yang D, Lavoie C, Bouvier M, Hebert TE, Lakatta EG, Cheng H, Xiao RP. Heterodimerization of beta1- and beta2-adrenergic receptor subtypes optimizes beta-adrenergic modulation of cardiac contractility. Circ Res. 2005;97(3):244-51.

10. Samoshkin A, Convertino M, Viet CT, Wieskopf JS, Kambur O, Marcovitz J, Patel P, Stone LS, Kalso E, Mogil JS, Schmidt BL, Maixner W, Dokholyan NV, Diatchenko L. Structural and functional interactions between six-transmembrane mu-opioid receptors and beta2-adrenoreceptors modulate opioid signaling. Sci Rep. 2015;5:18198.

11. Naga Prasad SV, Laporte SA, Chamberlain D, Caron MG, Barak L, Rockman HA. Phosphoinositide 3-kinase regulates beta2-adrenergic receptor endocytosis by AP-2 recruitment to the receptor/beta-arrestin complex. J Cell Biol. 2002;158(3):563-75.

12. Nienaber JJ, Tachibana H, Naga Prasad SV, Esposito G, Wu D, Mao L, Rockman HA. Inhibition of receptor-localized PI3K preserves cardiac beta-adrenergic receptor function and ameliorates pressure overload heart failure. J Clin Invest. 2003;112(7):1067-79.

13. Gregg CJ, Steppan J, Gonzalez DR, Champion HC, Phan AC, Nyhan D, Shoukas AA, Hare JM, Barouch LA, Berkowitz DE. beta2-adrenergic receptor-coupled phosphoinositide 3-kinase constrains cAMP-dependent increases in cardiac inotropy through phosphodiesterase 4 activation. Anesth Analg. 2010;111(4):870-7.